

**Analysis of the adaptor proteins,
gephyrin and GRIP1,
in KIF5-driven neuronal transport in *Mus musculus*,
(*Linnaeus, 1758*)**

Dissertation

**zur Erlangung des Doktorgrades
am Fachbereich Biologie der Fakultät für Mathematik, Informatik und
Naturwissenschaften der Universität Hamburg**

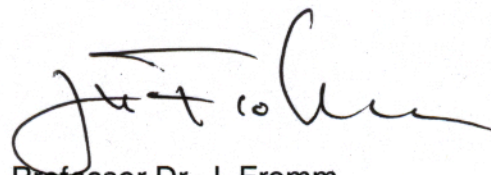
by

**Han Kyu Lee
from Republic of Korea**

**Hamburg
October, 2011**

Genehmigt vom Fachbereich Biologie
der Fakultät für Mathematik, Informatik und Naturwissenschaften
an der Universität Hamburg
auf Antrag von Prof. Dr. M. KNEUSSEL
Weiterer Gutachter der Dissertation:
Prof. Dr. C. LOHR
Tag der Disputation: 22. Juli 2011

Hamburg, den 08. Juli 2011

A handwritten signature in black ink, appearing to read 'J. Fromm', is written over the printed name.

Professor Dr. J. Fromm
Vorsitzender des Promotionsausschusses
Biologie



University of Hamburg

Center for Molecular Neurobiology (ZMNH)

Research group: Neuronal Translational Control

Katharine K. Miller

Hamburg, 23.05.2011

Falkenried 94

D-20251 Hamburg

Germany

Phone: +49 040 7410 57262

Fax: +49 040 7410 53436

Subject: English Language Declaration

To whom it may concern,

I, Katharine K. Miller, testify that I have fully read over the doctoral thesis of Han Kyu Lee and declare that the English it is written in to be clear and free of grammatical errors.

Sincerely,

Katharine K. Miller

Table of contents

1. Abstract	6
2. Introduction	8
2-1. The mammalian central nervous system	8
2-2. Neurons	9
2-2-1. Excitatory synapses.....	9
2-2-2. Inhibitory synapses.....	11
2-2-3. Ionotropic glutamate receptors.....	13
2-2-3-1. AMPA receptors.....	14
2-2-3-2. NMDA receptors.....	16
2-3. Motor proteins and motor-cargo complexes	19
2-3-1. Intracellular cargo transport.....	19
2-3-2. Anterograde motor proteins: Kinesin.....	19
2-3-3. Retrograde motor proteins: Dynein.....	23
2-3-4. Cytoskeletal tracks.....	25
2-3-4-1. Microtubules.....	26
2-3-4-2. Post-translational modifications:	
Polyglutamylation.....	27
2-3-5. Cargo adaptors.....	29
2-3-5-1. Gephyrin.....	29
2-3-5-2. GRIP1.....	30
2-4. Cell adhesion molecules	31
2-4-1. N-Cadherin.....	31
2-4-2. N-Cadherin and GRIP1.....	33
3. Aim of the study	35

4. Materials and Methods	37
4-1. Materials	37
4-1-1. Chemicals and enzymes.....	37
4-1-2. Instrumentations.....	37
4-1-3. Buffers and media.....	38
4-1-4. Cell lines.....	41
4-1-5. Bacterial strains.....	41
4-1-6. Antibodies.....	41
4-1-6-1. Primary antibodies.....	42
4-1-6-2. Secondary antibodies.....	43
4-1-7. Oligonucleotides.....	43
4-1-8. Vectors and their usage.....	45
4-1-9. Viruses.....	47
4-2. Molecular biology	48
4-2-1. Bacterial transformation.....	48
4-2-2. Isolation of plasmid DNA.....	48
4-2-2-1. Small-scale isolation of plasmid DNA.....	48
4-2-2-2. Large-scale isolation of plasmid DNA.....	49
4-2-3. Determination of DNA concentrations.....	49
4-2-4. PCR based amplification of DNA for cloning.....	49
4-2-5. Digestion of plasmids and PCR fragments with restriction enzymes.....	50
4-2-6. Agarose gel electrophoresis.....	51
4-2-7. Purification of plasmids and PCR fragments from an agarose gel.....	51
4-2-8. Ligation.....	51
4-2-9. DNA sequencing.....	51
4-3. Biochemistry	52
4-3-1. SDS-polyacrylamide gel electrophoresis.....	52
4-3-2. Western Blotting.....	52

4-3-3. Immunodetection.....	53
4-3-4. Co-immunoprecipitation.....	53
4-3-4-1. Precipitation of endogenous proteins from rodent brain extract.....	53
4-3-4-2. Precipitation of exogenous proteins from HEK293 cell line.....	54
4-3-5. Differential centrifugation.....	55
4-3-6. Detection of surface expressed proteins.....	55
4-4. Cell culture and immunocytochemistry	56
4-4-1. HEK293TN culture.....	56
4-4-2. Transfection of cultured HEK293 cell.....	56
4-4-3. Preparation of primary hippocampal neurons.....	57
4-4-4. Transfection of cultured hippocampal neurons.....	58
4-4-5. Virus infection.....	58
4-4-6. Immunocytochemistry.....	58
4-5. Time-lapse imaging	59
4-6. Quantitative and statistical analysis	60
5. Results	61
5-1. Project 1: Polyglutamylation specifically inhibits gephyrin-mediated KIF5 movement	61
5-1-1. Induced polyglutamylation by application of strychnine.....	61
5-1-2. Rescue gephyrin distribution by shRNA-mediated knockdown of PGs1 gene expression after application of strychnine.....	62
5-2. Project 2: KIF5-driven novel transport complex, N-Cadherin-GluR2-GRIP1-KIF5C	67

5-2-1. Interaction and co-localization of GluR2, GRIP1, KIF5C, and N-Cadherin.....	67
5-2-2. Transport of GluR2, GRIP1, and N-Cadherin by KIF5C.....	70
5-2-2-1. Subcellular distribution of mRFP-GRIP1 and mRFP-N-Cadherin by KIF5C in neurons.....	72
5-2-2-2. Surface expression of GluR2 and N-Cadherin by KIF5C.....	75
5-2-3. Interference of GluR2 and N-Cadherin surface expression	79
5-2-4. A transport complex carrying different transmembrane protein.....	84
5-2-4-1. Co-localization of GluR2 and N-Cadherin in the same vesicle.....	85
5-2-4-2. Co-migration GluR2 and N-Cadherin.....	87
5-2-5. Association of the complex with Sec8.....	90
5-2-6. Interference spine density by inhibiting the complex formation.....	91
 6. Discussion	 94
 6-1. Project 1: Polyglutamylation specifically inhibits gephyrin-mediated KIF5 movement	 94
6-1-1. Application of a glycine receptor antagonist induces polyglutamylation.....	94
6-1-2. Functional inactivation of polyglutamylases increases mRFP-gephyrin transport into neuritis.....	95
 6-2. Project 2: KIF5-driven novel transport complex, N-Cadherin-GluR2-GRIP1-KIF5C	 98
6-2-1. GRIP1 interacts to N-Cadherin through its PDZ2 domain...	98
6-2-2. N-Cadherin interacts and co-localizes with each of GluR2- GRIP1-KIF5C complex.....	99
6-2-3. KIF5C is a motor protein for N-Cadherin.....	101
6-2-4. Functional ablation of KIF5 and GRIP1 decreases GluR2	

and N-Cadherin surface expression.....	103
6-2-5. GluR2 and N-Cadherin are formed in the same vesicle and undergo co-transport.....	106
6-2-6. KIF5C and N-Cadherin/GRIP1 binding is involved in the regulation of spine numbers.....	109
6-3. Outlook	111
7. References	113
8. Appendices	143
8-1. Abbreviations and units	143
8-2. Figures and tables	146
8-3. Curriculum Vitae	148
8-4. List of publications	149
9. Acknowledgements	150

1. Abstract

Thousands of intra- and extracellular processes define the identity of a neuron at a given time. These processes require an interplay between different molecules, including the communication of the plasmamembrane with intracellular vesicle compartments. For instance, synaptic formation requires intra- and extracellular processes for the formation of precise molecular attachments between pre- and postsynaptic neurons. Motor proteins such as kinesins, dyneins, and myosins are highly involved in regulating intracellular turnover and synaptic formation in neurons. Kinesins mainly transport cargos toward anterograde direction along microtubules and have been implicated in the delivery of material to synapses. Despite many studies, which have discovered several different transport mechanisms, the transport mechanisms for specific cargos still remain elusive.

Here, I report that gephyrin and GRIP1 (glutamate receptor-interacting protein 1) act as adaptor proteins, which steer their respective cargos through different mechanisms. A gephyrin-mediated transport complex and a GRIP1-mediated transport complex, both of which use the same motor protein, KIF5, were investigated through two separate projects. The first project focuses on posttranslational modifications of microtubules and their impact on anterograde transport of a GlyR-gephyrin-KIF5 complex. In this project, I show that increasing neuronal activity through the application of 1 μ M strychnine up-regulates polyglutamylation of tubulins, which interferes with ability of the gephyrin-mediated transport complex to be targeted into neurites. After depleting polyglutamylation of tubulins by infecting cells with Lentivirus carrying shRNA-PGs1, distribution of the complex is recovered. These results indicate that changes in neuronal activity alter cellular function by a crosstalk with intracellular transport of synaptic cargo into neurites. The second project focuses on a novel transport complex, N-Cadherin-GluR2-GRIP1-KIF5. Several recent studies have proposed that N-Cadherin, a Ca^{2+} -dependent cell adhesion molecule, regulates synapse formation in mammalian central neurons. Independently, GRIP1 was previously shown to act as an adaptor protein for transporting GluR2-containing AMPA receptors driven by KIF5 motor proteins. Here, I show that N-Cadherin is also transported by KIF5 together with GRIP1. Expression of a dominant-negative KIF5C polypeptide,

characterized by the deletion of its motor domain, caused N-Cadherin aggregation in the cell body and significantly interfered with N-Cadherin transport into neurites. Furthermore, competitive interference with N-Cadherin/GRIP1 binding or depolymerization of microtubules decreased N-Cadherin surface membrane levels upon heterologous expression. Therefore, N-Cadherin, similar as reported for the GluR2-containing AMPA receptor, is driven by a GRIP1-KIF5 transport complex. Consequently, I investigated whether both N-Cadherin and the GluR2-containing AMPA receptor are co-transported by the same adaptor-motor protein complex in neurons. Co-immunoprecipitation and co-localization experiments pointed to a complex consisting of N-Cadherin, GluR2-containing AMPA receptor, GRIP1, and KIF5. In line with these observation, electron microscopy detected N-Cadherin and the GluR2-containing AMPA receptor to share the same intracellular vesicles. Finally, I observed the co-transport of both proteins in neurites of living neurons by applying time-lapse video microscopy. These results suggest that N-Cadherin is transported together with a GluR2-GRIP1-KIF5 complex in the same vesicle. To my knowledge, this is the first report that describes co-transport of a cell adhesion molecule together with neurotransmitter receptors, both of which are known to be essential for the identity of excitatory spine synapses. As a result, I expect the findings from my two projects to extend the current understanding of somata to synapse targeting.

2. Introduction

2-1. The mammalian central nervous system

The mammalian nervous system is a highly complex network, consisting of an intricate connection between neurons and glial cells. It is responsible for processing and integration of sensory and motor input, which is mediated by electrical and chemical signaling in the body. The nervous system is divided into two parts, the central nervous system (CNS) and the peripheral nervous system (PNS) (Kandel *et al.*, 2000). Information is detected by the PNS and is transmitted to the CNS for processing. The CNS is comprised of the spinal cord and the brain, which control many functions of the body. The spinal cord is a long and thin tubular bundle and is the main hub of communication signals, involving sensory information from the PNS to the brain and motor information from the brain to the PNS. Information is interpreted at the brain. Anatomically, the brain is divided into three specific regions: the forebrain (also known as the proencephalon), which consists of the cerebral hemispheres, thalamus, and hypothalamus, the midbrain (also known as the mesencephalon), and the hindbrain (also known as the rhombencephalon), which consists of the pons and cerebellum. Additionally, the CNS is also divided into three functional components: the sensory system, the motor system, and the homeostatic and higher brain functions. The sensory system is responsible for processing sensory information and consists of the somatosensory, viscerosensory, auditory, vestibular, olfactory, gustatory, and visual systems. The motor system is involved with movement, which is controlled by motor units, and the somatic system, which is made up of skeletal muscle, the spinal reflexes, the autonomic visceral system, the cerebellum, and several subcortical and cortical sites. The homeostatic and higher functional system are mainly involved in body maintenance and the interpretation of information. The homeostatic and higher functional system includes the hypothalamus, cortical areas involved in motivation, insight, personality, language, memory, imagination, creativity, thinking, judgement, mental processing, and subcortical areas involved in learning, thought, consciousness, memory, attention, emotional state, sleep and arousal cycles.

2-2. Neurons

Neurons, also known as nerve cells, are a major component of the CNS. A neuron is an excitable cell, which transmits information to other cells using electrical and chemical signals. Neurons, which are polarized, are connected to each other to form networks. There are three main specialized types of neurons: sensory neurons, interneurons, and motor neurons. The sensory neurons collect information from the sensory receptors in the body and transmit it to the brain. The interneurons interpret the information and communicate between the sensory neurons and the motor neurons. The motor neurons transmit the information signaling for the body to react. Each neuron consists of three distinct subcellular compartments, which are the cell body (also known as the soma), the dendrites, and the axon. Dendrites are extended over hundreds of micrometers and make multiple branches called the dendritic tree, whereas axons are extended for much longer distances (up to 1 m in humans and even more in other species). These dendrites and axons arise from the cell body. Various signals are detected at dendrites through synaptic connections with the axons or dendrites from other neurons. These signals are collected and interpreted in the cell body. Finally this information is transferred to neighboring neurons, which are connected through an axon of the cell.

In general, neurons are electrically excitable cells due to thousands of ion channels and ion pumps, which are embedded in the plasmamembrane of the neurons. The functions of neurons are dependent on differential ions concentration, such as sodium (Na^+), potassium (K^+), chloride (Cl^-), and calcium (Ca^{2+}), between the extracellular membrane and intracellular membrane. When a certain concentration of ions reaches a threshold level, an action potential is generated. This action potential rapidly propagates along the axon, changing the balance of ions between the extracellular and intracellular membrane. This is the basic signal transferring mechanism in the neuron.

2-2-1. Excitatory synapses

Two different types of synapses, chemical and electrical, are present in the CNS. Chemical synapses transmit signals using neurotransmitters through the synaptic cleft, which is located between the presynaptic and postsynaptic membranes. In

contrast, electrical synapses utilize electrical signals, which are transmitted by physiologically connecting regions, called gap junctions (Purves *et al.*, 2008).

Early electrophysiological studies have shown that glutamate is a major neurotransmitter that initiates molecular and physiological processes of excitatory synapses in the CNS (Curtis *et al.*, 1960; Krnjevic and Phillip, 1963). These processes can also be initiated by several other neurotransmitters, for instance, acetylcholine, catecholamines, serotonin, and histamine. Excitatory synapses, also known as glutamatergic synapses, are mainly localized on the dendritic spines, which are postsynaptic microcompartments. Around 80% of excitatory synapses are located in dendritic spines, whereas approximately 20% of excitatory synapses are located in dendritic shafts (Boyer *et al.*, 1998). The dendritic spines are classified by shape and size as either thin, stubby, mushroom, or cup-shaped (Harris *et al.*, 1992; Chang and Greenough, 1984; Peters and Kaiserman-Abramof, 1970). In terms of synaptogenesis, larger spines, which are mushroom or cup-shaped, are functionally stronger (strong connection between pre- and postsynapse and more receptors on postsynapse) meaning that they are more stable (Spacek and Harris, 1997). They were reported to contain high amounts of smooth endoplasmic reticulum and neurotransmitter receptors, whereas smaller spines, which are thin and stubby, may be more flexible, rapidly enlarging or shrinking in response to subsequent activation (Bourne and Harris, 2007). An enlarged spine head connects to its dendrite by a narrow neck. Dendritic spines provide a postsynaptic biochemical compartment that separates the synaptic space from the dendritic shaft. This allows each spine to function as a partially independent unit (Korkotian *et al.*, 2004). Functional excitatory synapses are governed by hundreds of macromolecular complexes separately expressed at the presynaptic and/or postsynaptic termini. In addition, a wide variety of cell-adhesion molecules (CAMs) hold pre- and postsynaptic membranes together at the appropriate distance (Scheiffele, 2003; Yamagata *et al.*, 2003).

At the presynaptic side, many synaptic vesicles, which are around 40 nm in diameter and contain a variety of neurotransmitters, are recruited to active zones (Bonanomi *et al.*, 2006). When an action potential arrives at the presynaptic bouton, neurotransmitters in the synaptic vesicles are released into the synaptic cleft and the released neurotransmitters are retrieved (Jin and Garner, 2008; Schoch and Gundelfinger, 2006; Sudhof, 2004). The synaptic cleft between the presynaptic bouton and the postsynaptic dendritic spine is a space separated by a

gap of 20 to 25 nm (Sheng and Hoogenraad, 2007). On the postsynaptic side, multiple protein complexes exist exactly opposite to the active zone of the presynaptic bouton (Kasai *et al.*, 2003). These complexes are called postsynaptic densities (PSD), which are ultrastructurally observed as electron-dense thickenings of the postsynaptic membrane where glutamate receptors and their associated proteins are highly concentrated (Sheng and Hoogenraad, 2007). Therefore, the dimensions of the spine head are highly correlated with the sizes of the PSDs and the associated active zone, as well as with the synaptic strength (Kasai *et al.*, 2003). Postsynaptic dendritic spines are divided into two regions, the PSD and the extrasynaptic region. The respective proteins, which are present on the extrasynaptic region and the PSD, are distinctively different. For example, the function of many proteins in the extrasynaptic region is related to endocytotic processes, whereas the PSD contains several proteins important for synaptic transmission (Racz *et al.*, 2004; Baude *et al.*, 1993).

In brief, excitatory neurotransmitters are released from the presynapse to the dendritic spine of the postsynaptic neuron, and the diffused neurotransmitters bind to their specific receptors, which are mainly ionotropic glutamate receptors (iGluRs) and metabotropic glutamate receptors (mGluRs). Upon binding their respective neurotransmitters, receptors allow positively charged ions to enter the postsynaptic neuron (iGluRs) or to activate biochemical cascades that modify other intracellular proteins (mGluRs). If the signal is sufficient and above the threshold, the neuron is subsequently depolarized (Sheng and Hoogenraad, 2007; Endoh, 2004). In addition, increased amounts of positively charged ions, especially calcium (Ca^{2+}) ions, in the postsynapse act as regulators and secondary messengers to the PSD and other subcellular compartments.

2-2-2. Inhibitory synapses

Unlike excitatory synapses, inhibitory synapses in the CNS use two agonists as neurotransmitters, γ -Aminobutyric acid (GABA) for GABA receptors and glycine for glycine receptors. It is well established that GABA is the major neurotransmitter of inhibitory synapses in the brain. Although glycine is widely distributed throughout the whole CNS (Danglot *et al.*, 2004; Aoki *et al.*, 1988; Ottersen *et al.*, 1987), early studies suggested that glycinergic synapses are mostly present in the spinal cord and the brainstem (Lynch, 2004). In general, inhibitory synapses are localized on

dendritic shafts or directly at the cell body of postsynaptic neurons. However, several studies showed that about 15% of inhibitory synapses are present on dendritic spines (Megias *et al.*, 2001). The main function of inhibitory synapses is to control neuronal excitability throughout the CNS.

At inhibitory synapses, GABA is originally synthesized from glutamic acid by the enzyme glutamic acid decarboxylase (GAD), which is mainly detected in GABAergic neurons. Once GABA is synthesized, it is transported into vesicles containing the vesicular inhibitory amino acid transporter (VIAAT), which are then translocated toward presynaptic terminals (Dumoulin *et al.*, 1999). Following GABA release from the presynaptic terminal, it binds to specific transmembrane receptors in the plasma membrane of both pre- and postsynaptic neuronal processes. Through this binding, the receptor channels open and allow either an influx of chloride (Cl^-) ions into the neuron or an efflux of potassium (K^+) from the neuron. The chloride ions diffusing into the neuron hyperpolarize the cell, thereby reducing the probability that an action potential is elicited. The GABA receptors can be divided into three types, GABA_A , GABA_B , and GABA_C , covering two general classes of GABA receptors, ionotropic and metabotropic GABA receptors. GABA_A and GABA_C are ionotropic receptors, which are ligand-gated ion channel complexes belonging to the cysteine (Cys) loop family of ion channels. In contrast, GABA_B is a metabotropic receptor, which is a G protein-coupled receptor (GPCR). In general, the fast inhibitory actions of GABA are mediated by the activation of GABA_A receptors in the brain and GABA_C receptors in the retina (Rudolph and Mohler, 2004; Chavas and Marty, 2003; Sieghart and Sperk, 2002; Bormann and Feigenspan, 1995). On the other hand, the slow inhibitory actions of GABA are mediated by the activation of GABA_B receptors (Bettler and Tiao, 2006; Chavas and Marty, 2003; Couver *et al.*, 2000). Ionotropic GABA_A receptors are pentamers assembled from eight different subunits (α , β , γ , δ , ϵ , θ , π , ρ). However, the majority of pentamers are composed of three subunits, α , β , and γ (Rudolph and Mohler, 2004). Each subunit harbours four transmembrane domains, which include two intracellular loops, one between the first and second transmembrane domains and the other between the third and fourth transmembrane domains. Conversely, the subunits of heterodimeric metabotropic GABA_B receptors harbour seven transmembrane domains. Like other neurotransmitter receptors, the diverse GABA receptor combinations have different physiological and pharmacological properties and are differentially expressed in a spatiotemporal manner.

Glycine, mainly expressed in the spinal cord, the brainstem, and the retina, is an inhibitory neurotransmitter in the CNS, like GABA. Glycine is synthesized from serine by the mitochondria isoform of serine hydroxymethyltransferase. Fully synthesized glycine is then translocated into vesicles by the action of VIAAT, similar as for the neurotransmitter GABA (Dumoulin *et al.*, 1999). Glycine molecules acting as neurotransmitters have similar properties in the spinal cord, the brainstem, and the retina as GABA molecules do in the brain. When glycine binds to the glycine receptor it allows an influx of chloride ions into the cell and the release of potassium from the neuron. Strychnine is a highly competitive antagonist for the glycine receptor, although other antagonists with a lower affinity to the receptor exist (Rajendra *et al.*, 1997). Similar to the GABA receptor, the strychnine-sensitive glycine receptor is a member of the Cys-loop family of ion channels and is comprised of five subunits that combine to form a pentamer (Miyazawa *et al.*, 2003). Four different α subunit isoforms and one β subunit isoform exist for the glycine receptor. In addition, the Cys-loop ion channel superfamily contains the nicotinic acetylcholine (AChR) and 5-HT₃ receptors, all of which are also composed of five protein subunits that assemble into pentamers (Sine and Engel, 2006). Glycine receptors composed from different subunit combinations are differentially expressed across the CNS and function under specific conditions (Malosio *et al.*, 1991). For example, the GlyR β subunit transcripts are highly expressed during neural development as well as in the adult CNS (Malosio *et al.*, 1991), whereas expression of GlyR α 2 subunits decrease after birth, and expression of GlyR α 1 and α 3 increase (Singer *et al.*, 1998)

2-2-3. Ionotropic glutamate receptors: AMPA receptor and NMDA receptor

Glutamate plays an essential role in many physiological functions, is a major excitatory transmitter in the CNS and acts through two classes of receptors. Ionotropic glutamate receptors (iGluRs) and metabotropic glutamate receptors (mGluRs) show different manners of activation for increasing the postsynaptic current (Palmada and Centelles, 1998). The iGluRs form ion channels and these channels are activated by glutamate binding to the receptor. However, the mGluRs, upon binding of glutamate, indirectly activate G-proteins that interact with intracellular loops of the receptor. The iGluRs are the principal mediators of fast

excitatory transmission in the CNS. These receptors are divided into three subfamilies by their specific binding and responses to agonists such as *N*-Methyl-D-aspartate (NMDA), α -amino-3-hydroxyl-5-methyl-4-isoxazole-propionate (AMPA), and kainite (Ozawa *et al.*, 1998; Wollmuth *et al.*, 2004). However, each receptor represents a multimeric assembly of four subunits. All iGluRs are ligand-gated non-selective cation channels that are permeable to K^+ , Na^+ , and Ca^{2+} in response to glutamate binding (in case of NMDA receptor, glycine co-agonist binding on the receptor is also required). Through this binding, sequential intramolecular rearrangements lead to an opening of the ion channel pore. The subsequent flow of cations into the cell increases the excitatory postsynaptic current (EPSC). If sufficient iGluRs are activated and the depolarization of the neuron reaches a certain threshold, an action potential can be triggered.

An important function of the iGluRs is the modulation of synaptic plasticity, which is considered to underlie the formation learning and memory. However, mGluRs are also involved in regulation of synaptic plasticity (Debanne *et al.*, 2003). Moreover, activation and persistence of long-term potentiation (LTP) and long-term depression (LTD) strongly depends on the number of iGluRs and mGluRs available for synaptic transmission at the synapse (Pérez-Otaño and Fhlers, 2005; Asztély and Gustafsson, 1996).

The AMPA receptor was first discovered through expression cloning from the rat (Hollmann *et al.*, 1989). Molecular cloning of receptor subunits further showed that the classes defined by molecular criteria were in good correlation with those defined earlier by pharmacological criteria (Dingledine *et al.*, 1999; Hollmann and Heinemann, 1994). To date, 18 genes have been identified in the iGluR family in mammals through expression cloning (Dingledine *et al.*, 1999).

Excitatory synapses contain AMPA receptors and NMDA receptors. These two receptors are essentially important for neural communication, which is considered to be the basis of learning and memory formation.

2-2-3-1. AMPA receptors

AMPA receptors, which are non-NMDA type ionotropic glutamate receptors, are the primary synaptic receptors for fast excitatory transmission in the CNS and are commonly detected in many regions of the brain. The receptors were named after the synthetic agonist, α -amino-3-hydroxyl-5-methyl-4-isoxazole-propionate (AMPA), which elicits a relative AMPA-induced activation of members of the

glutamate receptor subfamily. The AMPA receptor subfamily comprises genes for four subunits. From these genes, four proteins containing about 900 amino acids with approximately 70% sequence homology are encoded and are designated as GluR1, GluR2, GluR3, and GluR4 (Song and Huganir, 2002; Shi *et al.*, 1999). These receptor subunits combine to form heterotetramers (Greger *et al.*, 2007; Mayer, 2005). In this class of receptor, posttranscriptional modifications are abundant, including alternative splicing of exons and selective nuclear editing of transcripts (Greger *et al.*, 2003; Seeburg PH, 1993). Although each modification of the four subunits separately regulates the receptor, modification of the GluR2 subunit, which is Q (Glutamine)/R (Arginine) editing, is more important for receptor function. In general, several cations, sodium (Na^+), potassium (K^+), and calcium (Ca^{2+}), diffuse through the channel pore of AMPA receptors lacking the GluR2 subunit upon their activation by glutamate. However, the presence of the GluR2 subunit in AMPA receptor heterotetramers results in the blockage of calcium permeability. This mechanism, which prevents extracellular calcium ion entry by the Q/R edited GluR2 subunit, is believed to protect the neuron from excitotoxicity (Kim *et al.*, 2001). On a molecular level, Q/R editing regulates the exit of GluR2 from the endoplasmic reticulum, thereby controlling AMPA receptor assembly at the step of tetramerization (Greger *et al.*, 2003). As a result of posttranscriptional modifications, diverse AMPA receptor variants exist in the neuron, and possess different functional properties under various conditions.

A single AMPA receptor has four agonist binding sites, one at each receptor subunit (Mayer, 2005), which is located at the extracellular loop between the third and fourth transmembrane domains (Armstrong *et al.*, 1998). AMPA receptor subunits consist of four transmembrane domains: three domains spanning the entire membrane and a kinked domain within the membrane. Therefore, the N-terminal region of each subunit locates extracellularly, whereas the C-terminal region is located intracellularly. Upon binding of the agonist, the pore is opened by intramolecular loop rearrangements and currents are increased (Platt, 2007; Rosenmund *et al.*, 1998). Once the pore is opened, the AMPA receptor is quickly desensitized, which stops the current flow and allowing it to return to its resting stage. The AMPA receptor has three stages: resting stage, active stage, and desensitization stage (Horning and Mayer, 2004). Through this gating mechanism, AMPA receptors open and close quickly, thereby mediating a fast excitatory synaptic transmission in the CNS (Platt *et al.*, 2007).

AMPA receptors can interact with several scaffolding proteins, which contain PDZ domains, via their C-terminal region. The PDZ domain (postsynaptic density protein (PSD95)/Drosophila disc large tumor suppressor (DlgA)/zonula occludens-1 protein (zo-1) domain) is a protein-protein interaction motif, which plays a role in receptor targeting and localization (O'Brien *et al.*, 1998; Kornau *et al.*, 1997; Sheng and Wyszynski, 1997; Ehlers *et al.*, 1996; Sheng, 1996; Sheng and Kim, 1996). These scaffolding proteins have been intensively studied with respect to their functions and interactions with the AMPA receptors. For example, synapse-associated protein 97 (SAP97) interacts with GluR1-containing AMPA receptors through a type I PDZ domain (Leonardo *et al.*, 1998), while glutamate receptor interacting protein (GRIP; GRIP1 and GRIP2), AMPA receptor binding protein (ABP), and protein interacting with C kinase 1 (PICK1) directly interact with GluR2-containing AMPA receptors through their type II PDZ domains (Chung *et al.*, 2003; Dong *et al.*, 1999; Xia *et al.*, 1999; Osten *et al.*, 1998; Srivastava *et al.*, 1998; Dong *et al.*, 1997). A well-studied example of physiological consequences of these interactions is GluR2 phosphorylation by PKC. GRIP proteins and PICK1 interact with GluR2 at the same site but this interaction is differentially regulated by PKC-dependent phosphorylation of GluR2 at serine 880. When GluR2 interacts with PICK1, GluR2-containing AMPA receptors are internalized by PKC-dependent phosphorylation (Chung *et al.*, 2000; Xia *et al.*, 2000; Matsuda *et al.*, 1999) and LTD is induced. In a similar fashion, phosphorylation regulates many functions such as localization, conductance, and open probability of AMPA receptors. Synaptic plasticity is believed to be strongly regulated by these modifications.

2-2-3-2. NMDA receptors

iGluRs, including AMPA and NMDA receptors, mediate most of the excitatory synaptic transmission in the CNS. In contrast to AMPA receptors, NMDA receptors are coincidence detectors, because their activation not only requires ligand binding of glutamate but also depends on the postsynaptic membrane potential. Upon glutamate binding, NMDA receptors are highly permeable to calcium ion influx in a voltage-dependent manner using slow gating kinetics, since the channel pore is blocked by a magnesium ion at resting membrane potential (Mcbain and Mayer, 1994). Therefore, the postsynaptic neuron first needs to be depolarized in order to release Mg^{2+} from the channel pore of NMDA receptors. This calcium ion influx through the NMDA receptors is thought to play a critical role for synaptic

plasticity, learning and memory. The NMDA receptors also allow entry of other cations such as sodium (Na^+), potassium (K^+) (Paoletti and Neyton, 2007; Cull-Candy *et al.*, 2001; Liu and Zhang, 2000; Dingledine *et al.*, 1999). AMPA and NMDA receptors, both of which are present at excitatory synapses, work in concert to depolarize neurons in the CNS. It is believed that AMPA receptors are activated first and by depolarizing the neuron then trigger NMDA receptor activation. In detail, glutamate activated AMPA receptors conduct the flow of cations into the neuron and the magnesium ions blocking the NMDA receptors are released by the increased amount of intracellular positively charged ions. Ca^{2+} can flow into the neuron after the Mg^{2+} ions are expelled from the NMDA receptor channel pore. Ca^{2+} can in turn act as a secondary messenger in various signaling pathways. These sequential mechanisms are believed to be the basis of excitatory synaptic transmission underlying the induction and persistence of LTP and LTD.

Unlike AMPA receptors, NMDA receptors were originally identified through selective activation from an agonist, *N*-methyl *D*-aspartate (NMDA). NMDA receptors, are considered unique, given that glutamate/NMDA are not sufficient agonists for activation of the NMDA receptors. Glycine, as a co-agonist, is essentially required for activation of the NMDA receptors (Danysz and Parsons, 1998). Binding of these two neurotransmitters, glutamate and glycine, is therefore needed for activation of the NMDA receptors.

The NMDA receptors are comprised from members of two major subunits, NR1 and NR2 (Nakanishi and Masu, 1994) although an additional subunit, NR3, has been cloned (Andersson *et al.*, 2001). The NMDA receptor mainly forms a heterotetramer between two NR1 and two NR2 subunits. A single NMDA receptor subunit has a structure similar to the other iGluRs subunits, which have four transmembrane domains and show an extracellular N-terminal region and an intracellular C-terminal region. Functional NMDA receptors contain an NR1 subunit that has a binding site for glycine (Hirai *et al.*, 1996). The NR1 gene has 22 exons, three of which undergo alternative splicing. These three exons are exon 5, located in the N-terminal region, and exons 21 and 22 located in the C-terminal region (called the N, C1, and C2 cassettes, respectively). The alternative splicing can generate eight variants of the NR1 subfamily (Zukin and Bennett, 1995). The alternative splicing variant forms are denoted as NMDAR1-1a, -2a, -3a, -4a, -1b, -2b, -3b, and -4b (Zukin and Bennett, 1995; Hollmann and Heinemann, 1994; Sugihara *et al.*, 1992). Certain properties of heteromeric NMDA receptors are

dependent on the specific NR1 splice variants (Seeburg, 1993). For example, NMDA receptors that contain an N-cassette-lacking NR1 subunit show a higher affinity for glutamate and lower affinity for competitive antagonists (Zukin and Bennett, 1995). On the other hand, the NR2 subfamily contains four individual subunits, NR2A, -2B, -2C, and -2D, all of which contain a binding site for glutamate (Laube *et al.*, 1997). A kinetics approach shows that NMDA receptors contain two glutamate and two glycine agonist-binding sites (Mayer and Armstrong, 2004; Laube *et al.*, 1997; Hirai *et al.*, 1996). Although the NR2 subunits do not form a functional channel by themselves, heteromeric channels together with NR1 exhibit greatly increased currents compared to NR1 homomeric channels. From the members of the NR2 subfamily, splicing variant forms have been detected only from NR2C and NR2D (Daggett *et al.*, 1998; Ishii *et al.*, 1993). The sequence homology of the amino acid composition of the NR2 subunits is about 50% while the sequence homology between NR1 and NR2 is less than 30% (Hollmann, 1999). From these various alternative splicings and combinations of the NR1 and NR2 subunits, a large number of different NMDA receptors are generated that respond to different biological and pharmacological environments (Sucher *et al.*, 1996) and appear to have many characteristically different properties. For example, NR2C- or NR2D-containing receptors have less sensitivity for Mg^{2+} or channel-blocking antagonists and exhibit a lower concentration of Ca^{2+} influx than other NMDA receptors containing NR2A or NR2B subunits (Monyer *et al.*, 1994). *In situ* hybridization shows that NR2A mRNA is ubiquitously expressed in the hippocampal area, whereas NR2B mRNA is predominately expressed in the forebrain. NR1 mRNA is expressed in both of these brain regions. NR2C mRNA is, however, mainly distributed in the cerebellum (Tolle *et al.*, 1993), showing that NMDA receptor subunits and subunits variants are expressed in a spatiotemporal manner.

2-3. Motor proteins and motor-cargo complexes

2-3-1. Intracellular cargo transport

A specific distribution of molecules within neurons is necessary for maintaining neuronal homeostasis and response to extracellular stimuli. Intracellular transport

refers not only to the movement of proteins from the endoplasmic reticulum (ER) to their designated targets such as the cell membrane through anterograde transport, but also to proteins that are internalized from the cell membrane for subsequent degradation or recycling. Like proteins, cellular organelles and even RNAs are actively transported to their specific locations. In neurons, transport of proteins, RNAs, and organelles to the dendrites is required for LTP. Therefore, transport in these cells is fundamental for their function.

In the past decades, hundreds of studies have suggested that many proteins are involved in intracellular transport either as cargos, adaptors (linker protein to connect between cargos and motor proteins), or motors, which power the movement of cargo along cytoskeletal tracks (Vale, 2003; Cheney and Baker, 1999; Karki and Holzbaur, 1999; Hirokawa, 1998). Three motor protein groups, kinesin, dynein, and myosin, exist in the cell. Kinesin and dynein mainly transport cargos in anterograde and retrograde directions along microtubules, respectively. In contrast, myosin transports cargo in both directions along actin filaments.

The direction of movement as well as other properties of motor proteins are controlled by interactions with trafficking factors (Maas *et al.*, 2009; Muresan and Muresan, 2005; Nakata and Hirokawa, 2003; Setou *et al.*, 2002; Verhey *et al.*, 2001). Figure 2-1 shows an example of motor proteins in their characteristic oligomerization state.

2-3-2. Anterograde motor proteins: Kinesin

Kinesin is an abundant and well-studied motor protein. It is present in most cell types and transports many cargos to different locations (Figure 2-2). In neurons, kinesin transport appears to be bidirectional. Cargo is moved from the cell body to the periphery, which is termed as anterograde transport, and from the periphery to the cell body, which is retrograde transport. Kinesin is mainly involved in anterograde transport.

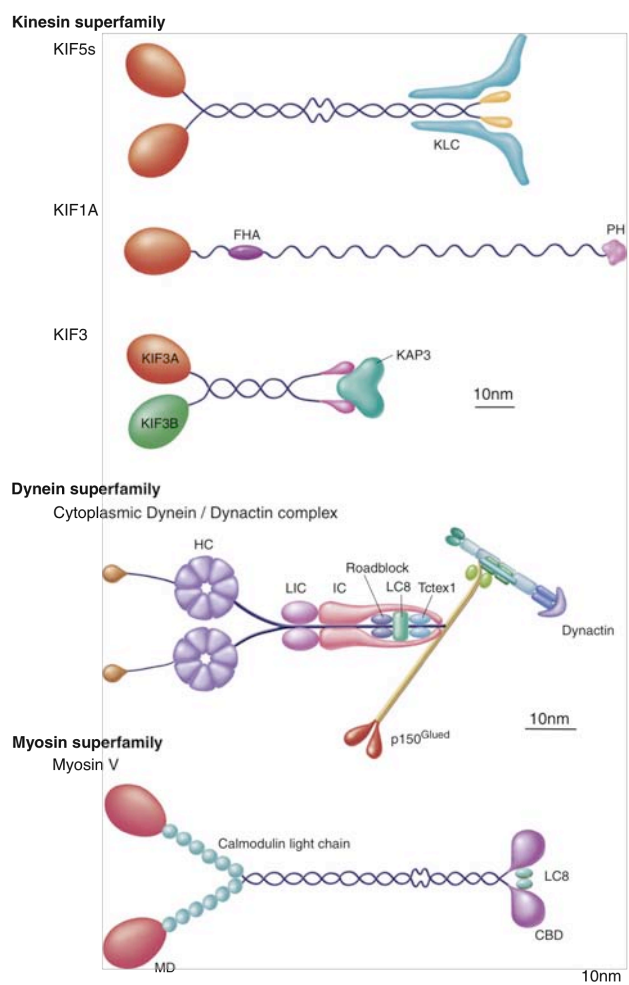


Figure 2-1. Structure of motor proteins

Kinesin superfamily proteins: KIF5, also known as kinesin 1, is homo- or heterodimerized and the dimerized form of KIF5 transports cargos with or without an association with kinesin light chain. KIF1A, also known as kinesin 3, is a monomeric motor. KIF3, also known as kinesin 2, is trimerized with KIF3A, KIF3B, and KAP3.

Dynein superfamily protein. Cytoplasmic dynein is a huge protein complex and is composed of heavy chains: light intermediate chains, intermediate chains, and light chains. This complex interacts with several dynactin components to transport different cargos.

Myosin superfamily protein: Myosin V is composed of two heavy chains and its neck domain binds to calmodulin light chains. Dynein light chain 8 binds at the tail region of the myosin V heavy chains.

CBP, calmodulin light chain; FHA, forkhead associated; HC, heavy chain; IC, intermediate chain; KAP3, kinesin-associated protein 3; KLC, kinesin light chain; LC, light chain; LIC, light intermediate chain; MD, motor domain; PH, pleckstrin homology.

(This figure is adapted from Hirokawa *et al.*, 2010)

In mammals, 45 kinesin genes have been identified (Lawrence *et al.*, 2004; Miki *et al.*, 2001; Noda *et al.*, 1995; Goldstein, 1993; Hirokawa, 1993; Aizawa *et al.*, 1992). The kinesin superfamily proteins (KIFs) are largely classified in three major groups, which are related to the location of their motor domain: N-terminal motor domain KIFs (N-KIFs), middle motor domain KIFs (M-KIFs), and C-terminal motor domain KIFs (C-KIFs). In certain cases, kinesins have a different direction of movement because of the location of their motor domain. For instance, N-KIFs and C-KIFs move in the anterograde and retrograde directions, respectively. M-KIFs, however, depolymerize microtubules in an ATP-dependent manner but are not directly involved in the transport of cargo. Despite this, most kinesins move in the anterograde direction. Kinesins are composed of a motor domain, a neck domain, a stalk domain, and a tail domain and most kinesins form homomeric or heteromeric dimers (Figure 2-1). However, the KIF1A (kinesin 3) motor functions as a monomer. Two conserved sequences, the ATP binding motif and the microtubule binding domain exist within the motor domain of kinesins. Kinesins transverse along microtubules by hydrolysis of ATP (Hirokawa and Noda, 2008; Kim and Endow, 2000; Vale and Fletterick, 1997).

Kinesins associate with different cargos through specific adaptor proteins (Figure 2-2). The association of the transport complexes is precisely regulated by when cargo has to be loaded, how cargo is loaded and unloaded, and by the final destination of the transport complex. All these mechanisms occur distinctly in the axon and dendrites.

Both fast transport, which involves membrane organelles, and slow transport, which involves cytoplasmic and cytoskeleton proteins, exist in the axon. Fast transportation is characterized by velocities of around 50 – 400 mm/day, whereas slow transportation constitutes slow velocities of less than 8 mm/day. Recent studies have observed that slow transport is not due to a slow velocity, but rather that the frequency of pauses is quite high (Roy *et al.*, 2007; Brown, 2003). Transport of cytoplasmic proteins by slow transport is more essential for maintaining neuronal homeostasis, although both types of transport, fast and slow, seem to be necessary. Many cargos in the axon are transported by the fast transport mechanism. For example, synaptic vesicle precursors are transported by KIF1A and KIF1B β (Wagner *et al.*, 2009; Niwa *et al.*, 2008; Zhao *et al.*, 2001; Okada *et al.*, 1995), plasma membrane precursor by KIF3 (Takeda *et al.*, 2000), phosphatidylinositol 3,4,5-triphosphate (PIP₃) vesicles by KIF13B (Horiguchi *et al.*,

2006). KIF5 has been implicated in the transport of many cargos such as presynaptic membrane, active zone vesicles, mitochondria, amyloid precursor protein (APP)-containing vesicles, APOER2 vesicles, and TrkB vesicles (Arimura *et al.*, 2009; Cai *et al.*, 2005; Guo *et al.*, 2005; Muresan and Muresan, 2005; Su *et al.*, 2004; Kamel *et al.*, 2001; Verhey *et al.*, 2001; Bowman *et al.*, 2000). It has been suggested that KIF5 is involved in both fast and slow axonal transport (Roy *et al.*, 2008; Xia *et al.*, 2003; Terada *et al.*, 2000). Hsc70, a protein linking cytoplasmic proteins to motor proteins, acts as an adaptor and is transported to the axon by KIF5 through an association with kinesin light chain (KLC) (Terada *et al.*, 2010). Mice overexpressing a dominant-negative form of Hsc70 showed significantly delayed slow transport, while the levels of fast transport increased, indicating that Hsc70 is a factor that promotes slow axonal transport. In dendrites, it has been observed that a variety of cargos, which are mainly receptor proteins, mRNA complexes, and some cellular organelles, are also transported by KIFs. In dendritic spines, different receptors need to be translocated into this compartment in order to fulfill their physiological function important for synaptic activity. For instance, KIF5 is the main motor protein implicated in the transport of AMPA receptors. In dendrites, KIF5 associates with GluR2-containing AMPA receptors through the adaptor protein glutamate receptor interacting protein 1 (GRIP1) (Setou *et al.*, 2002; Figure 2-2). Other receptors, such as NR2B-containing NMDA receptors are transported to the dendritic spines by KIF17 through a Mint 1 scaffolding complex acting as an adaptor (Jeyifous *et al.*, 2009; Guillaud *et al.*, 2008; Setou *et al.*, 2000; Figure 2-2). In this respect, Guillaud *et al.* suggested a cargo unloading mechanism whereby NR2B-containing NMDA receptors are released from KIF17, when Ca^{2+} concentrations increase near the postsynaptic site leading to subsequent phosphorylation of KIF17 which then releases the cargo (Guillaud *et al.*, 2008).

At inhibitory synapses, GABA and glycine receptors are transported by KIF5 through huntingtin-associated protein 1 (HAP1) and gephyrin, respectively (Twelvetrees *et al.*, 2010; Maas *et al.*, 2009). In addition, *Arc* and *CaMKIIa* mRNAs are transported to postsynaptic regions by KIF5. Local protein synthesis in response to synaptic activity is believed to be necessary to induce long-lasting LTP. *Arc* and *CaMKIIa* mRNA associate with a large mRNP complex made up of several components. This mRNP complex interacts with KIF5 for transport to dendritic synapses (Kanai *et al.*, 2004). Like all kinesin transport mechanisms, the

anterograde transport by KIFs is important for cellular activities, responses, and survival.

In terms of cargo transport, KIF5-mediated transport seems to occur more frequently than transport through other KIFs, although all members of the KIF superfamily are involved in transport of many different types of cargo. KIF5 comprises three subfamilies: KIF5A, KIF5B, and KIF5C. It has been shown that the expression profile of these subfamilies differs (Miki *et al.*, 2001). KIF5A and KIF5C are mainly expressed in neurons, whereas KIF5B is ubiquitously expressed. However, they all function similarly as motor proteins. There are three genetic defect studies for the KIF5 genes. Xia *et al.* investigated KIF5A using *Kif5a* knockout mice and identified a loss of large caliber axons and an accumulation of neurofilaments in neuronal cell bodies of these mice (Xia *et al.*, 2003). Kanai *et al.* studied KIF5C using *Kif5c* knockout mice and found that the knockout mice had smaller brain sizes and a higher loss of motor neurons than control mice (Kanai *et al.*, 2000). Tanaka *et al.* deleted KIF5B using *Kif5b* knockout mice and observed that the knockout mice are embryonic lethal. Studies on embryonic tissue revealed a perinuclear clustering of lysosomes and mitochondria (Tanaka *et al.*, 1998). Concerning KIF5A and KIF5C knockout mice, it is postulated that their viability stems from compensation by other genes. KIF5B knockout mice are embryonic lethal although KIF5A and KIF5C could act as compensators. However, differences in gene distribution and expression might explain the lethality. For instance, KIF5B is also expressed and functions in non-neuronal cells. All KIF5s form homodimers or heterodimers and certain types of KIF5 associate with kinesin light chain (KLC), which interacts with the tail region of KIF5. This association has been shown to be essential for the transport of specific cargos (Hirokawa *et al.*, 1989; Brady, 1985; Vale *et al.*, 1985).

2-3-3. Retrograde motor proteins: Dynein

Dynein is mainly involved in retrograde transport processes, from the periphery of the cell toward the cell body. For cargo transport, dynein moves along microtubules by hydrolyzing ATP as an energy source. Dynein is largely divided into two major groups: cytoplasmic dyneins, which are a general form of dynein for intracellular transport, and axonemal dyneins, which are ciliary or flagellar dyneins. Cytoplasmic dynein is comprised of a mega protein complex, which is

approximately 1.5 megadaltons and contains two heavy chains, two intermediate chains, four intermediate light chains, and additional light chains (Pfister *et al.*, 2005; Karki and Holzbaaur, 1999). Additionally, cytoplasmic dynein has several accessory proteins: p24, p27, p62, p150^{Glued}, actin-related protein 1 (Arp1), CAPZ α , CAPZ β , and dynamitin. These accessory proteins are part of a large complex called dynactin, which importantly controls dynein activity and regulates cargo binding to the dynein motor (Schroer, 2004). There are only two members of the cytoplasmic dynein heavy chains, which are cytoplasmic dynein heavy chain 1 (Dync1h1) and cytoplasmic dynein heavy chain 2 (Dync2h1) (Pfister *et al.*, 2006; Tanaka *et al.*, 1995). Furthermore, only Dync1h1 is mainly involved in retrograde intracellular transport in neural axons and dendrites (May *et al.*, 2005). Therefore, in contrast to kinesin, the specificity of cargo binding to the motor is thought to be achieved by a higher number of adaptor proteins.

However, it has been observed that dynein can recognize specific cargos for transport to different regions. For example, dynein intermediate chain 1 (DIC1) interacts with vesicles, which contain TrkB (Ha *et al.*, 2008), and dynein light chain 1 and 2 (DLC1 and 2) directly interact with the bassoon protein (Fejtova *et al.*, 2009). Dynein also recognizes specific cargos containing gephyrin, which is a scaffolding protein. Gephyrin can interact with DLC1 and DLC2 (Fuhrmann *et al.*, 2002) and acts as an adaptor protein for glycine receptors (Maas *et al.*, 2006). Using several binding interfaces, cytoplasmic dynein transports cargos, such as myosin V (Huang *et al.*, 1999), TrkB-containing vesicles (Ha *et al.*, 2008), mitochondria (Hollenbeck and Saxena, 2005), brain-derived neurotropic factor (BDNF) vesicles (Colin *et al.*, 2008; Gauthier *et al.*, 2004), the piccolo/bassoon complex (Fejtova *et al.*, 2009), and others from the axon toward the cell body. On the other hand, glycine receptor vesicles (Maas *et al.*, 2006; Fuhrmann *et al.*, 2002), mRNA complexes (di Penta *et al.*, 2009), Rab5 and Rab7 containing endosomes (Sato *et al.*, 2008; Johansson *et al.*, 2007), and cargo designated for import into the nucleus (Perry and Fainzilber, 2009) are transported to the cell body in the case of dendrites.

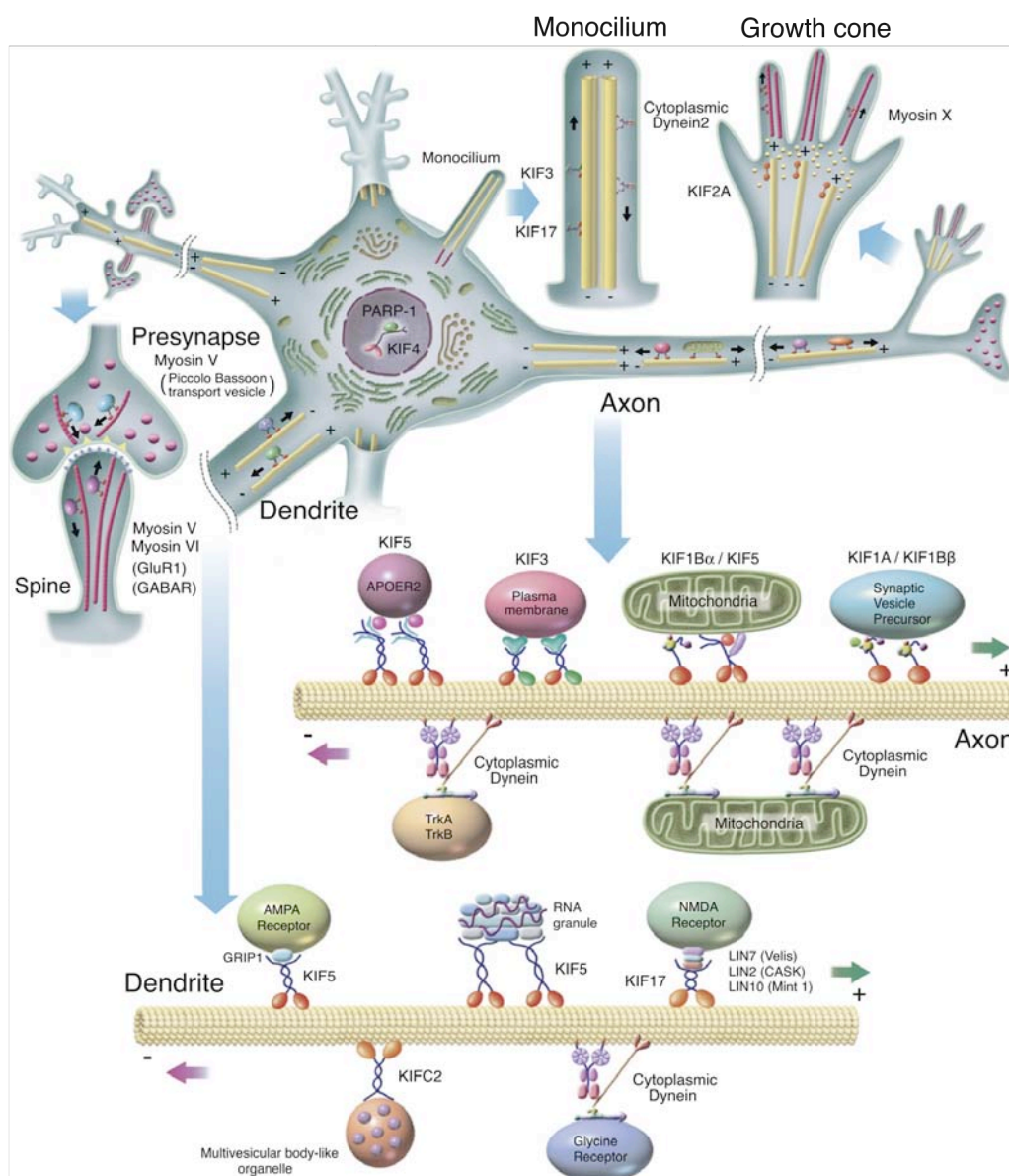


Figure 2-2. Intracellular transport in neurons

Three motor protein superfamilies transport many cargos at different regions in neurons. In the axon and dendrites, KIFs transport a variety of cargos, including cellular organelles, in the anterograde direction along microtubules, whereas cytoplasmic dynein transfers cargos in the opposite direction, retrogradely.

(This figure is adapted from Hirokawa *et al.*, 2010)

2-3-4. Cytoskeletal tracks

The cytoskeleton provides cellular structure and shape as an intracellular multi-protein skeleton and is involved in cellular division. There are three types of

cytoskeletal filaments: actin filaments, intermediate filaments, and microtubules (Doherty and McMahon, 2008; Minton, 1992).

Actin filaments, also known as microfilaments, are the thinnest filaments of the three types. They undergo constant polymerization at one end and depolarization on the other, a mechanism also referred to as treadmilling. In neurons, actin filaments are mainly localized below the plasmamembrane, especially in dendritic spines and filopodia where they are used as tracks for motor proteins by the myosin superfamily (Thompson and Langford, 2002).

In contrast, intermediate filaments are more stable filaments about 10 nm thick, which is between the thickness of actin filaments and microtubules (Fuchs and Cleveland, 1998). Intermediate filaments mainly play a role in the formation and persistence of cell-cell and cell-matrix junctions. Several types of intermediate filaments exist, which are generated from vimentins, keratin, neurofilaments, and lamin. Each type of intermediate filament is found in different areas of the cell and has been implicated in different cytoskeletal based processes.

Microtubules are comprised of alpha (α)- and beta (β) tubulins. GTP-dependent polymerization of these two tubulins generates hollowed-cylindrical microtubules, which are the thickest filaments (about 25 nm in diameter). Microtubules originate from the microtubule organizing center (MTOC), located at perinuclear regions. They are used as a cytoskeletal track by kinesin and dynein motor proteins.

Actin filaments and microtubules are highly organized within cells and together with the motor proteins kinesin, dynein, and myosin provide a framework for the redistribution and organization of cellular components.

2-3-4-1. Microtubules

Microtubules are highly dynamic and unstable assemblies of tubulin monomers. This means that assembly and disassembly of microtubules occurs simultaneously, although one end, in contrast to actin filaments, is more or less stable. α - and β -tubulin polymerize in a GTP-dependent fashion at the (+) end of microtubulins. This microtubule end, which is characterized by a dynamic turnover of tubulin monomers, becomes unstable in the absence of further polymerization of additional monomers or due to other reasons, resulting in depolymerization of microtubules, also referred to as microtubule catastrophe. In contrast, the (-) end of microtubules, is characterized by a stable anchorage at the MTOC, involving a third class of tubulin monomers, γ -tubulin. In neurons, the (+) end mainly points

into the distal axon and dendrites, whereas the polarities are mixed at the soma (Conde and Caceres, 2009; Dombek *et al.*, 2003; Stepanova *et al.*, 2003; Baas *et al.*, 1989; Baas *et al.*, 1988). Polymerization of microtubules utilizes GTP as an energy source. In general, GTP binding to α - and β tubulins allows these monomers to polymerize. GTP-bound β tubulin is hydrolyzed to GDP-bound β tubulin after assembly while GTP-bound α tubulin is more stable. The assembly kinetics of GDP-bound tubulin differ from those of GTP-bound tubulin, since the GDP-bound β tubulin is easily removed from the microtubule assembly. During polymerization, each GTP-bound α - and β tubulin dimer is consecutively added to the microtubule. Shortly thereafter, β tubulin is hydrolyzed to the GDP-bound form followed by hydrolyzation of GTP-bound α -tubulin, thereby explaining the rapid turnover of tubulin monomers at the microtubulin (+) end. Therefore, growing microtubules are not depolymerized because of a protection mechanism where the (+) end of the filament is capped by the GTP-bound stable α tubulin (Karp, 2005). When sufficient monomers are not added to the (+) end of microtubules, they are rapidly depolymerized. Through polymerization and depolymerization, microtubules are dynamically controlled, growing and shrinking at their (+) end region is characteristic for those cytoskeletal elements (Mitchison and Kirschner, 1984).

Taken together, microtubules are involved in many cellular processes, which include: mitosis, cytokinesis, cell remodeling, and cargo trafficking. In the latter case, microtubules serve as tracks for intracellular cargo trafficking involving kinesin and dynein motor proteins, which mainly transport cargos along microtubules.

2-3-4-2. Post-translational modifications: polyglutamylation

Microtubules carry out many essential functions in cells. However, many questions have been raised about the diversity of microtubule functions and how individual microtubules can carry out several different events (Luduena, 1998). In the past decades, a number of studies have discovered that post-translational modifications (PTMs) are one possible answer for the functional diversity of tubulin (MacRae, 1997). Several reversible forms of PTMs on microtubules have been found, such as acetylation, tyrosination, detyrosination, $\Delta 2$ tubulin modification, phosphorylation, palmitoylation, glycylation, and glutamylation (Janke and Kneussel, 2010; Hammond *et al.*, 2008; Verhey and Gaertig, 2007; Westermann

and Weber, 2003). Through these tubulin modifications, microtubules are given specific functions with respect to cell division, mitosis, motility, shape, intracellular structure, and intracellular trafficking. The majority of PTMs events occur on the C-terminal domain of α - and β tubulins, which is generally located on the outside of polymerized microtubules (Nogales *et al.*, 1999).

Glutamylation is the attachment of a glutamate residue onto the C-terminal tail of α - and β tubulins (Verhey and Gaertig, 2007; Westermann and Weber, 2003; Mary *et al.*, 1994; Redeker *et al.*, 1994; Rudiger *et al.*, 1992; Alexander *et al.*, 1991), originally identified in the mammalian brain by mass spectrometry (Ebbe *et al.*, 1990). These glutamate residues are attached and detached by two classes of enzymes, glutamylases and deglutamylases, respectively (Janke *et al.*, 2005; Audebert *et al.*, 1993). Additionally, glutamylase enzymes are a member of the tubulin tyrosine ligase-like (TTL) protein family (Rogowski *et al.*, 2009; Wloga *et al.*, 2009; Janke *et al.*, 2005). In case of glutamylation, a large number of glutamate side chains, called polyglutamylation, are generally detected along different areas of microtubules (Bobinnec *et al.*, 1998; Fouquet *et al.*, 1994). Neuronal polyglutamylation preferentially occurs on microtubules found in centrioles, axonemes, and the mitotic spindle. However, the occurrence of polyglutamylation is not limited to microtubules. For the nucleosomal assembly proteins, NAP1 and NAP2, this modification has been implicated in the regulation of chromatin structure (Rengnard *et al.*, 2000). Recently, several studies have suggested that intracellular transport by kinesin motor proteins is also regulated by polyglutamylation. A reduction of α tubulin polyglutamylation in TTL1 mutant mice altered the distribution of KIF1A (kinesin 3) but not KIF3a (kinesin 2) and KIF5 (kinesin 1). In addition, the mutant mouse showed a decreased number of synaptic vesicles in the axonal terminal (Ikegami *et al.*, 2007). Moreover, a related study has recently suggested that polyglutamylation regulates transport of cargo complexes in a specific manner. Increasing the polyglutamylation of tubulins by induction of neuronal activity interfered with a transport complex, containing a glycine receptor (GlyR), gephyrin (a cargo adaptor protein), and KIF5 (kinesin 1) (Maas *et al.*, 2009). Interestingly, the same study shows that the movement of different transport complexes, including the GluR2-containing AMPA receptor, GRIP1 (an adaptor protein), and KIF5 (kinesin 1), is not affected by polyglutamylated microtubules, although they use the same motor proteins as the

complexes that are affected. Therefore, polyglutamylation seems to control transport of specific motor-cargo complexes, dependent on neuronal activity.

2-3-5. Cargo adaptors: Gephyrin and GRIP1

2-3-5-1. Gephyrin

Gephyrin, which is closely associated with glycine or GABA receptors, is a component of the postsynaptic protein network for inhibitory synapses but is also known to function as co-factor for molybdenum (Moco) biosynthesis (Feng *et al.*, 1998). Molybdenum-dependent enzymes are required for the reduction of nitrate and the oxidation of sulfite to sulfate. These two processes are crucial for survival of autotrophic and heterotrophic organisms. However, gephyrin was first discovered as a GlyR-associated protein (Pfeiffer *et al.*, 1982). Gephyrin consists of three major domains: the G domain, the C domain, and the E domain. Multiple isoforms of gephyrin are generated by alternative RNA splicing. Three gephyrins can trimerize through their G domain, which is located at N-terminal region. Subsequently, two different trimers can dimerize through the E domain, which is located at the C-terminal region of gephyrin. The G and E domains are linked by a central domain, which is known as the C domain. Multimerized gephyrins function as scaffolding proteins at the postsynaptic protein network of inhibitory synapses. In particular, the dimerized E domain binds to the GlyR intracellular loop, which is located between the transmembrane domains 3 and 4 of the GlyR β subunit (Kim *et al.*, 2006; Sola *et al.*, 2004; Meyer *et al.*, 1995). The C domain includes binding sites for several gephyrin-interacting proteins, such as Pin1, dynein light chain 1 and 2 (DLC1 and 2), and collybistin (Fuhrmann *et al.*, 2002; Betz *et al.*, 2000). Several studies have identified that gephyrin is an essential component of intracellular transport complexes. Specifically, β subunit-containing glycine receptors bind to a gephyrin-dynein complex that retrogradely moves along microtubules (Maas *et al.*, 2006). Another recent study has shown that gephyrin also serves as an adaptor for the kinesin motor protein, which moves in the anterograde direction (Maas *et al.*, 2009). This β subunit-containing GlyR-gephyrin-KIF5 complex moves in anterograde directions along microtubules (Maas *et al.*, 2009). Therefore, gephyrin seems to function as an adaptor protein for both anterograde and retrograde transport complexes. Additionally, Maas *et al.* suggest

that gephyrin might act a trafficking factor that detects modifications of microtubules in response to neuronal activity. Therefore, Maas *et al.* speculated that synaptic transmission is in crosstalk with intracellular protein turnover, regulating the transport along microtubules modified by neuronal activity (Maas *et al.*, 2009).

2-3-5-2. GRIP1

Glutamate receptor-interacting protein 1 (GRIP1) is a major component required for synaptic localization and the clustering of ion channels and receptors in dendritic spines of excitatory synapses. GRIP1 has seven PDZ domains, most of which have been suggested to play a role in receptor targeting or localization. These PDZ domains specifically bind to the C-terminal end of a variety of membrane proteins (O'Brien *et al.*, 1998; Kornau *et al.*, 1997; Sheng and Wyszynski, 1997; Ehlers *et al.*, 1996; Sheng, 1996; Sheng and Kim, 1996). It was first identified that GRIP1 specifically interacts with the C-terminus of the GluR2 and GluR3-AMPA receptor subunits, via the PDZ4, PDZ5, and to the additional 30 amino acids on the N-terminal side of PDZ4 (Dong *et al.*, 1997). It was later shown that GRIP2 performs the same function (Dong *et al.*, 1999). Three members of the GRIP family have been identified and consist of, GRIP1, GRIP2, and AMPA receptor binding protein (ABP), although in some cases GRIP2 is also termed as ABP (Dong *et al.*, 1999; Osten *et al.*, 1998; Srivastava *et al.*, 1998; Dong *et al.*, 1997). The GRIP family has a high sequence homology. GRIP2 and ABP have perfectly matched sequences across PDZ1 to PDZ6, although GRIP2 has an additional PDZ domain, PDZ7 (Dong *et al.*, 1999). In addition, the PDZ6 domain of GRIP1 can interact with the C-terminal of the ephrin-B1 ligand, EphB2/EphA7 receptor tyrosine kinases (Bruckner *et al.*, 1999; Lin *et al.*, 1999; Torres *et al.*, 1998), and with the C-terminal of the liprin- α family of multidomain proteins (Wyszynski *et al.*, 2002). Concerning its PDZ domains, the PDZ456 domains of GRIP1 allow it to form homo- and heterodimers (Dong *et al.*, 1999).

A different study demonstrated that GRIP1 could directly interact with KIF5 through a region located between the PDZ6 and PDZ7 domains of GRIP1 (Setou *et al.*, 2002). Taken together, GRIP1 is a well-defined adaptor protein in its regulation of KIF5-dependent targeting of GluR2-containing AMPA receptors into neuronal dendrites.

2-4. Cell adhesion molecules

Cell adhesion molecules (CAMs) are located at the cellular surface being involved in binding to other cells or to function within the extracellular matrix (ECM). Through this adhesion, CAMs control fundamental processes such as cellular differentiation, propagation of both intracellular and extracellular signals, and cellular responses (Cavallaro and Dejana, 2011). In other words, CAMs maintain tissue integrity and detect the surrounding microenvironment in order for the cells to respond.

Mostly, the CAMs are transmembrane receptors and they have been shown to interact with each other to form homodimers or heterodimers. Each CAM is divided into three domains: an intracellular domain, which interacts with cytoplasmic proteins or cytoskeletal proteins, a transmembrane domain, and an extracellular domain, which interacts either with other CAMs or with extracellular elements. CAMs are defined according to their types for adhesion: adherent junction forming CAMs such as cadherins, tight junction forming CAMs such as claudin, and intercellular boundary forming CAMs such as immunoglobulin-like CAMs (Ig-CAMs) (Dejana *et al.*, 2009; Takai *et al.*, 2008a; Takai *et al.*, 2008b; Vestweber, 2008; Wallez and Huber, 2008; Bazzoni and Dejana, 2004).

The CAM family contains four main members: Ig-CAMs, integrins, cadherins, and selectins. These members are functionally separated between calcium-dependent CAMs, which are cadherins and selectins, and calcium-independent CAMs, which are Ig-CAMs and integrins (Brackenbury *et al.*, 1981).

2-4-1. N-Cadherin

Cadherins are calcium-dependent cell adhesion molecules, which belong to the type-1 class of transmembrane proteins. Cadherins are important in regulating and maintaining cellular processes and in establishing tissue polarity (Makrigiannakis *et al.*, 1999; Ong *et al.*, 1998). The cadherin superfamily consists of classical cadherins, protocadherins, desmosomal cadherins, and cadherin-like proteins. The classical cadherins are in turn categorized according to the regions where they are mainly expressed. For example, R-, E-, and N-Cadherin are expressed at retinal tissue, epithelial tissue, and neural tissue, respectively (Gumbiner, 2005).

Thus, N-Cadherin is mainly expressed in neural tissue and generally comprises

three domains: an intracellular domain, a transmembrane domain, and an extracellular domain. The C-terminal intracellular domain binds to cytoskeletal actin filaments through α - and β -catenin (Yamada *et al.*, 2005). The N-terminal extracellular domain has 5 ectodomains, which can bind either other cadherins or calcium ions. Two types of N-Cadherin dimerization exist, *cis*- and *trans*-dimerization, which are lateral and opposed association, respectively. The *cis*-dimerization is much stronger than the *trans*-dimerization because a higher number of N-Cadherins is involved in the clustering (Shapiro *et al.*, 1995). N-Cadherin expression at the excitatory and inhibitory synapses regulates diverse neural processes through its structure and dimerization.

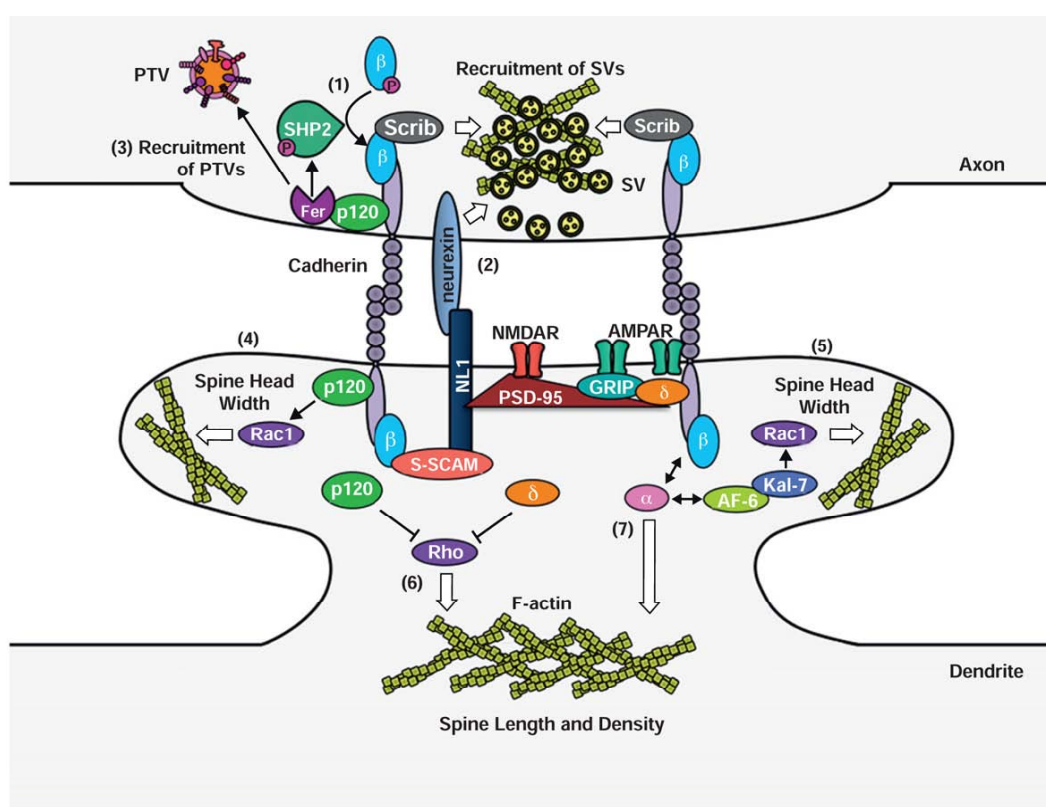


Figure 2-3. Schematic depiction of the N-Cadherin complex at excitatory synapses

The N-Cadherin, calcium-dependent cell adhesion molecules, complex together with α - and β -catenin and p120-catenin mediates many synaptic activities through regulation of different components in pre- and postsynaptic synapses. α , α -catenin; β , β -catenin; δ , δ -catenin; p120, p120-catenin; PTV, Piccolo-Bassoon transport vesicle; SV, synaptic vesicle. Black bidirectional arrows denote dynamic interaction; black arrows denote interaction or activation; white arrows denote outcomes at synapses.

(This figure is adapted from Brigidi and Bamji, 2011)

Figure 2-3 illustrates several functions of N-Cadherin at the excitatory synapse (represented by numbers in Figure 2-3). Synaptic vesicles in the presynapse and several molecules in the postsynapse are recruited by functions of N-Cadherin. Neural processes are functionally regulated by these mechanisms. In detail, p120-catenin recruits dephosphorylated β -catenin (1) to N-Cadherin by regulating the tyrosine kinase Fer (3) and recruits Piccolo-Bassoon transport vesicles (PTVs) and tyrosine phosphatase SHP-2 to the synapse. Postsynaptic N-Cadherin and catenin complexes recruit synaptic scaffolding molecule (S-SCAM) to neuroligin-1 (NL1). NL1 then dimerizes with neurexin (2). With functions of (1), (2), and (3), synaptic vesicles are recruited to the active zone in the presynapse (Aiga *et al.*, 2010; Stan *et al.*, 2010; Sun *et al.*, 2009; Lee *et al.*, 2008). Activation of the Rac1 GTPase, by either p120-catenin (4) or α -catenin (5) enhances spine head width, while inhibition of RhoA GTPase (6) by the release of p120-catenin and δ -catenin or by the interaction of α -catenin (7) with actin filaments increases spine length and density (Kim *et al.*, 2008; Xie *et al.*, 2008; Elia *et al.*, 2006; Abe *et al.*, 2004). Overall, N-Cadherin as a cell adhesion molecule plays a critical role for communications between pre- and postsynapse and these communications are essential for synaptic function.

2-4-2. N-Cadherin and GRIP1

Over the past decades, it has been suggested that N-Cadherin and its interaction partners are important to maintain and regulate neuronal functions. Recently, several studies have provided more evidence showing that N-Cadherin indirectly interacts with GRIP1 through δ -catenin and that this interaction regulates AMPA receptor function to increase synaptic activity (Arikkath *et al.*, 2009; Ochiishi *et al.*, 2008; Silverman *et al.*, 2007). For instance, Silverman *et al.* demonstrated that δ -catenin interacts with GRIP1 through its PDZ2 domain and that this complex forms strong interactions with postsynaptic multimers. This is because δ -catenin also binds to PSD-95, which has been identified as a linker for the NMDA receptor (Silverman *et al.*, 2007). In addition, δ -catenin was reported to regulate surface expression of GluR2-containing AMPA receptors through this complex (Ochiishi *et al.*, 2008). Neurons devoid of δ -catenin following genetic ablation or acute knockdown of *δ -catenin*, show abnormal spine formation and function in neural circuitry during development (Arikkath *et al.*, 2009).

However, a different study has reported that N-Cadherin directly interacts with GRIP1 through its PDZ2 domain (Schurek, 2006; Figure 2-4). This direct interaction between N-Cadherin and GRIP1 might point to a novel transport complex processed by KIF5, given that only a few studies have investigated N-Cadherin's transport by motor proteins (Teng *et al.*, 2005; Yanagisawa *et al.*, 2004; Chen *et al.*, 2003; Mary *et al.*, 2002).

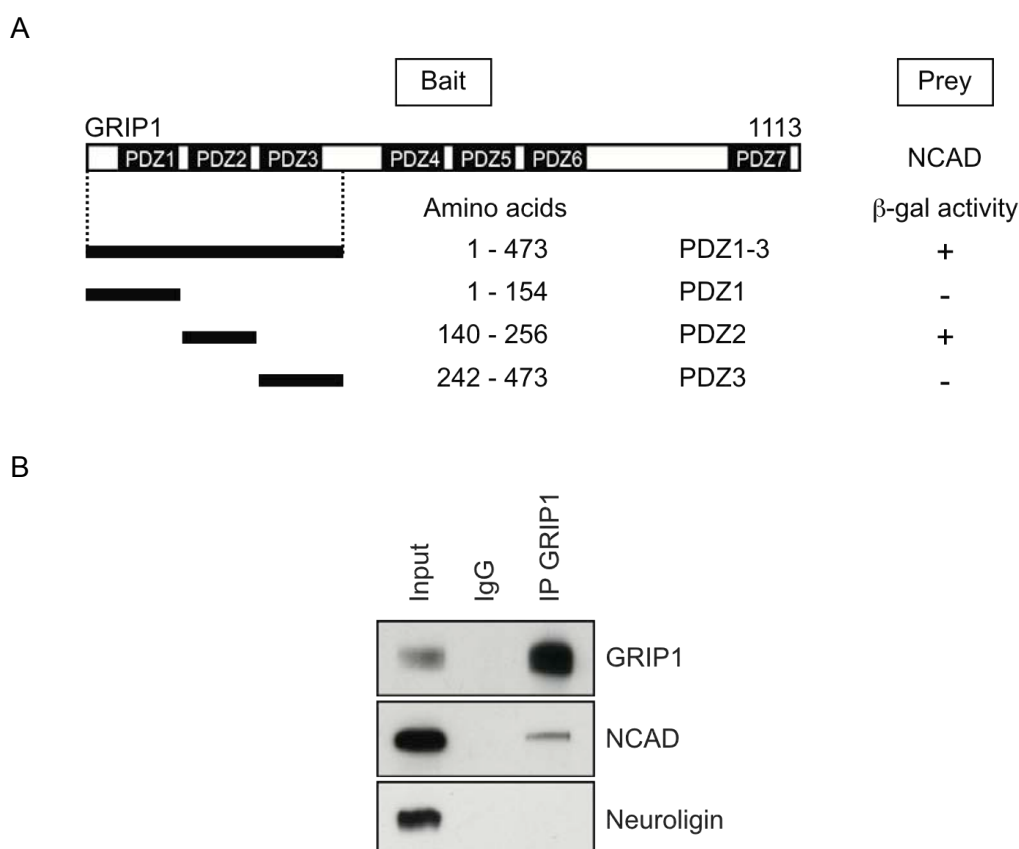


Figure 2-4. Interaction of GRIP1 and N-Cadherin

(A) Through yeast two-hybrid screening, N-Cadherin was found to directly interact with the bait protein, GRIP1. The PDZ2 domain of GRIP1 was further mapped to interacts with N-Cadherin. To screen the interaction, truncated N-Cadherin (102-907 amino acids) was generated with pJG4-5 vector. Interaction between GRIP1 and N-Cadherin is indicated with (+). (B) The interaction by yeast-hybrid assay was confirmed by co-immunoprecipitation experiment using vesicle-enriched P3 fraction of mouse whole brain lysate. Rabbit IgG and Neuroigin were used as a negative control.

(This figure is modified from Schurek, 2006)

3. Aim of the study

The precise intracellular composition of molecules and organelles is essential for maintaining, processing, and responding to information between extracellular and intracellular compartments. Particularly in neurons, thousands of different units of information are interpreted under different conditions at locations, such as excitatory and inhibitory synapses. For each process, every single molecule that is involved must be located at a certain subcellular position. Three different motor protein superfamilies, kinesin, dynein, and myosin, participate in these active transport mechanisms.

This study focuses mainly on a kinesin motor protein, which anterogradely transports cargos. My goal was to better understand specific functions of KIF5 under varying conditions of neuronal activity and in complex with different cargos and adaptors.

In the first study, I aimed to investigate how a transport complex, GlyR-gephyrin-KIF5, can migrate toward an activated synaptic condition. Gephyrin is known as a scaffolding protein that interacts with the GlyR β subunit at inhibitory synapses but it also interacts with the KIF5 motor protein as an adaptor protein (Maas *et al.*, 2009). Moreover, microtubules, which act as the track for the motor protein KIF5, are highly modified by neuronal activity. KIF5 mobility may be altered through modifications like polyglutamylation of the respective microtubule tracks. To examine the contribution of the proposed mechanisms, neuronal activity was increased by application of strychnine. Subsequently the polyglutamylation of tubulin was monitored through detection with two polyglutamylation specific antibodies, B3 and GT335. Furthermore, I aimed to investigate the effect on the movement of the respective cargo after knocking-down gene expression of polyglutamylase by Lentivirus-carrying shRNA-PGs1. Through this study, I expected to determine the existence of a crosstalk between neuronal activity and modification of cytoskeletal tracks.

In the second study, I aimed to investigate whether an already described transport complex consisting of GluR2, GRIP1, and KIF5 is also linked to intracellular transport of cell adhesion molecules. A previous study has shown that the motor protein KIF5 transports GluR2-containing AMPA receptors via GRIP1 as an

adaptor protein (Setou *et al.*, 2002). However, GRIP1 was also identified as a direct interaction partner of N-Cadherin by another study (Schurek, 2006). To determine whether a GRIP1-N-Cadherin association also binds to KIF5, I first intended to perform co-immunoprecipitation and co-localization experiments. Further, given that I found the intracellular distribution of N-Cadherin to be dependent on KIF5 motor protein activity, similar as it was observed for GluR2, I examined whether N-Cadherin and GluR2 functionally undergo co-transport within the same vesicle. To address this question, I planned to carry out time-lapse microscopy of living neurons. Given that co-transport of N-Cadherin and GluR2 fusion particles could be observed in the neurites, I next intended to confirm this result by electron microscopy. By using a biotinylation approach to detect cell surface proteins, I aimed to detect changes in plasmamembrane targeting of N-Cadherin and GluR2 by specifically interfering with components of the transport complex.

A novel transport complex consisting of N-Cadherin, GluR2, GRIP1, and KIF5, for instance, would allow efficient delivery of synaptic molecules, N-Cadherin and GluR2-containing AMPA receptor, to dendrites.

4. Materials and Methods

4-1. Materials

4-1-1. Chemicals and enzymes

All chemicals for this study were purchased from SIGMA-Aldrich (Steinheim, Germany), Carl-Roth GmbH & Co. KG (Karlsruhe, Germany), Roche (Mannheim, Germany), AppliChem (Darmstadt, Germany), Invitrogen (Carlsbad, USA), and VWR (Darmstadt, Germany).

Restriction enzymes and their specific buffers were purchased from Roche (Mannheim, Germany), Fermentas (St. Leon-Rot, Germany), and New England Biolabs (Hertfordshire, UK). The T4-DNA-Ligase and *Taq*. DNA polymerase were purchased from Invitrogen (Carlsbad, USA).

Finally, the *Pfu Turbo* DNA polymerase and *Phusion* DNA polymerase were purchased from Stratagene (La Jolla, California, USA) and New England Biolabs (Hertfordshire, UK), respectively.

4-1-2. Instrumentations

- PCR cycler: T-1 Thermocycler (Biometra, Göttingen, Germany)
- Gel Electrophoresis for agarose gel: B2, B1A (Owl Separation Systems, Portsmouth, USA)
- Photometer: Ultraspec 3000 (GE Healthcare, Buckinghamshire, UK)
- NanoDrop: ND-1000 (PeqLab, Erlangen, Germany)
- UV-Illuminator: UVT2035 (Herolab, Wiesloch, Germany)
- Gel electrophoresis for PAGE: Mini-PROTEAN 3 Cell (Biorad, Munich, Germany)
- Western Blot apparatus: Mini Trans-Blot Cell (Biorad, Munich, Germany)
- Homogenizator: *Potter S* (B. Braun Melsungen AG, Melsungen, Germany)
- Centrifuge: TL-100 Ultracentrifuge, L7 Ultracentrifuge, and J2-21 M/E (Beckman, Fullerton, USA) and Eppendorf Centrifuge 5417C (Eppendorf, Hamburg, Germany)
- Rotors: TLA 100.3, JA-10, JA-14, JA-20, SW-40Ti (Fullerton, USA)

- Cell culture bench: SterilGARD Class II TypA/B3 from Baker Company (Beckman, Standford, USA)
- Cell culture incubators: NUAIRE IR AUTOFLOW CO₂ (Zapf Instruments, Sarstad, Germany) and Heraeus-Incubator and Hera-Cell Incubator (Heraeus, Hannau, Germany)
- Confocal microscope: Laser-scanning Confocal Microscopes Fluoview FV1000 with Olympus Fluoview Software Ver. 2.1.b (Olympus, Hamburg, Germany)
- Time-lapse imaging device: Zeiss Axiovert 200M light microscopy (Zeiss, Göttingen, Germany), Mac5000 (Visitron System, Puchheim, Germany), and Sony CCD-Camera 12.0 Monochrome w/o IR-18 (Diagnostic Instruments Inc., Sterling Height, USA)
- Sequencing analyzer: ABI Prism (Leica, Wetzlar, Germany)
- Magnetic particle concentrator: Dynal MPC-S (Dynal, Oslo, Norway)

4-1-3. Buffers and media

All buffers and media were made with Milli-Q-System filtered water (Millipore, Eschborn, Germany). When they need to be precise, pH values were adjusted with NaOH, KOH, or HCl. Buffers or solutions were sterilized by autoclaving at 120 °C for 20 min or by sterile-filtrating through a 0.22 µm Millipore membrane (Millipore, Eschborn, Germany). Each buffers and media were slightly modified from the Molecular cloning (Sambrook *et al.*, 1989) for their special usages.

The buffers and media that were used are listed below.

Blocking buffer for Immunoblotting

5% Non-fat milk in 1x TBS-T

Blocking buffer for Immunocytochemistry

3% Bovine Serum Albumin (BSA) in 1x PBS

Cell lysis buffer

1% Triton X-100, 1 mM PMSF, 1 mM Complete Protease Inhibitor (Roche, Mannheim, Germany) in 1x PBS

D-MEM/F-12 complete for hippocampal neuronal cell culture

500 ml D-MEM/F-12 (1:1, w/o L-Glu); 10% (v/v) FCS; 2 mM L-Glutamine; 25 μ g/ml Pyruvate; Penicillin/Streptomycin (50,000 U)

6x DNA loading dye

7.5 g Ficoll; 0.125 g Bromophenol Blue (BPB) in 50 ml H₂O (Aliquots were kept at -20 °C)

2x HBS for transfection

1.6 g NaCl; 0.074 g KCl; 0.027 g Na₂HPO₄•2H₂O; 0.2 g Dextrose; 1 g HEPES in 100 ml H₂O (pH 7.05, sterile filtered and aliquots were kept at -20 °C)

HEPES buffer for Time-lapse imaging and washing cultured neuron

135 mM NaCl; 5 mM KCl; 2 mM CaCl₂; 10 mM HEPES; 15 mM (D)-Glucose (pH 7.4, sterile-filtered)

HEK293TN medium

500 ml D-MEM (+4500 mg/l Glucose, +GlutaMAX I, - Pyruvate); 5 ml Penicillin/Streptomycin buffer (10,000 U/ml) in H₂O

IM-Ac buffer

20 mM HEPES; 100 mM K-Acetate; 40 mM KCl; 5 mM EGTA; 5 mM MgCl₂ in H₂O (pH 7.2, sterile-filtered)

IP washing buffer

20 mM Tris; 150 mM NaCl; 5 mM MgCl₂ in H₂O (pH 7.5, sterile-filtered)

LB (Luria-Bertani) Agar

1% (w/v) Pepton; 0.5% Yeast extract; 1% (w/v) NaCl; 2%

(w/v) Agar (Add 100 µg/ml Ampicillin or 50 µg/ml Kanamycin after autoclave)

LB medium

1% (w/v) Pepton; 0.5% Yeast extract; 1% (w/v) NaCl (Keep at 4 °C after autoclave)

Neurobasal medium

500 ml Neurobasal medium (Invitrogen, Carlsbad, USA); 2 mM L-Glutamine; 25 µg/ml Pyruvate; 5 ml Penicillin/Streptomycin buffer (10,000 U/ml); 2% (v/v) B27

4 % Paraformaldehyde (PFA)

40 g Paraformaldehyde; 40 g Sucrose in 1 L 1x PBS (pH 7.2)

1x PBS

8 g NaCl; 0.2 g KCl; 1.44 g Na₂HPO₄ in 1 L H₂O (pH 7.5, autoclave)

SDS-running buffer (10x)

250 mM Tris; 2.5 M Glycine; 1% (w/v) SDS in 1 L H₂O (pH 8.3)

4x SDS-loading dye

220 mM Tris (pH 6.8); 40% (v/v) Glycine; 8% (w/v) SDS; 0.8% (w/v) Bromophenol Blue in H₂O (for using 100 µl / 8 µl β-Mercaptoethanol)

Stripping buffer

25 mM Glycine; 1% SDS in H₂O (pH 2.0)

50x TAE

2 M Tris-HCl; 100 mM EDTA in H₂O (pH 8.0)

TBS-T

10 mM Tris-HCl; 150 mM NaCl; 0.2% (v/v) Tween-20 in H₂O (pH 7.4)

Western transfer buffer

20% (v/v) Methanol; 250 μM Tris; 192 μM Glycine in H₂O (pH 8.0)

4-1-4. Cell lines

HEK293TN cell line (293T/17)

Human embryonic kidney (ATCC, CRL-11268; Manassas, USA)

4-1-5. Bacterial strains

XL 1-Blue

supE44 hsdR17 recA1 endA1 gyrA96(nal^R) thi-1 recA1 relA1 lac glnV44 F' [::Tn10 proAB⁺ lacI^q Δ (lacZ)M15] hsdR17(rk⁻ m_K⁺) (Stratagene, La Jolla, California, USA)

Nalidixic acid resistant

Tetracycline resistant (carried on the F plasmid)

DH5α

F- *φ80/lacZΔM15 Δ(lacZYA-argF)U169 deoR recA1 endA1 hsdR17(rk⁻, mk⁺) phoA supE44 thi-1 gyrA96 relA1 λ-* (Invitrogen, Carlsbad, USA)

Nalidixic acid resistant

4-1-6. Antibodies

The listed antibodies were used for Co-Immunoprecipitation (Co-IP), Electron Microscopy (EM), Immunoblotting (IB), and Immunocytochemistry (ICC).

4-1-6-1. Primary antibodies

Antibodies	Species	Dilution factors	Sources
Anti- α -Tubulin	Mouse	1:5000 for IB	SIGMA (Steinheim, Germany)
Anti-B3	Mouse	1:3000 for IB	SIGMA (Steinheim, Germany)
Anti-GFP	Rabbit	1:4000 for IB 4 μ g for Co-IP	Invitrogen (Carlsbad, USA)
Anti-GluR2	Mouse	1:3000 for IB 1:1000 for ICC 4 μ g for Co-IP 1:100 for EM	Chemicon (Temecula, USA)
Anti-GRIP1	Rabbit	1:3000 for IB 1:1000 for ICC 4 μ g for Co-IP	Upstate (New York, USA)
Anti-GT335	Rabbit	1:2000 for IB	Dr. Carsten Janke (Montpellier, France)
Anti-KIF5C	Rabbit	1:2000 for IB 1:1000 for ICC 4 μ g for Co-IP	Thermo Scientific (Waltham, USA)
Anti-N-Cadherin	Mouse	1:3000 for IB 1:1000 for ICC 2 μ g for Co-IP 1:100 for EM	BD Biosciences (California, USA)
Anti-N-Cadherin	Mouse	1:1000 for ICC	SIGMA (Steinheim, Germany)
Anti-Neurologin	Mouse	1:2000 for IB	Synaptic System (Göttingen, Germany)
Anti-panKHC	Mouse	1:3000 for IB	Millipore (California, USA)
Anti-PGs1	Rabbit	1:1000 for IB	Carsten Janke (Montpellier, France)
Anti-Sec8	Mouse	1:3000 for IB 4 μ g for Co-IP	BD Biosciences (California, USA)
Anti-SV2 (Synaptic Vesicle)	Mouse	1:500 for ICC	Harvard Medical School (Boston, USA)

Anti-TRPC1	Mouse	1:1000 for IB	Santa Cruz Biotechnology (Heidelberg, Germany)
IgG	Mouse	4 µg for Co-IP	SIGMA (Steinheim, Germany)
IgG	Rabbit	4 µg for Co-IP	SIGMA (Steinheim, Germany)

Table 4-1. Primary antibodies and their information

4-1-6-2. Secondary antibodies

Antibodies	Species	Dilution factors	Sources
Anti-mouse-HRP	Donkey	1:15,000 for IB	Dianova (Hamburg, Germany)
Anti-rabbit-HRP	Donkey	1:20,000 for IB	Dianova (Hamburg, Germany)
Anti-mouse-Alexa488	Donkey	1:1000 for ICC	Dianova (Hamburg, Germany)
Anti-rabbit-Alexa488	Donkey	1:1000 for ICC	Dianova (Hamburg, Germany)
Anti-mouse-CY3	Donkey	1:1000 for ICC	Dianova (Hamburg, Germany)
Anti-rabbit-CY3	Donkey	1:1000 for ICC	Dianova (Hamburg, Germany)
Anti-mouse-CY5	Donkey	1:1000 for ICC	Dianova (Hamburg, Germany)
Anti-rabbit-CY5	Donkey	1:1000 for ICC	Dianova (Hamburg, Germany)

Table 4-2. Secondary antibodies and their information

4-1-7. Oligonucleotides

The following unmodified HPSF quality oligonucleotides for PCR and sequencing were purchased from MWG biotech (Ebersberg, Germany).

Oligonucleotides	Sequences (5' to 3')	Usage
YP-mCherry-Agel	GTACCGGTCGCCACCATGGT GAGCAAG	To obtain an mCherry-coding PCR fragment, which has an <i>AgeI</i> restriction enzyme site at the 5' end, for further cloning into the pGEM-T Easy vector

HK-mCherry-SacI	CCGAGCTCGTGATTGAGTCG CGGCCGA	To obtain an mCherry-coding PCR fragment, which has a <i>SacI</i> restriction enzyme site at the 3' end, for further cloning into the pGEM-T Easy vector. This was additionally used as a sequencing primer
HK-dnKIF5c3-S	CCCAAGCTTGGGACAGTCTC TGTGAACTTGGA	To obtain a KIF5 Δ MD PCR fragment, which has a <i>HindIII</i> restriction enzyme site at the 5' end, for further cloning into the pEGFP-C3 vector
HK-dnKIF5c3-AS	GGGGTACCCCTTACTTCTGG TAGTGAGTGGA	To obtain a KIF5 Δ MD PCR fragment, which has a <i>KpnI</i> restriction enzyme site at the 3' end, for further cloning into the pEGFP-C3 vector
HK-glur2-92-S	CCCAAGCTTGGGATGCAAAA GATTATGCATATT	To obtain a GluR2N PCR fragment, which has a <i>HindIII</i> restriction enzyme site at the 5' end, for further cloning into the pEGFP-N1 vector
HK-glur2-92-AS	CGAATTCGATAAAAATCCAAA AATTGCGTA	To obtain a GluR2N PCR fragment, which has an <i>EcoRI</i> restriction enzyme site at the 3' end, for further cloning into the pEGFP-N1 vector
T7 Promotor	TAATACGACTCACTATAGGG	Sequencing primer for pGEM-T Easy-mCherry vector
SP6 Promotor	TATTTAGGTGACACTATAG	Sequencing primer for

		pGEM-T Easy-mCherry vector
HK-pEGFP-C-S	ATGGTCCTGCTGGAGTTCGTG	Sequencing primer for pEGFP-C3-KIF5CΔMD vector
HK-dnKIF5c-mid-R3	CCAGATGCTGGATGACACTC	Sequencing primer for pEGFP-C3-KIF5CΔMD vector
DB-KIF5C-seq-1S	GCAACAGATGTTGGATCAGG	Sequencing primer for pEGFP-C3-KIF5CΔMD vector
DB-KIF5C-seq-4AS	GGTCGTAATTGACAGCCAGC	Sequencing primer for pEGFP-C3-KIF5CΔMD vector
DB-KIF5C-seq-2S	GTACATTAGCAAGATGAAGT	Sequencing primer for pEGFP-C3-KIF5CΔMD vector
HK-KIF5c C-term-S	TTCGTGATGAGATTGAGGAG	Sequencing primer for pEGFP-C3-KIF5CΔMD vector
HK-pEGFP-C-AS	CCTCTACAAATGTGGTATGG	Sequencing primer for pEGFP-C3-KIF5CΔMD vector
HK-pEGFP-GFP-AS	GGCTGTTGTAGTTGTACTCC	Sequencing primer for pEGFP-N1-GluR2N vector
HK-GluR2 mid1-AS	ACCTCCAAATTGTCGATATG	Sequencing primer for pEGFP-N1-GluR2N vector

Table 4-3. Oligonucleotides and their usage

4-1-8. Vectors and their usage

Vectors	Sources	Usage

pGEM-T Easy	Promega (Mannheim, Germany)	Generation of pGEM-T Easy-mCherry vector
pGEM-T Easy-mCherry	mCherry sequence was inserted into the pGEM-T Easy vector with <i>AgeI</i> and <i>SacI</i> restriction sites	Amplification of mCherry-coding sequence
pmCherry-C3	GFP from pEGFP-C3 vector was replaced with mCherry using <i>AgeI</i> and <i>SacI</i> restriction sites	Expression of pmCherry fusion protein in eukaryotic cells
pmCherry-C3-KIF5C	GFP from pEGFP-C3-KIF5C vector was replaced with mCherry using <i>AgeI</i> and <i>SacI</i> restriction sites	Expression of pmCherry fused to KIF5C in eukaryotic cells
pmCherry-C3-KIF5C Δ MD	GFP from pEGFP-C3-KIF5C Δ MD vector was replaced with mCherry using <i>AgeI</i> and <i>SacI</i> restriction sites	Expression of pmCherry fused to KIF5C Δ MD in eukaryotic cells
pEGFP-C3-KIF5C	Dr. Michelle Peckham (Leeds, UK)	Expression of pEGFP fused to KIF5C in eukaryotic cells
pEGFP-C3-KIF5C Δ MD	KIF5C deleted motor domain was generated from a rat brain cDNA library using <i>HindIII</i> and <i>KpnI</i> restriction sites. This fragment was inserted into the pEGFP-C3 vector.	Expression of pEGFP fused to KIF5C with deleted motor domain in eukaryotic cells. This construct was used as a dominant-negative form
pmRFP	Dr. R. Y. Tsien (San Diego, USA)	Expression of pmRFP fusion protein in eukaryotic cells
pEGFP-N1	Clontech (Heidelberg, Germany)	Expression of pEGFP fusion protein in eukaryotic cells
pEGFP-C3	Clontech (Heidelberg, Germany)	Expression of pEGFP fusion protein in eukaryotic cells
pEGFP-GluR2	Dr. Peter Seeburg (Heidelberg, Germany)	Expression of pEGFP fused to GluR2 in eukaryotic cells
pEGFP-N1-	Extracellular domain of GluR2,	Expression of pEGFP fused

GluR2N	which is the N-terminal region, was generated from a rat brain cDNA library using <i>HindIII</i> and <i>EcoRI</i> restriction sites. This fragment was inserted into the pEGFP-N1 vector	to GluR2N in eukaryotic cells. This construct was used as a competitive form of GluR2
pmRFP-GRIP1	Department of Molecular Neurogenetics (Kneussel, Hamburg, Germany)	Expression of pmRFP fused to GRIP1 in eukaryotic cells
pEGFP-C1-GRIP1	Department of Molecular Neurogenetics (Kneussel, Hamburg, Germany)	Expression of pEGFP fused to GRIP1 in eukaryotic cells
pEGFP-GRIP1-PDZ2	Department of Molecular Neurogenetics (Kneussel, Hamburg, Germany)	Expression of pEGFP fused to GRIP1, which only contains PDZ2 domain, in eukaryotic cells
pmRFP-N-Cadherin	Department of Molecular Neurogenetics (Kneussel, Hamburg, Germany)	Expression of pmRFP fused to N-Cadherin in eukaryotic cells

Table 4-4. Plasmids and their information

4-1-9. Viruses

Viruses	Sources	Usage
X171 (FUGWinker)	Dr. Carsten Janke (Montpellier, France)	Lenti-virus for expression of GFP alone. This virus was used as a control
X175 (pCJ494-1)	Dr. Carsten Janke (Montpellier, France)	Lenti-virus for expression of GFP and shRNA for PGs1

Table 4-5. Viruses and their information

4-2. Molecular biology

4-2-1. Bacterial transformation

Two different types of competent bacterial cell lines, DH5 α and XL 1-Blue, were used for transformation. Aliquots of DH5 α or XL 1-Blue were thawed on ice for 15 min. 100 ng of plasmid DNA were added to 100 μ l of bacterial competent cell and incubated for 15 min on ice. The competent cells mixed with plasmid DNA were heat shocked at 42 °C for less than 50 sec and then incubated for 2 min on ice. To recover the competent cells, 500 μ l of LB-medium without antibiotic were added. The competent cells were then incubated for 1 h at 37 °C with constant shaking. The incubated cells were harvested by centrifugation at 12,000 rpm for 1 min at room temperature and resuspended in 50 μ l LB-medium. Finally, the transformed bacterial cells were plated on LB-agar plate containing the appropriate antibiotic (e.g. 100 μ g/ml of Ampicillin or 50 μ g/ml of Kanamycin) and incubated at 37 °C overnight to observe transformed single bacterial colonies.

4-2-2. Isolation of plasmid DNA

4-2-2-1. Small-scale isolation of plasmid DNA (Mini-preparation)

A small-scale bacterial culture was started from a single bacterial colony selected from the transformed bacterial agar plate. The colony was inoculated in 5 ml LB-medium containing the appropriate antibiotic and incubated at 37 °C overnight with constant shaking. Before starting plasmid DNA isolation, 50 μ l of grown-bacterial cells were saved in 50% glycerol and kept at -80 °C until further use. Grown-bacterial cells were precipitated by centrifugation and resuspended using the 'NucleoSpin Plasmid QuickPure' plasmid purification kit (Macherey-Nagel GmbH & Co. KG, Düren, Germany). 250 μ l of Buffer A1 were added to harvested bacterial cells and transferred to a new 1.5 ml Eppendorf reaction tube (Eppendorf, Hamburg, Germany) after resuspension. Immediately, 250 μ l of Buffer A2, a lysis buffer, were added and the tube was gently inverted a few times to mix well. After a 5 min incubation at room temperature, 300 μ l of Buffer A3, a neutralization buffer, were added and the tube was again gently inverted a few times. The neutralized solutions were placed in centrifuge 5417C (Eppendorf, Hamburg, Germany) for centrifugation at 4 °C for 10 min at 12,000 rpm. After this step,

supernatants were carefully taken and transferred to a new tube. Using a column from the kit, plasmid DNA from the supernatants was concentrated on the column's silica membrane with repeated centrifugation. 600 μ l of Buffer AQ were then added 2 times to wash the silica membrane and the column was dried by centrifugation for 1 min at 12,000 rpm. To elute the pure plasmid DNA, 100 μ l pure-distilled H₂O were added to the silica membrane and the column was centrifuged.

4-2-2-2. Large-scale isolation of plasmid DNA (Maxi-preparation)

To produce high concentrated plasmid DNA, confirmed and saved bacterial cells from small-scale isolation of plasmid DNA (see 4-2-2-1) were re-inoculated in 150 ml LB-medium containing appropriate antibiotic and incubated at 37 °C overnight with constant shaking. Grown-bacterial cells were harvested by centrifugation and resuspended using plasmid purification kit 'PureLink HiPure Plasmid Maxiprep Kit' (Invitrogen, Carlsbad, USA) or 'QIAGEN Plasmid Maxi Kit' (QIAGEN, Hilden, Germany). To keep the plasmid DNA, 200 μ l grown-bacterial cells were saved in 50% glycerol. The kit (Invitrogen, Carlsbad, USA) is not much different from the 'NucleoSpin Plasmid QuickPure' (Macherey-Nagel GmbH & Co. KG, Düren, Germany). General steps for isolation of plasmid DNA were followed according to the manufacturer's instructions.

4-2-3. Determination of DNA concentrations

DNA concentration was determined by Ultraspec 3000 (GE Healthcare, Buckinghamshire, UK) to measure optical density (OD) using 260 nm and 280 nm wavelengths. An OD₂₆₀ of 1 corresponds to 50 μ g/ml for double-stranded DNA, 40 μ g/ml for single-stranded DNA and RNA, and 20 μ g/ml for single-stranded oligonucleotides. The plasmid DNA concentration was also determined by agarose gel electrophoresis by comparing the apparent thicknesses of the DNA bands with those of the ladder bands (HyperLadder I from BIOLINE, Luckenwalde, Germany).

4-2-4. PCR based amplification of DNA for cloning

Fragments of interest were amplified by PCR using specific oligonucleotides (see 4-1-7). Each oligonucleotide was 27 to 33 bp long, 18 to 22 bp of which exactly

matched their target sequences, 6 bp of which encoded an enzyme restriction site, and 5 to 9 bp of which added an overhang or additional nucleotides in order to facilitate enzymatic digestion and to protect frame shift, respectively.

The PCR reaction was done with following reagents:

Double-stranded DNA template	100 ng
PCR buffer	1x
MgCl ₂	1.5 mM
dNTPs	250 µM each
Sense preimer	10 pmol
Antisense primer	10 pmol
Phusion or Pfu turbo DNA polymerase	1 to 2 units
H ₂ O up to 40 µl	

The PCR reaction was done under the following conditions:

1x	at 95 °C for 5 min
38x	at 95 °C for 30 sec
	at from 50 °C to 65 °C for 40 sec
	at 72 °C for 1 min
1x	at 72 °C for 5 min

4-2-5. Digestion of plasmids or PCR fragments with restriction enzymes

Plasmids or PCR fragments were digested with appropriate restriction enzymes. 1 µg to 2 µg of plasmids or PCR fragments were digested with the appropriate number of units (depending on reaction time) of restriction enzymes in the presence of 1x appropriate buffer according to their manufacturer's instructions. The digestion was normally performed for 2 h at optimal temperature (Generally, enzymatic reaction temperature is 37 °C. However, some enzymes have optimal endonuclease activity at higher or lower temperatures.). For non-compatible enzymes, the digestions were sequentially done with appropriate buffers.

4-2-6. Agarose gel electrophoresis

Digested DNA fragments were separated by electrophoresis in 0.8% to 2% agarose gels. The 6x loading dye (see 4-1-3) was mixed with the samples before loading them onto the gel. To check precise sizes of the digested plasmids or PCR fragments, 1 Kb DNA ladder 'HyperLadder I' (BIOLINE, Luckenwalde, Germany) was loaded into another lane. 90 V to 130 V was applied on the gel to separate DNA fragments by migration from negative charge to positive charge. After separation, ethidium bromide (EtBr; 0.5 µg/ml) pre-stained DNA fragments were subsequently visualized under UV-light. Photo was taken with UV-Gel Documentation System 'UVT2035' (Herolab, Wiesloch, Germany).

4-2-7. Purification of plasmids and PCR fragments from an agarose gel

After separation, DNA fragments were excised from the agarose gel and purified with Agarose Gel DNA Extraction Kit (Roche, Mannheim, Germany) according to the manufacturer's instructions. DNA was eluted by incubating beads with 40 µl distilled H₂O at room temperature for 10 min followed by centrifuging.

4-2-8. Ligation

Ligations were performed by mixing 20 ng to 30 ng of digested plasmid DNA with 3 to 5-fold molar excess of the digested insert. 1 unit of T4-DNA-Ligase (Invitrogen, Carlsbad, USA) and 1x buffer were added to reaction tubes, adding H₂O up to 20 µl. The mixture was incubated at 4 °C for either 3 h or overnight. 5 µl of ligation mixtures were used for transformation of competent DH5α or XL 1-Blue cells without any further purification.

4-2-9. DNA sequencing

DNA sequencing was performed by a sequencing service facility (PD Dr. S. Hoffmeister-Ullerich) in the ZMNH (Center for Molecular Neurobiology Hamburg). Based on the Dideoxynucleotide chain termination method by Sanger (Sanger et al., 1977), DNA sequencing was performed with ABI Prism 377 DNA-Sequencer (Applied Biosystems, Darmstadt, Germany) and BigDye Terminator v1.1 Cycle

Sequencing Kit (Applied Biosystems, Darmstadt, Germany) according to the manufacturer's instructions.

The sequencing results were analyzed with Macintosh-Software DNA Strider TM 1.3f9 (CEA, France).

4-3. Biochemistry

4-3-1. SDS-polyacrylamide gel electrophoresis (SDS-PAGE)

Proteins of different molecular weight were separated by use of discontinuous SDS-polyacrylamide gel electrophoresis (SDS-PAGE) using the Mini-Protean III System (BioRad, Munich, Germany). The SDS-polyacrylamide gels consisted of a 5% acrylamide (v/v) stacking gel and 8% to 15% acrylamide (v/v) running gel created using 40% (w/v) Acrylamide/Bis-acrylamide (Roth, Karlsruhe, Germany). Before loading the proteins onto the gel, samples were diluted in 4x SDS-loading dye and denatured by incubation for 5 min at 95 °C. Samples were then loaded onto the gel alongside protein marker 'Precision Plus Protein Standards Dual Color' (BioRad, Munich, Germany) to check the precise sizes of the proteins. Samples were run at a constant voltage of 80 V in 1x SDS-running buffer until the samples reached the running gel. The voltage was then increased to 100 V for further migration.

4-3-2. Western Blotting

To immunodetect a specific protein with its antibody, the proteins separated on the gel were transferred onto a 'PVDF-Membrane Hybond-P (0.45 µm pore size)' membrane (Amersham, Freiburg, Germany) using a constant voltage of 120 V for 60 min to 90 min (depending on the protein size). The protein is able to be electrically transferred through this system because it is negatively charged by the SDS and therefore travels toward the positively charged electrode.

Transfer was performed by the Wet-Blot Mini Trans-Blot Cell Apparatus (BioRad, Munich, Germany). The gel and PVDF membrane were sandwiched between sponge and paper (sponge/paper/gel/membrane/paper/sponge) and all were clamped tightly together ensuring no air bubbles between gel and membrane.

4-3-3. Immunodetection

The protein attached-PVDF membrane was blocked with 5% (w/v) non-fat milk in TBS-T for 1 h at room temperature with constant agitation to prevent non-specific background binding of primary and/or secondary antibodies to the membrane. Primary antibodies were introduced to the membrane with appropriate dilution range of each antibody (see 4-1-6) with 5% (w/v) non-fat in 1x TBS-T and the membrane was incubated with agitation at room temperature for 1 h to 2 h or at 4 °C overnight. Most primary antibody incubations were preferentially performed at 4 °C. After primary antibody incubation, the membrane was washed 6 times for 30 min with 1x TBS-T. Appropriate secondary antibodies (see 4-1-6) were then introduced in order to conjugate horseradish peroxidase (HRP) to the primary antibody. Secondary antibodies in 5% (w/v) non-fat in 1x TBS-T were incubated with the membrane for 1 h at room temperature with agitation. The membrane was then underwent 6 washes for 5 min each with 1x TBS-T. To detect protein, an enhanced chemiluminescence (ECL) solution 'Immobilon™ Western' (Millipore, Eschborn, Germany) was applied to the membrane for 1 min at room temperature. The ECL solution was mixed well, using the same amount of HRP Substrate Luminol Reagent and HRP Substrate Peroxide Solution, before application to the membrane. Finally the membrane was exposed to 'Hyperfilm™ ECL' film (Amersham, Freiburg, Germany) in a dark room under red light in order to visualize specific protein. The exposure time changed based on the resulting band intensity.

If the membrane was to be used to detect another protein, the membrane was stripped with stripping buffer for 30 min at room temperature.

4-3-4. Co-immunoprecipitation

Co-immunoprecipitation was performed using either rat or mouse brain extract for the precipitation of endogenous proteins and transfected HEK293 cells for the precipitation of exogenous proteins. All of the steps were done on ice.

4-3-4-1. Precipitation of endogenous proteins from rodent brain extract

Co-immunoprecipitation from rat or mouse brain extract only used the microsomal vesicle fraction (P3) from differential centrifugation (see 4-3-5). Before solubilizing the P3 fraction with 1% (v/v) Triton X-100, 20 µl of the appropriate type of

Dynabeads (Dynabead® Protein A or Dynabead® Protein G) (Invitrogen, Carlsbad, USA) was added into a reaction tube containing 800 µl of ice-cold 1x IP-Washing buffer and was subsequently washed 2 to 3 times with the same buffer using the Magnetic Particle Concentrator (Dyna, Oslo, Norway). The appropriate antibody (4-1-6) for specific protein precipitation was introduced into a reaction tube containing 800 µl of ice-cold 1x IP-Washing buffer and incubated at 4 °C for 4 h with constant rotation for antibody conjugation onto the bead. An aliquot of P3 fraction sample stored at -80 °C was thawed on ice and 1% Triton-X100 (v/v) was added to the P3 fraction. The sample was solubilized through discontinuous vortexing for 1 h. After solubilization, 10% (v/v) of the solubilized P3 fraction was saved for input control on the western blot. For precipitation, antibody conjugated Dynabeads were washed and equilibrated with IP-Washing buffer and IM-Ac buffer, respectively, and solubilized P3 sample was introduced into the antibody conjugated Dynabead containing tube. The reaction tube was incubated at 4 °C overnight with constant rotation. The next day, the sample was washed 3 times with ice-cold 1x IP-Washing buffer using the Magnetic Particle Concentrator from Dynal (Oslo, Norway). 45 µl H₂O were added into the reaction tube containing the Dynabeads along with 15 µl 4x SDS-loading dye and the total solution was boiled at 95 °C for 5 min. In parallel, IgG control was processed without antibody. In order to detect precipitated protein, SDS-polyacrylamide gel electrophoresis (see 4-3-1), Western Blot (see 4-3-2), and Immunodetection (see 4-3-3) were performed.

4-3-4-2. Precipitation of exogenous proteins from HEK293TN cell line

Co-immunoprecipitation from transfected HEK293TN cells was performed to figure out whether the introduced exogenous proteins fused with specific tags (see 4-1-8) were well expressed and whether they interacted with each other. Cells were transfected (see 4-4-2) with several exogenous protein combinations and incubated for over 18 h. Transfected HEK293TN cells were harvested with 1% (v/v) Triton X-100, 1 mM PMSF (SIGMA, Steinheim, Germany), and Complete Mini Protease Inhibitor Tablet (Roche, Mannheim, Germany) in 1x PBS. Precipitation of exogenous protein from HEK293TN cells was followed by a protocol for the precipitation of endogenous protein from rodent brain extract described in 4-3-4-1, but skipped the addition of solubilization buffer. For solubilization of transfected HEK293TN cells, 1x PBS containing 1% (v/v) Triton X-

100, 1 mM PMSF (SIGMA, Steinheim, Germany), and Complete Mini Protease inhibitor cocktail (Roche, Mannheim, Germany) was used instead of IM-Ac buffer.

4-3-5. Differential centrifugation

Differential centrifugation was performed to separate certain organelles from whole cells. Differential centrifugation was slightly modified from the protocol from Saito *et al.* (Saito *et al.*, 1997). All steps for differential centrifugation were done at 4 °C. In brief, 10 day old (P10) rats or mice were decapitated and the brains were sunk into buffer 1 (320 mM sucrose, 10 mM HEPES/KOH, 1 mM DTT, 1 mM EGTA, and 1 mM EDTA pH 7.9) with Complete Mini Protease Inhibitor Tablet (Roche, Mannheim, Germany) and 1 mM PMSF (SIGMA, Steinheim, Germany) and homogenated using a Glass-Teflon Homogenator (B. Braun Melsungen AG, Melsungen, Germany). Extracts were centrifuged for 10 min at 1,000 g, the P1 spin, using a Beckman JA-20 Rotor, and the supernatant, S1, was further centrifuged for 10 min at 10,000 g, the P2 spin step. The remaining supernatant, S2, was centrifuged for 1 h at 100,000 g, the P3 spin, with a Beckman SW40Ti Rotor and the supernatant, S3, was retained. Protein content was determined using a BCA Protein Assay Kit (Pierce Biotechnology, Rockford, USA). Each fraction was aliquoted and kept at -80 °C until they were used.

4-3-6. Detection of surface expressed proteins

HEK293TN cells were seeded on 35 mm cell culture dishes from Sarstedt (Newton, USA) and transfected with fused proteins of interest (see 4-4-2) when the cells showed over 60 % of confluency. Transfected HEK293TN cells were incubated for over 18 h to allow the transfected fusion proteins to express. After removing the HEK293TN cell medium, 1 mM Biotin Reagent (Biotinamidohexanoic acid 3-sulfo-N-hydroxysuccinimide ester sodium salt) (SIGMA, Steinheim, Germany) in HEPES buffer was applied to the transfected HEK293TN cells and cells were incubated on ice for 20 min. The reaction was quenched by adding 100 mM glycine in HEPES buffer to the cells twice and washing once with 1x PBS. The cells were harvested with 1% (v/v) Triton X-100, 1 mM PMSF (SIGMA, Steinheim, Germany), and Complete Mini Protease Inhibitor Tablet (Roche, Mannheim, Germany) in 1x PBS and incubated for 1 h on ice with discontinuous vortexing to

solubilize the cells. The solubilized cells were centrifuged at 4 °C for 10 min at 1,000 g. Supernatant was taken to detect biotinylated surface expressed proteins. For investigation of biotinylated proteins, 40 µl of Dynabeads® MyOne™ Streptavidin C1 (Dynal AS, Oslo, Norway) were used after washing twice with IP-Washing buffer using the Magnetic Particle Concentrator (Dynal, Oslo, Norway). The solubilized supernatant was added to the washed Streptavidin beads and incubated for 4 h at 4 °C with constant rotation. The beads were washed with IP-Washing buffer containing 1% (v/v) Triton X-100 using the Magnetic Particle Concentrator (Dynal, Oslo, Norway). 45 µl of H₂O with 15 µl of 4x SDS-loading dye were added to the beads and the whole solution was then boiled for 5 min at 95 °C. To detect biotinylated proteins, SDS-polyacrylamide gel electrophoresis (see 4-3-1), Western Blot (see 4-3-2), and Immunodetection (see 4-3-3) were performed.

4-4. Cell culture and immunocytochemistry

4-4-1. HEK293TN culture

HEK293 cell (see 4-1-4) culture and related experiments were done in a cell culture hood and the cells were incubated at 37 °C in 95% (v/v) O₂ and 5% (v/v) CO₂. The cells were subcultured every 2 to 3 days at a 1:6 to 1:8 subcultivation ratio using HEK293TN medium (see 4-1-3). The cells were washed with 1x PBS after removal of the HEK293TN medium. The cells were incubated with 1x Trypsin-EDTA (Invitrogen, Carlsbad, USA) at 37 °C for 2 min to detach the cells from the plates. The cells were then added to 100 mm or 35 mm culture dishes (Sarsted, Newton, USA) using 10ml for 100mm and 3 ml for 35mm of HEK293TN medium.

4-4-2. Transfection of cultured HEK293TN cell

HEK293TN (see 4-1-4) cell transfection was performed using the Calcium Phosphate Transfection Method. This method was slightly modified from the standard method (Chen and Okayama, 1987). The day before transfection, the

cells were subcultured to 60% confluency. For 100 mm dish, 5 to 10 μg of DNA was used in sterilized 225 μl H_2O and mixed with 75 μl of 1 M CaCl_2 . The mixture was transferred into a tube containing 300 μl of 2x HBS (N, N-bis-[2-hydroxyethyl]-2-aminoethane sulfonic acid-buffered saline, pH 6.9) and mixed well by pipetting or vortexing. The final mixture was added onto the plate in a drop wise manner after a 15 min incubation at room temperature. The cells were then placed into the incubator at 37 °C in 95% (v/v) O_2 and 5% (v/v) CO_2 . The general time of incubation after transfection for the HEK298TN cells was over 18 h for this study.

4-4-3. Preparation of primary hippocampal neurons

Primary cultures of hippocampal neurons were prepared from mice (C57Bl/J6 strain) or rats (Wistar strain) at postnatal day 0 (P0) to 1 (P1), as previously described (Fuhrmann *et al.*, 2002; Neuhoff *et al.*, 2005). In brief, hippocampi were dissected from newborn (P0 or P1) mice or rats and incubated with 0.5 mg/ml papain and 10 $\mu\text{g}/\text{ml}$ DNase in PBS containing 10 mM glucose for 25 min at 37 °C. After washing once with 10 ml Dulbecco's Modified Eagle Medium DMEM/F12-complete (Invitrogen, Carlsbad, USA), 2 ml DMEM/F12-complete were added to the hippocampi and hippocampal neurons were disaggregated by sequential pipetting with a glass-pipette. Using a hemocytometer, disaggregated hippocampal neurons were titrated and seeded at a density of 140,000 cells for mice or 110,000 cells for rats onto a 14 mm glass coverslip or glass based time-laps plate '4-Well-Lab-Tek™ chambered coverglass System' (Nunc International, Roskilde, Denmark). After incubation for 3 h to 5 h at 37 °C in 95% (v/v) O_2 and 5% (v/v) CO_2 , DMEM/F12-complete was replaced with Neurobasal medium (GIBCO BRL, Karlsruhe, Germany) containing 25 $\mu\text{g}/\text{ml}$ pyruvate, 2 mM glutamine, 50 units/ml of Penicillin and Streptomycin and 2% (v/v) B27 supplement (Invitrogen, Carlsbad, USA). At 3 days in vitro (DIV3), 3 μM of 1- β -D-arabinofuranosyl-cytosine (AraC) (SIGMA, Steinheim, Germany) was added to suppress astrocyte division. Every 7 days, one-third of the culture medium was replaced with fresh medium. The coverslip and plate were previously coated with 50 $\mu\text{g}/\text{ml}$ Poly-L-Lysin (SIGMA, Steinheim, Germany) in 1x PBS through a 10 h incubation and then washed 3 times with sterilized H_2O . The coverslip and plate were again coated with 20 $\mu\text{g}/\text{ml}$ Laminine (Roche, Mannheim, Germany) in H_2O

and finally washed 3 times with H₂O. The coated coverslips and plates were kept at 4 °C until used.

4-4-4. Transfection of cultured hippocampal neuron

Hippocampal neurons were cultured at 37 °C in 95% (v/v) O₂ and 5% (v/v) CO₂ in vitro (see 4-4-3). 9 day in vitro (DIV9) cells were transfected by the Calcium Phosphate Transfection Method as described for the transfection of cultured HEK293TN cells (see 4-4-2). In brief, the Calcium Phosphate Transfection Method was performed by mixing 1 µl of DNA with 250 mM CaCl₂ in 30 µl H₂O and the mixture was transferred and mixed with 30 µl of 2x HBS. After a 15 min incubation at room temperature, the final mixture was applied to the cells in a drop wise manner (500 µl of conditioned Neurobasal medium were saved from the well and kept during transfection) and the cells were incubated for 1 h at 37 °C in 95% (v/v) O₂ and 5% (v/v) CO₂. Transfected cells were washed two times with pre-warmed HEPES buffer and 500 µl of freshly conditioned Neurobasal medium mixed with 500 µl of used Neurobasal medium were added to the cells (see 4-4-3). Transfected cells were incubated until the cells were used to perform further studies.

4-4-5. Virus infection

Two different Lenti-virus preparations (see 4-1-9) from Carsten Janke (Montpellier, France) were used for the 'Project 1' study. For PGs1 knockdown, DIV 8 neurons were infected with Lenti-viruses carrying either GFP with shRNA-PGs1 or GFP only and then incubated for two days. At DIV10, infected neurons were transfected with mRFP-gephyrin after checking the viruses' expression through GFP levels. 1 µM Strychnine was applied 2 hr after transfection and the neurons were fixed or harvested for further studies.

4-4-6. Immunocytochemistry

Surface staining exclusively allows the visualization of surface proteins. Some receptor proteins are, however, difficult to stain under living cellular conditions. For that reason, surface immunocytochemistry was performed after fixation with 4% (w/v) paraformaldehyde (PFA) and 4% (w/v) sucrose in 1x PBS for 10 min. Fixed neurons were incubated with 3% (w/v) Bovine Serum Albumin (BSA) in 1x PBS at

4 °C for 1 h and stained for surface proteins with appropriate antibodies (see 4-1-6-1) in 3% (w/v) BSA at 4 °C 2 h with constant shaking. The antibodies were washed 5 times with 1x PBS for 30 min and the cells were permeabilized with 0.2% (v/v) Triton X-100 for 10 min. The neurons were blocked with 3% (w/v) BSA for 1 h at room temperature with constant shaking. In order to stain for other proteins, antibodies (see 4-1-6-1) in 3% (w/v) BSA in 1x PBS were applied to the neurons and the neurons were incubated overnight at 4 °C with constant shaking. The neurons underwent five 30 min washes with 1x PBS and were stained with the appropriate secondary antibodies (see 4-1-6-2) in 3% (w/v) BSA for 1 h at room temperature with constant shaking. After staining with secondary antibodies, unspecific secondary antibody binding was eliminated by washing 5 times with 1x PBS. A coverslip was then applied with mounting solution 'Aqua Poly/Mount' from Polysciences Inc. (Warrington, USA) on the slide-glass after washing once with H₂O to eliminate the salt from the 1x PBS. The mounted coverslip was completely dried without any light and then kept at -20 °C.

4-5. Time-lapse imaging

For time-lapse imaging, 110,000 to 140,000 hippocampal neurons were plated on 0.16 mm thick glass based time-lapse plate '4-Well-Lab-Tek™ chambered coverglass System' from Nunc International (Roskilde, Denmark) and cultured for 10 days in vitro (DIV10). The neurons were transfected by the Calcium Phosphate Transfection Method (see 4-4-4) and the imaged with time-lapse imaging. During time-lapse imaging, temperature and CO₂ concentration were maintained at 37 °C and 5% (v/v) CO₂, respectively. Temperature was controlled via a large plastic hood from Harnischmacher-Labtechnik (Kassel, Germany) surrounding the whole microscope. The time-lapse chamber and microscope were heated 1 to 2 h before imaging in order to maintain a stable temperature. All doors were closed and air-conditioning was switched off to avoid cold airflow into the hood. During time-lapse imaging, a constant flow of carbogen (5% (v/v) CO₂) was applied in the chamber to keep the CO₂ concentration constant. Images were taken with a Zeiss Axiovert 200M light microscopy from Zeiss (Göttingen, Germany). Images from time-lapse experiments were taken at a 5 sec interval. The total duration of the movies ranged up to 5 min.

4-6. Quantification and statistical analysis

All numerical data were presented in this study as group mean values with standard error of mean (SEM). All immunodetection signals (see 4-3-3) from western blots (see 4-3-2) were scanned by a scanner (Epson Perfection 3200 Photo) with 300 dpi resolution and quantified with ImageJ Software, Version 1.38 from the National Institute of Health (NIH; West Chester, USA). The quantified signal intensity was normalized to control signal intensity and analyzed. Images of cellular signal intensity, distribution, and movement were visualized by Laser-scanning Confocal Microscopes Fluoview FV1000 with Olympus Fluoview Software Ver. 2.1.b from Olympus (Hamburg, Germany) and Zeiss Axiovert 200M light microscopy from Zeiss (Göttingen, Germany). The images were saved in TIF-Format and analyzed using MetaMorph 7.1 from Universal Imaging (Downingtown, USA). To assess the statistical significance of all data, standard error of mean values and p-values were analyzed using SigmaPlot version 10 from Systat Software Inc. (Chicago, USA). The level of significance was given through three different levels of significance probability: $p < 0.05$ (*), $p < 0.01$ (**), and $p < 0.001$ (***)

5. Results

5-1. Project 1: Polyglutamylation specifically inhibits gephyrin-mediated KIF5 movement

5-1-1. Induced polyglutamylation by application of strychnine

To examine whether polyglutamylation of tubulin is induced by increased neuronal activity, I analyzed the levels of polyglutamylation, a process involving posttranslational modification of tubulins, under control or strychnine-mediated conditions.

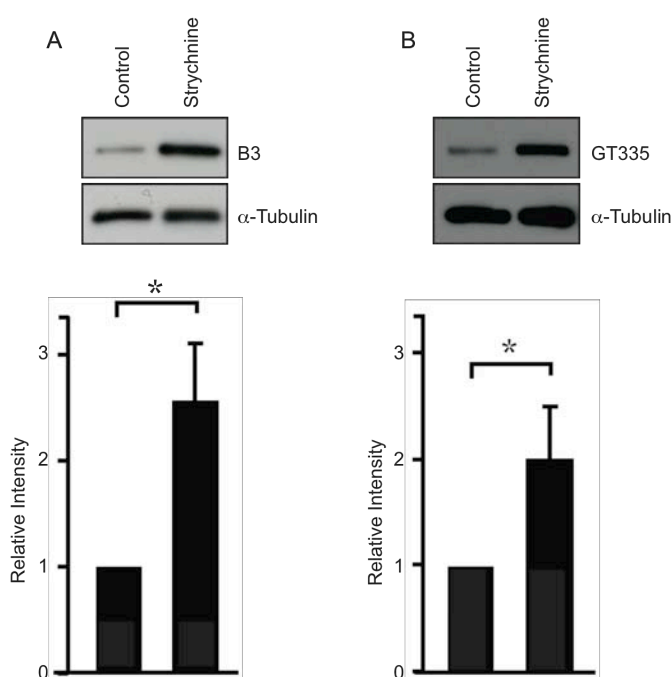


Figure 5-1. Increase of polyglutamylation by strychnine-mediated blockade of GlyR.

1 μ M strychnine was applied for 8 h on cultured hippocampal neurons (DIV 11-14). Cytoskeletal fractions were used to detect polyglutamylation from the microtubules using 2 independent antibodies, B3 and GT335, 8 h after drug application. Immunodetection of polyglutamylation was compared with or without strychnine treatment using B3 (A) and GT335 (B) antibodies. α -tubulin was used as a loading control. The graph analyzes the levels of polyglutamylation after normalization to loading control. B3: 2.60 ± 0.57 (n= 8 experiments); GT335: 2.03 ± 0.51 (n= 11 experiments). * $p < 0.05$. Data: means \pm SEM.

DIV11-14 cultured hippocampal neurons were either untreated or treated with 1 μ M strychnine for 8 h. The preparation of cytoskeletal fraction was performed to eliminate soluble cytoplasmic proteins from the neurons. Using two independent antibodies specific to polyglutamylated tubulin, B3 and GT335, the level of polyglutamylation from 1 μ M strychnine treated neurons was analyzed and compared with control neurons. The two experiments, which utilized two independent antibodies, B3 and GT335, showed that tubulin polyglutamylation levels increased after strychnine treatment. The quantification of these results revealed a significant increase in tubulin polyglutamylation levels after normalization to α -tubulin (Figure 5-1. A and B). These results suggest that the level of tubulin polyglutamylation is altered by changes in neuronal activity following strychnine treatment.

5-1-2. Rescue of gephyrin distribution by shRNA-mediated knockdown of PGs1 gene expression after application of strychnine

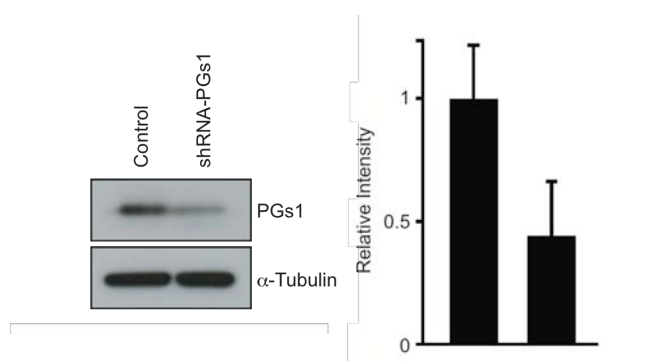


Figure 5-2. Knock-down of polyglutamylase by Lentivirus carrying shRNA-PGs1.

DIV8 cultured hippocampal neurons were infected with one of two different Lentiviruses (see 4-1-9), a control Lentivirus carrying GFP construct with no insert or a Lentivirus carrying GFP and shRNA-PGs1. Two days after Lentivirus infection, neurons were determined Lentivirus infection by GFP autofluorescent and harvested. Immunodetection were performed using PGs1 specific antibody. α -tubulin was used as a loading control. The graph analyzes the expression of polyglutamylase (PGs) after normalization to the loading control. PGs1 detection: 0.44 ± 0.21 ($n = 3$ experiments). Data: means \pm SEM.

It has been reported that eight different polyglutamylase enzymes exist in mammals and that neuronal polyglutamylase activity is exclusively due to one enzyme (van Dijk *et al.*, 2007; Janke *et al.*, 2005). Furthermore, the neuronal polyglutamylase, which is a multiprotein complex, is comprised of five subunits, PGs 1-5 (Janke *et al.*, 2005).

To reduce neuronal polyglutamylase gene expression, Lentivirus carrying shRNA-PGs1 were used to infect DIV8 cultured hippocampal neurons, which were then incubated for 2 days. The level of neuronal polyglutamylase was detected with a PGs1 specific antibody and compared with control neurons infected with Lentivirus carrying GFP. PGs1 is a subunit of the neuronal polyglutamylase complex. Compared to control neurons, the level of PGs1 was reduced in the neurons infected by Lentivirus carrying shRNA-PGs1 (Figure 5-2). Consistent with the depletion of neuronal polyglutamylase in the infected neurons, I used an antibody specific for tubulin polyglutamylation (B3) to determine polyglutamylation levels. These results showed that tubulin polyglutamylation levels were also decreased (Figure 5-3).

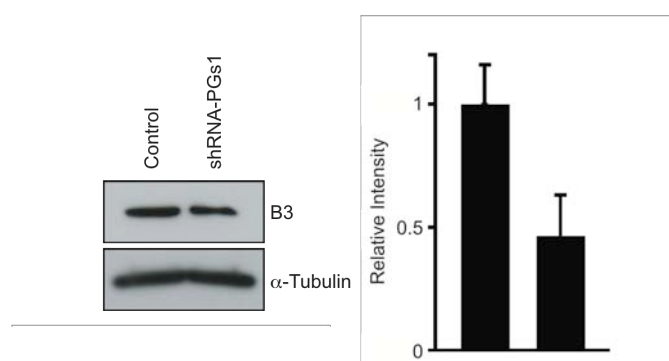


Figure 5-3. Decrease of polyglutamylation by Lentivirus carrying shRNA-PGs1.

DIV8 cultured hippocampal neurons were infected with either a control Lentivirus carrying GFP construct with no insert or a Lentivirus carrying GFP and shRNA-PGs1. Two days after Lentivirus infection, neurons were determined Lentivirus infection by GFP autofluorescent and harvested for cytoskeletal fractionation. Immunodetection were performed using B3 specific antibody. α -tubulin was used as a loading control. The graph analyzes the expression of polyglutamylation after normalization to the loading control. B3 detection: 0.46 ± 0.16 ($n = 4$ experiments). Data: means \pm SEM.

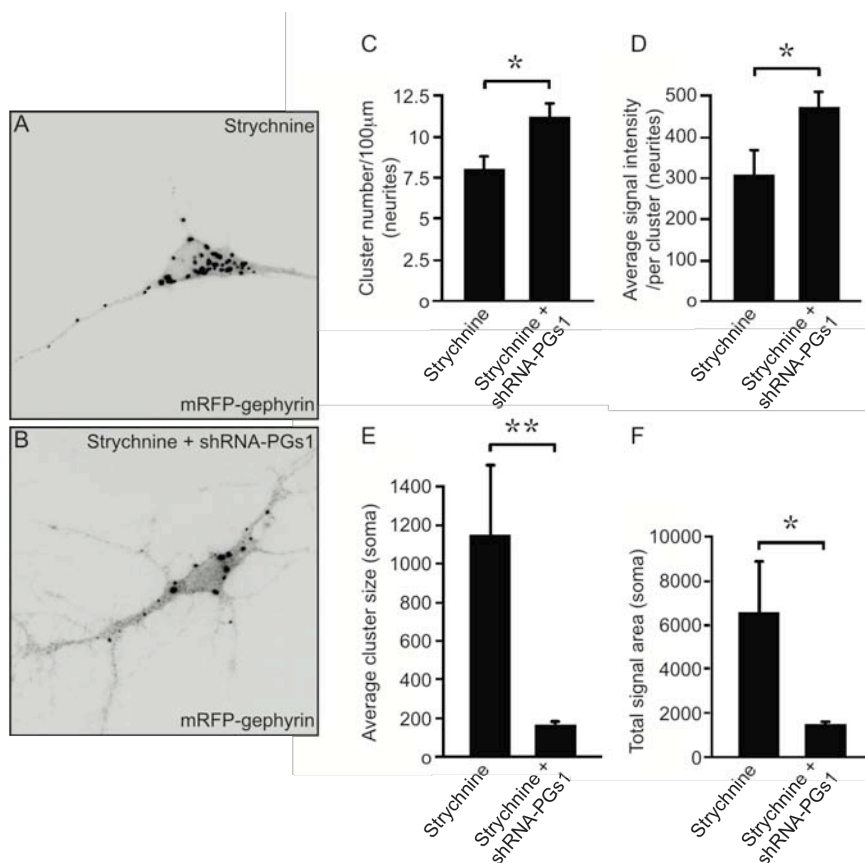


Figure 5-4. Rescue of mRFP-gephyrin transport by Lentivirus carrying shRNA-PGs1.

DIV10 neurons infected by either a control Lentivirus or a Lentivirus carrying shRNA-PGs1 were transfected with mRFP-gephyrin after confirming GFP autofluorescent. 2 h after transfection, 1 µM Strychnine was applied to the neurons and the neurons were fixed for immunocytochemistry (see 4-4-6). The neurites and soma of control neurons (A) and PGs1 knockdown neuron (B) were analyzed by MetaMorph 7.1 software. Signal number (C) and signal intensity (D) for the neurites and the cluster size (E) and signal intensity (F) on the soma were analyzed. Cluster number in neurites: (Strychnine) 8.04 ± 0.80 (n= 160 clusters); (Strychnine + shRNA-PGs1) 11.19 ± 1.00 (n= 156 clusters). Average signal intensity in neurites: (Strychnine) 306.89 ± 63.30 (n= 11 neurons); (Strychnine + shRNA-PGs1) 476.12 ± 43.33 (n= 11 neurons). Average cluster size in somata: (Strychnine) $1,153.64 \pm 379.28$ (n= 235 clusters); (Strychnine + shRNA-PGs1) 160.47 ± 24.09 (n= 153 clusters). Total signal area in somata: (Strychnine) $6,548.01 \pm 2,490.43$ (n= 11 neurons); (Strychnine + shRNA-PGs1) 850.40 ± 154.48 (n= 15 neurons). * $p < 0.05$ and ** $p < 0.01$. Data: means \pm SEM.

A recent study has identified that polyglutamylation is involved in transport mechanisms (Ikegami *et al.*, 2007). Decreased polyglutamylation of α tubulin in

TLL1 mutant mice that lack functional PGs1, a noncatalytic subunit of the TLL1 α tubulin glutamylase, showed abnormal distribution of KIF1A (kinesin 3) and decreased synaptic vesicles in the axons (Ikegami *et al.*, 2007). This finding suggests that polyglutamylation might be responsible for the regulation of cellular transport mechanisms.

In relation to this project, a previous approach demonstrated that the distribution of mRFP-fused gephyrin is significantly inhibited in neurons treated with strychnine compared to controls (Maas *et al.*, 2009). Furthermore, treatment of glycine, known to increase the activity of GlyR, did not show any alteration of mRFP-fused gephyrin distribution (Maas *et al.*, 2009). To further analyze whether polyglutamylation is involved in the transport mechanism of gephyrin, I analyzed the distribution pattern of mRFP-fused gephyrin after PGs1 knockdown gene expression, and with or without strychnine treatment. As an adaptor protein, gephyrin is associated with the KIF5 (kinesin 1) motor protein as a component of the transport complex (Maas *et al.*, 2009). Similar to the previous experiment, DIV8 neurons were separately infected with either control Lentivirus carrying GFP construct with no insert or Lentivirus carrying shRNA-PGs1 and were incubated for 2 days. After confirming GFP autofluorescence in neurons, the neurons were transfected with the mRFP-fused gephyrin construct. 2 h after transfection, the neurons were incubated with 1 μ M strychnine for 6 h to induce neuronal activity. The neurons were then fixed to visualize the distribution of mRFP-gephyrin. It has been shown previously that mRFP-gephyrin requires at least 6 h in order to detect an autofluorescence signal after transfection.

In parallel with a previous result, both increased mRFP-fused gephyrin clusters in the soma and decreased mRFP-fused gephyrin clusters in the neurites were observed neurons treated strychnine (Figure 5-4. A). However, re-distribution of mRFP-gephyrin was rescued in the neurons where neuronal polyglutamylase was knocked-down by Lentivirus carrying shRNA-PGs1 (Figure 5-4. B). The distribution pattern of mRFP-gephyrin was analyzed in terms of fluorescent signal intensity, cluster size and numbers in two different neuronal areas: the soma and the neurites. In the neurites, more clusters and a higher signal intensity were observed when neuronal gene expression of polyglutamylase was reduced by Lentivirus carrying shRNA-PGs1 (Figure 5-4. C and D). In contrast, the size of clusters and total signal intensity in the soma were significantly decreased compared to controls (Figure 5-4. E and F). Given that gephyrin is a known

component of a transport complex (Maas *et al.*, 2009), these results indicate that activity-induced tubulin polyglutamylation controls the gephyrin-mediated transport. Remarkably, the distribution of gephyrin was rescued when polyglutamylation was blocked by infection with Lentivirus carrying shRNA-PGs1.

5-2. Project 2: KIF5-driven novel transport complex, N-Cadherin-GluR2-GRIP1-KIF5C

5-2-1. Interaction and co-localization of GluR2, GRIP1, KIF5C, and N-Cadherin

Several studies have shown that GluR2-containing AMPA receptors and the motor protein KIF5 interact through the adaptor protein, GRIP1, to form a transport complex (Setou *et al.*, 2002; Dong *et al.*, 1997). This complex is essential for the localization of GluR2-containing AMPA receptors to synapses, which regulate several synaptic functions in the neurons. Moreover, a recent study showed via a yeast-two hybrid assay and co-immunoprecipitation study that the N-Cadherin cell adhesion protein directly interacts with GRIP1 (Schurek, 2006).

Since N-Cadherin as a cell adhesion molecule is important for many synaptic functions, I investigated whether an additional interactor binds to the interacting N-Cadherin and GRIP1 complex. To identify further interactors, independent co-immunoprecipitation experiments were performed with N-Cadherin, GluR2, or GRIP1 specific antibodies using vesicle-enriched intracellular fractions (P3) from postnatal day 10 (P10) mouse whole brain lysate. As expected, GRIP1 interacted either with N-Cadherin or with GluR2 (Figure 5-5). Interestingly, an interaction between N-Cadherin and GluR2 was observed from these experiments (Figure 5-5) as previous approaches showed an extracellular interaction of N-Cadherin and GluR2 (Zhou *et al.*, 2011; Saglietti *et al.*, 2007).

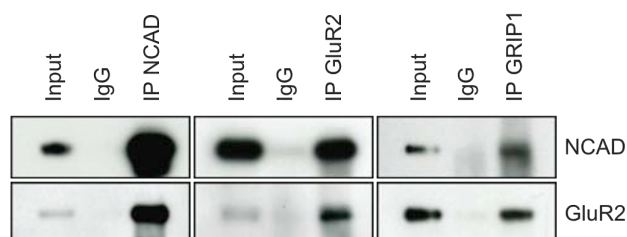


Figure 5-5. Interaction N-Cadherin with GluR2, and GRIP1.

N-Cadherin, GluR2, and GRIP1 were separately precipitated with their specific antibodies from vesicle-enriched P3 fraction of mouse whole brain (see 4-3-5). The precipitated samples were immunolabeled with either N-Cadherin or GluR2 antibodies. Rabbit IgG was used as a negative control.

To confirm the interaction of N-Cadherin and GluR2 with GRIP1, triple co-localization staining was performed with DIV11 cultured hippocampal neurons. DIV10 cultured hippocampal neurons were transfected with a GFP-GRIP1 fusion construct and incubated for 18 h. Subsequently the neurons were fixed and the localization of proteins was analyzed. Together with detection of GFP-GRIP1, endogenous N-Cadherin and GluR2 molecules were immunostained to observe their autofluorescence subcellular localization. GFP-GRIP1, GluR2, and N-Cadherin were visualized with green, red, and blue color, respectively, and triple co-localization was conveyed as white puncta indicated by red arrows in each inset (Figure 5-6).

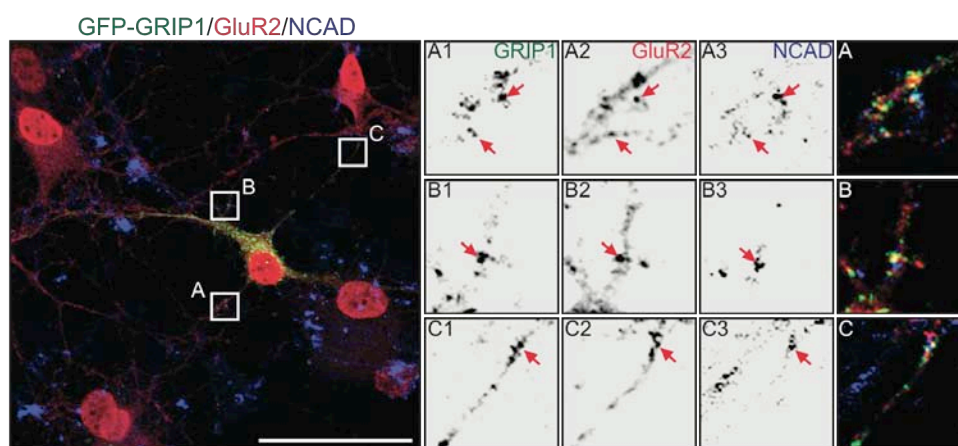


Figure 5-6. Triple co-localization of GRIP1, GluR2, and N-Cadherin.

DIV10 cultured hippocampal neurons were transfected with GFP-GRIP1. 18 h after transfection, the neurons were fixed and double immunolabeled with GluR2 (red) and N-Cadherin (blue). Magnified images display each individual protein signals as well as a merged image of all three signals. Fluorescence triple co-localization is shown by red arrows in three different insets. Scale bar: 50 μ m.

The results from the triple co-localization and co-immunoprecipitation experiments suggested that a novel transport complex might exist consisting of N-Cadherin, GRIP1, GluR2, and the motor protein KIF5. In control stainings, each member of the previously known transport complex, GluR2-GRIP1-KIF5, was independently stained alongside N-Cadherin in order to determine whether they might localize together. Co-localization of endogenous N-Cadherin with either GluR2 or GRIP1 was observed in DIV15 cultured hippocampal neurons (Figure 5-7). Furthermore, a member of the KIF5 family, KIF5C, co-localized with N-Cadherin (Figure 5-7).

This result suggested that KIF5 might be a motor protein for N-Cadherin that binds to GRIP1. In support of this hypothesis, it has been reported that KIF5 is a motor protein for N-Cadherin via p120-catenin (Yanagisawa *et al.*, 2004; Chen *et al.*, 2003; Mary *et al.*, 2002).

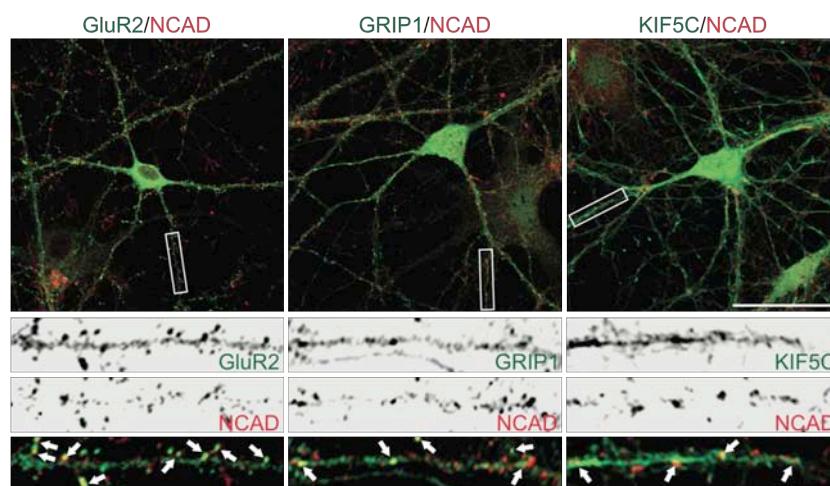


Figure 5-7. Localization of N-Cadherin with each component of GluR2-GRIP1-KIF5C.

DIV15 cultured hippocampal neurons were double immunolabeled with anti-N-Cadherin antibody (red) and antibodies against components of a well-known transport complex, using anti-GluR2 (left), anti-GRIP1 (middle), and anti-KIF5C (right). Immunofluorescence co-localization is shown in yellow color. Magnified images (white box regions) were captured from distal parts of dendrites. Scale bar: 50 μ m.

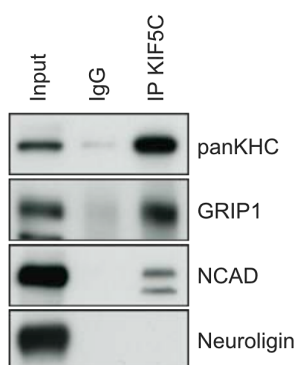


Figure 5-8. Association of N-Cadherin and GRIP1 with KIF5.

Co-immunoprecipitation was performed with KIF5C antibody using vesicle-enriched intracellular P3 fraction of mouse whole brain extract. The immunoprecipitated protein was detected with panKHC (kinesin heavy chain), GRIP1, N-Cadherin, and Neurologin antibodies. Rabbit IgG and Neurologin was used as a negative control.

To confirm the possibility that KIF5 interacts with N-Cadherin and GRIP1, co-immunoprecipitation was performed from vesicle-enriched intracellular P3 fractions of mouse whole brain lysate using a KIF5C specific antibody. N-Cadherin and GRIP1 were precipitated by KIF5C and were detected with their respective antibodies, whereas no proteins were precipitated by control IgG (Figure 5-8). Moreover, KIF5C did not interact with Neuroligin, which is a cell adhesion molecule and is transported by the KIF21B motor protein (Schapitz, 2009).

Together, these results support the idea that the KIF5 motor protein interacts with N-Cadherin and GRIP1. Based on the previous study showing that N-Cadherin directly interacts to GRIP1 (Schurek, 2006), it is conceivable that a novel KIF5-driven transport complex, N-Cadherin-GRIP1-KIF5, may exist.

5-2-2. Transport of GluR2, GRIP1, and N-Cadherin by KIF5C

To further characterize the relationship between N-Cadherin, GRIP1, and KIF5, the respective GFP fusion proteins were used whereby they mimicked the localization of their endogenous counterparts.

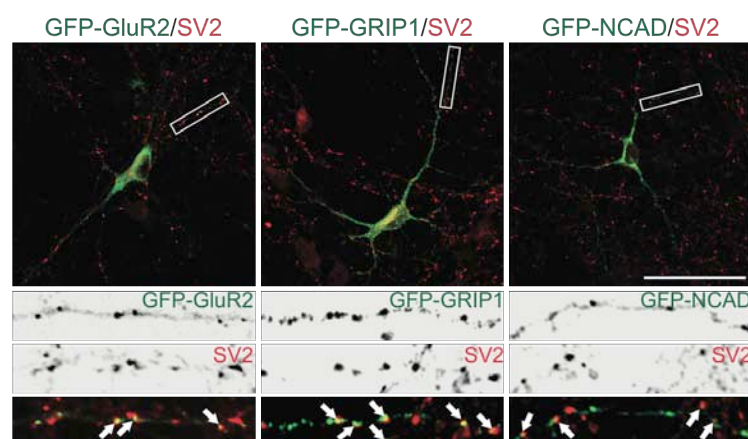


Figure 5-9. Co-localization of GFP-fused GluR2, GRIP1, and N-Cadherin with synaptic vesicle 2 (SV2). GFP fusion proteins GluR2 (left), GRIP1 (middle), and N-Cadherin (right) were expressed into DIV10 cultured hippocampal neurons. The Neurons transfected with different fusion proteins were labeled with SV2 (red; pre-synaptic marker). Co-localization signals are shown in yellow color. Magnified images (white box regions) were captured from distal parts of neurons. Scale bar: 50 μ m.

First, co-localizations of GFP-fused GluR2, GRIP1, and N-Cadherin with SV2 were determined by immunocytochemistry, since the endogenous proteins, which are postsynaptic proteins, co-localize with the presynaptic vesicle marker SV2. Using GFP-fused GluR2, GRIP1, and N-Cadherin, DIV10 cultured hippocampal neurons were separately transfected for 18 h. Subsequently, the neurons were fixed and analyzed. Each GFP-fused protein co-localized with SV2 at synapses (Figure 5-9). The white arrows in the inset point to the co-localized synaptic puncta. In line with the expected synaptic localization of endogenous GluR2, GRIP1, and N-Cadherin postsynaptic proteins, positive autofluorescence puncta of the respective GFP fusion proteins co-localized with the SV2 presynaptic marker.

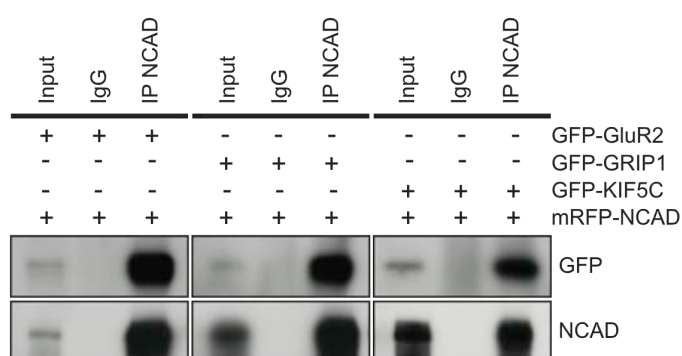


Figure 5-10. Co-immunoprecipitation of GluR2, GRIP1, and KIF5C with N-Cadherin in vitro. HEK293TN cells were separately transfected with each GFP-fused protein combinations (GFP-GluR2/mRFP-N-Cadherin, GFP-GRIP1/mRFP-N-Cadherin, and GFP-KIF5C/mRFP-N-Cadherin). Co-immunoprecipitation was performed with N-Cadherin specific antibody and detected with GFP and N-Cadherin specific antibodies. Mouse IgG was used as a negative control for each combination.

Second, fusion proteins were examined to determine whether they could reproduce their endogenous counterpart. To do this, co-immunoprecipitation was conducted to test these interactions. HEK 293TN cells were separately co-transfected with mRFP-N-Cadherin and either GFP-GluR2, GFP-GRIP1, or GFP-KIF5C, and incubated for 18 h. An N-Cadherin specific antibody was used for precipitation of proteins from transfected HEK293TN cells. The precipitated samples were probed with either GFP or N-Cadherin specific antibodies in order to observe their protein partners. All three GFP-fused proteins were seen to interact independently with mRFP-N-Cadherin (Figure 5-10), as shown in Figure 5-7.

Based on the data from these control experiments, GFP- and mRFP-fused constructs reproduced their endogenous counterparts and were used further investigations such as immunocytochemical and biochemical techniques.

5-2-2-1. Subcellular distributions of mRFP-GRIP1 and mRFP-N-Cadherin by KIF5C in neurons

It appears that a novel transport complex for N-Cadherin might exist because N-Cadherin was previously shown to interact with GRIP1 (Schurek, 2006) or with GRIP1 and KIF5 from my results. To examine whether this transport complex is driven by KIF5 motor proteins, I investigated the subcellular distribution of individual GRIP1 and N-Cadherin components in neurons expressing two different forms of GFP-fused KIF5C motor proteins: full-length KIF5C (GFP-KIF5C) and GFP-fused dominant-negative KIF5C (characterized by the deletion of its motor domain; GFP-KIF5C Δ MD).

First, mRFP-GRIP1 was characterized in neurons expressing the two different motors, GFP-KIF5C and GFP-KIF5C Δ MD, in order to examine for changes in the distribution pattern of mRFP-GRIP1. DIV10 cultured hippocampal neurons were transfected with mRFP-GRIP1 and co-expressed with either GFP-KIF5C or GFP-KIF5C Δ MD. Neurons were incubated for 18 h and then fixed in order to observe the distribution of mRFP-GRIP1. A GFP construct with no insert was used for control experiments (data not shown). The distribution of mRFP-GRIP1 in each experiment was quantitatively analyzed for signal intensity, cluster number and size.

In neurons expressing GFP-KIF5C Δ MD, mRFP-GRIP1 was strongly aggregated in the somata and a few clusters were seen in neurites (Figure 5-11. B, B1, and B2). In contrast, mRFP-GRIP1 distribution in neurons expressing GFP-KIF5C was widespread in the somata, and more clusters were seen in neurites (Figure 5-11. A, A1, and A2). In neurons expressing GFP-KIF5C Δ MD, cluster size and signal intensities in the somata were significantly increased compared with neurons expressing GFP-KIF5C. Conversely, the number of clusters in neurites was markedly decreased compared to neurons expressing GFP-KIF5C (Figure 5-11. C, D, and F). However, signal intensities in the neurites were largely unaltered in neurons expressing either GFP-KIF5C or GFP-KIF5C Δ MD (Figure 5-11. E), indicating that the distribution of mRFP-GRIP1 is regulated by endogenous KIF5C motor protein.

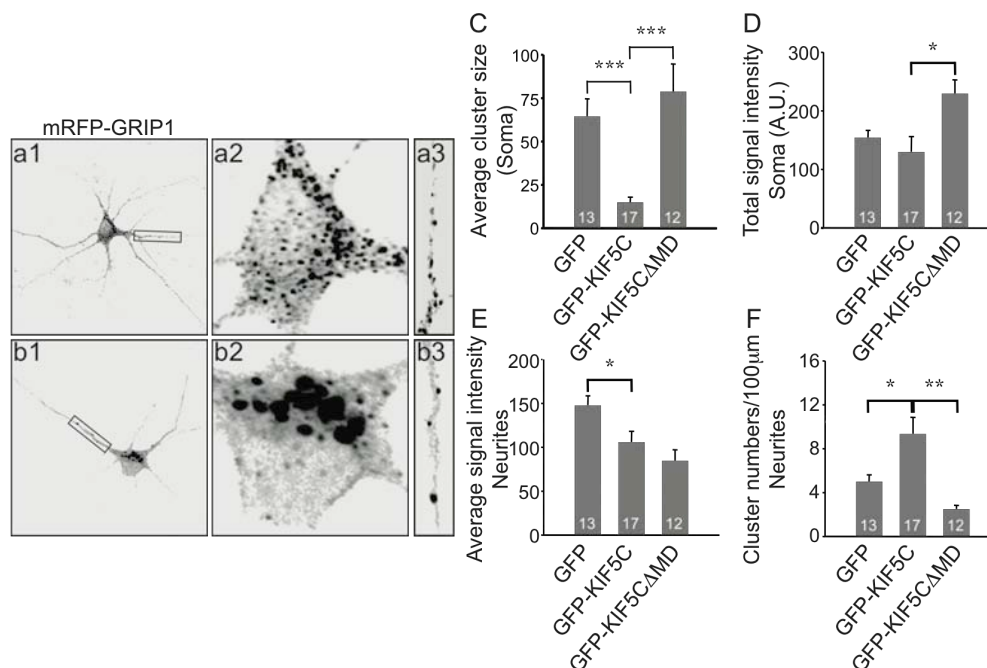


Figure 5-11. Subcellular distribution of mRFP-GRIP1 by motor protein, KIF5C.

DIV10 cultured hippocampal neurons were co-transfected with either GFP-fused full-length KIF5C (GFP-KIF5C) or GFP-fused KIF5C lacking its motor domain (GFP-KIF5CΔMD) along with mRFP-GRIP1. A GFP construct with no insert was used as controls. Distribution of mRFP-GRIP1 was analyzed in GFP-KIF5C (A) and GFP-KIF5CΔMD (B) co-transfected cells and the resulting expression in neurites and somata were analyzed by MetaMorph 7.1 software. Representative somata and neurites were magnified in (A1) and (B1) for somata and (A2) and (B2) for neurites from GFP-KIF5C and GFP-KIF5CΔMD transfected cells, respectively. Graphs show cluster size (C) and signal intensity (D) from somata and signal intensity (E) and cluster number (F) from neurites. Cluster number in neurites: (GFP) 4.99 ± 0.63 (n= 103 clusters); (GFP-KIF5C) 9.35 ± 1.51 (n= 211 clusters); (GFP-KIF5CΔMD) 2.49 ± 0.35 (n= 53 clusters). Average signal intensity in neurites: (GFP) 147.72 ± 10.75 (n= 13 neurons); (GFP-KIF5C) 105.85 ± 12.38 (n= 17 neurons); (GFP-KIF5CΔMD) 84.78 ± 12.36 (n= 12 neurons). Average cluster size in somata: (GFP) 64.51 ± 10.10 (n= 155 clusters); (GFP-KIF5C) 14.90 ± 3.07 (n= 685 cluster); (GFP-KIF5CΔMD) 78.78 ± 15.85 (n= 187 clusters). Total signal area in somata: (GFP) $154,067 \pm 12,677.97$ (n= 13 neurons); (GFP-KIF5C) $129,871.71 \pm 26,168.58$ (n= 17 neurons); (GFP-KIF5CΔMD) $229,612.25 \pm 23,155.16$ (n= 12 neurons). * $p < 0.05$, ** $p < 0.01$, and *** $p < 0.001$. Data: means \pm SEM.

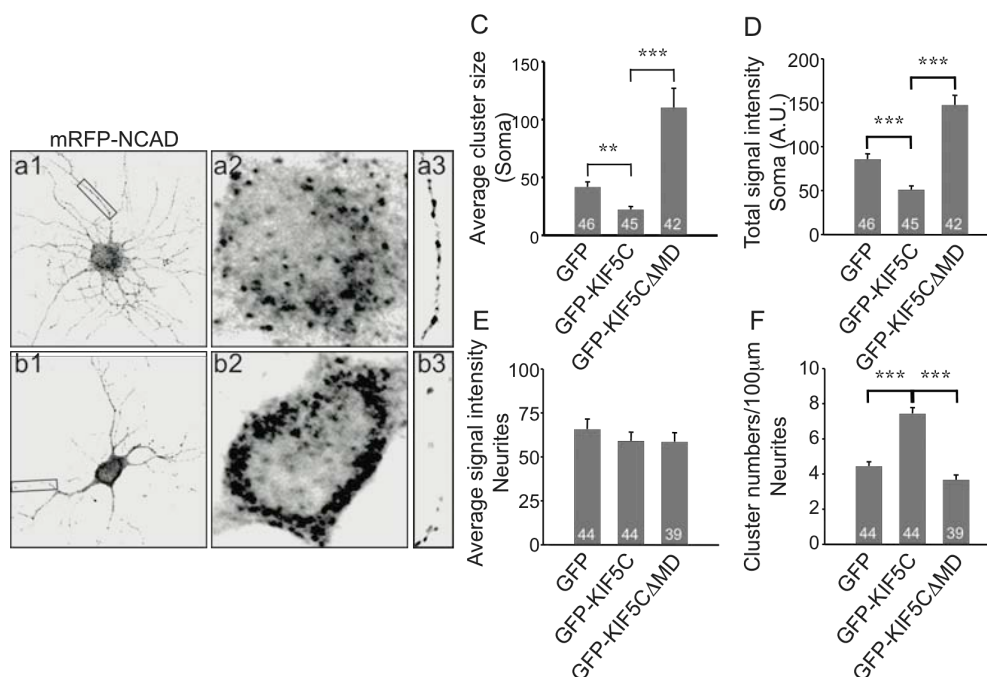


Figure 5-12. Subcellular distribution of mRFP-N-Cadherin by motor protein, KIF5C.

DIV10 cultured hippocampal neurons were co-transfected with either GFP-fused full-length KIF5C (GFP-KIF5C) or GFP-fused KIF5C lacking its motor domain (GFP-KIF5CΔMD) along with mRFP-GRIP1. A GFP construct with no insert was used as controls. Distributions of mRFP-N-Cadherin in the neurites and somata were analyzed in GFP-KIF5C (A) and GFP-KIF5CΔMD (B) transfected neurons and the results were analyzed by MetaMorph 7.1 software. Representative somata and neurites were magnified in (A1) and (B1) for somata and (A2) and (B2) for neurites from GFP-KIF5C and GFP-KIF5CΔMD transfected cells, respectively. Graphs show cluster size (C) and signal intensity (D) from somata and signal intensity (E) and cluster number (F) from neurites. Cluster number in neurites: (GFP) 4.44 ± 0.25 (n= 376 clusters); (GFP-KIF5C) 7.43 ± 0.35 (n= 640 clusters); (GFP-KIF5CΔMD) 3.67 ± 0.28 (n= 303 clusters). Average signal intensity in neurites: (GFP) 65.65 ± 5.92 (n= 44 neurons); (GFP-KIF5C) 59.03 ± 5.04 (n= 44 neurons); (GFP-KIF5CΔMD) 58.49 ± 5.25 (n= 39 neurons). Average cluster size in somata: (GFP) 41.69 ± 4.41 (n= 526 clusters); (GFP-KIF5C) 22.10 ± 2.78 (n= 569 cluster); (GFP-KIF5CΔMD) 110.28 ± 16.72 (n= 372 clusters). Total signal area in somata: (GFP) $85,486.20 \pm 6,392.20$ (n= 46 neurons); (GFP-KIF5C) $50,802 \pm 4,448.49$ (n= 45 neurons); (GFP-KIF5CΔMD) $147,283.74 \pm 11,068.03$ (n= 42 neurons). ** $p < 0.01$, and *** $p < 0.001$. Data: means \pm SEM.

It is worthwhile to consider that large aspects of transportation might be disrupted because GFP-KIF5CΔMD is a dominant-negative form of KIF5C and might

interfere with the function of other KIF5s. Therefore, obstructing the trafficking of mRFP-GRIP1 by GFP-KIF5C Δ MD might in turn, lead to the aggregation of endogenous GRIP1 in the neurites.

Next, mRFP-N-Cadherin was analyzed by using the same procedure that was used to analyze mRFP-GRIP1 distribution. In neurons expressing GFP-KIF5C, mRFP-N-Cadherin distribution was widespread, with small clusters seen throughout the entire neuron especially in the somata and neurites (Figure 5-12. A, A1, and A2). Notably, dominant-negative GFP-KIF5C Δ MD expressing neurons revealed more aggregated clusters in the somata compared with neurons expressing GFP-KIF5C (Figure 5-12. B, B1, and B2). Quantitatively, the cluster size and signal intensities in the somata or cluster numbers in the neurites were significantly increased or decreased in neurons expressing GFP-KIF5C Δ MD, respectively, compared with neurons transfected with GFP-KIF5C (Figure 5-12. C, D, and F). Signal intensities in the neurites did not change (Figure 5-12. E).

5-2-2-2. Surface expression of N-Cadherin and GluR2 by KIF5C

To examine the relationship between N-Cadherin and KIF5, surface expression levels of N-Cadherin were determined under three conditions: control (GFP alone), overexpressed KIF5C (GFP-KIF5C), and functionally interfered KIF5C (GFP-KIF5C Δ MD). Because endogenous N-Cadherin is already distributed evenly along synapses of young hippocampal neurons in culture (DIV5-6) (Elste and Benson, 2006), mRFP-fused N-Cadherin together with either GFP alone, GFP-KIF5C, or GFP-KIF5C Δ MD were introduced into neurons in order to specifically observe the relationship between mRFP-N-Cadherin and GFP-KIF5C. After endogenous N-Cadherin surface staining, co-localized signals of surface expressed N-Cadherin and mRFP-N-Cadherin were counted and quantified in order to determine the expression of N-Cadherin by GFP-KIF5C.

To perform this experiment, GFP, GFP-KIF5C, or GFP-KIF5C Δ MD were expressed together with mRFP-N-Cadherin in separate DIV10 hippocampal neuron cultures. Cells were incubated for 24 h and fixed without permeabilization. Surface expressed N-Cadherin was stained with its extracellular domain specific antibody and the neurons were analyzed.

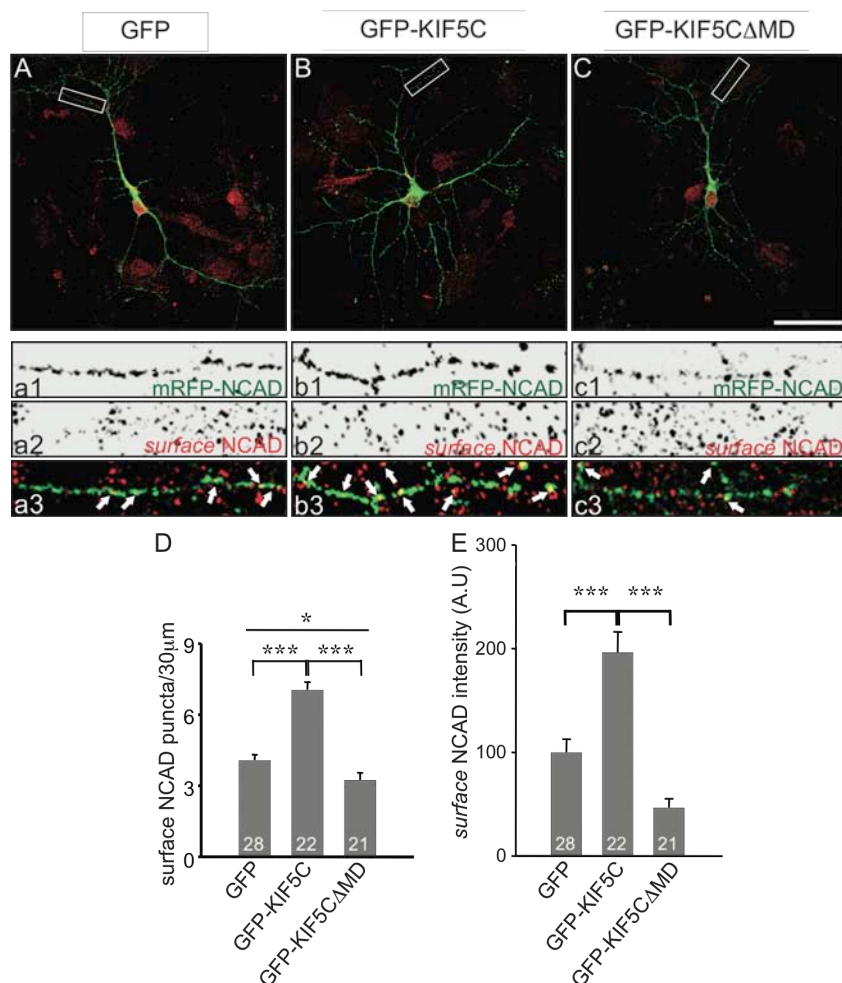


Figure 5-13. Increase of N-Cadherin surface expression by motor protein, KIF5.

DIV10 cultured hippocampal neurons were co-transfected with GFP alone, GFP-fused full-length KIF5C (GFP-KIF5C), and GFP-fused KIF5C lacking its motor domain (GFP-KIF5CΔMD) along with mRFP-N-Cadherin. One day after transfection, the neurons were fixed and labeled with an extracellular domain specific N-Cadherin antibody to show surface staining. The green fluorescence signals of GFP alone, GFP-KIF5C, and GFP-KIF5CΔMD were removed after confirming the expression of these plasmids. Images were analyzed by MetaMorph 7.1 software. Fluorescence of mRFP-N-Cadherin and surface N-Cadherin were changed to green and red fluorescence, respectively. Fluorescent co-localization is shown as a yellow color which was considered to be surface expression for control (A), GFP-KIF5C (B), and GFP-KIF5CΔMD (C) transfected cells. Magnified gray images show mRFP-N-Cadherin (A1, B1, and C1) green and surface N-Cadherin (A2, B2, and C2) red from control (A), KIF5C (B), and KIF5CΔMD (C) transfected cells. Fluorescent co-localizations shown in a yellow color from merged images (A3, B3, and C3) were used for analysis. Graphs show surface N-Cadherin punta (D) and surface N-Cadherin intensity (E). Surface N-Cadherin number: (GFP) 4.07 ± 0.24 (n= 28 neurites from 28 neurons);

(GFP-KIF5C) 7.05 ± 0.33 (n= 22 neurites from 22 neurons); (GFP-KIF5C Δ MD) 3.14 ± 0.29 (n= 21 neurites from 21 neurons). Surface N-Cadherin intensity: (GFP) 100.00 ± 12.83 (n= 28 neurites from 28 neurons); (GFP-KIF5C) 196.24 ± 19.77 (n= 22 neurites from 22 neurons); (GFP-KIF5C Δ MD) 46.50 ± 8.77 (n= 21 neurites from 21 neurons). * $p < 0.05$, and *** $p < 0.001$. Data: means \pm SEM. Scale bar: 50 μ m.

In the analysis of N-Cadherin surface expression, GFP signals were used only to confirm whether the constructs were expressed into neurons. The colors of mRFP-N-Cadherin and surface expressed N-Cadherin were switched to green and red, respectively. This resulted in a yellow signal when they co-localized. In cells expressing GFP-KIF5C, a higher number of N-Cadherin clusters were seen on the surface compared to control cells expressing GFP alone. In addition, N-Cadherin surface expression levels were markedly reduced in neurons expressing GFP-KIF5C Δ MD compared with controls.(Figure 5-13. A-C). A direct comparison between GFP-KIF5C and GFP-KIF5C Δ MD expressing cells showed a significant difference in the surface expression of N-Cadherin (Figure 5-13. B and C). The number of surface expressed N-Cadherins as well as their signal intensities were significantly increased GFP-KIF5C expressing cells (Figure 5-13. D and E).

The same experimental concept was used to examine the functional relationship between the KIF5 motor protein and the GluR2-containing AMPA receptor, since it has been shown that GluR2 is mainly transported by the KIF5 motor protein (Setou *et al.*, 2002). For this experiment, GFP-GluR2 and mCherry-fused KIF5C constructs were used. DIV10 cultured hippocampal neurons were transfected with GFP-GluR2 and co-expressed with either mCherry alone, mCherry-KIF5C, or mCherry-KIF5C Δ MD. Cells were incubated for 24 h and fixed without permeabilization. GFP-fused GluR2 and surface expressed GluR2 stainings were switched to green and red, respectively. All parameters used for analysis were the same, as previously stated. In comparison with controls, the surface expression of GluR2 was considerably increased in mCherry-KIF5C expressing cells, whereas surface expression of GluR2 was decreased in neurons co-expressed with GFP-KIF5C Δ MD (Figure 5-14. A-C).

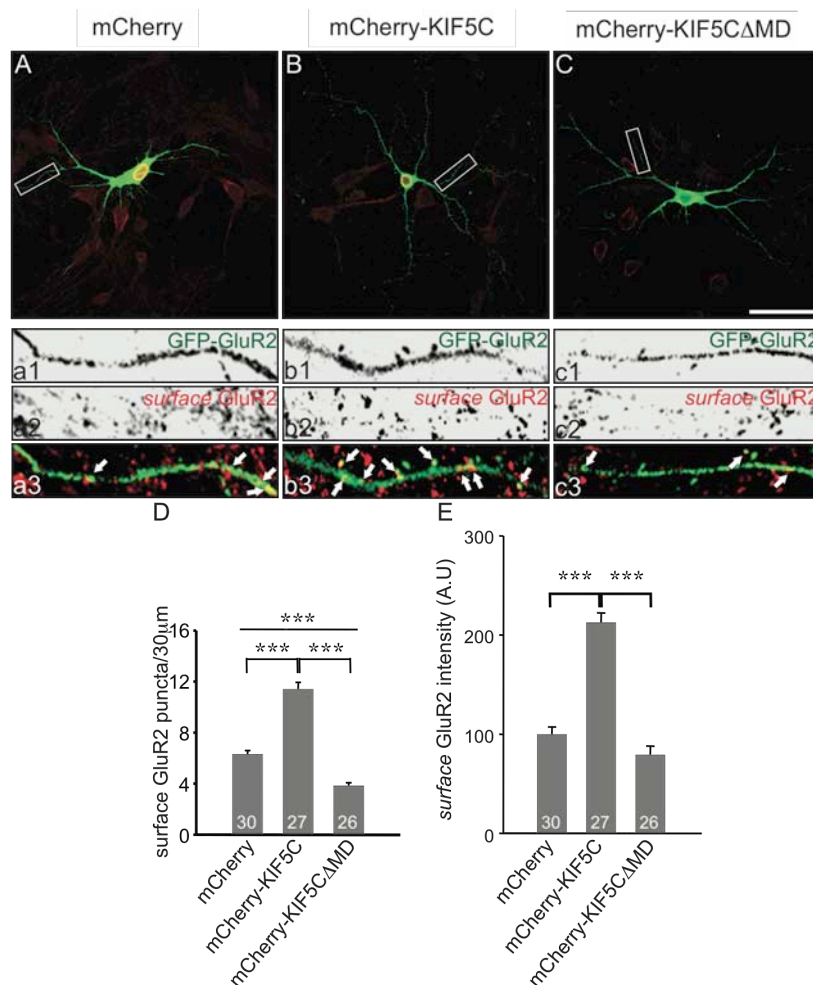


Figure 5-14. Increase of GluR2 surface expression by the motor protein, KIF5.

DIV10 cultured hippocampal neurons were co-transfected with mCherry alone, mCherry-fused full-length KIF5C (mCherry-KIF5C), and mCherry-fused KIF5C lacking its motor domain (mCherry-KIF5CΔMD) along with GFP-GluR2. One day after transfection, the neurons were fixed and labeled with extracellular domain specific GluR2 antibody for surface staining. The red autofluorescence signals of mCherry alone, mCherry-KIF5C, and mCherry-KIF5CΔMD were removed after confirming the expression of the vectors. The images were analyzed by MetaMorph 7.1 software. Fluorescence of GFP-GluR2 and surface expressed GluR2 were changed to green and red colors, respectively. Co-localization is shown as a yellow color which indicates surface expression of GluR2 for control (A), mCherry-KIF5C (B), and mCherry-KIF5CΔMD (C) transfected cells. Magnified gray images represent GFP-GluR2 (A1, B1, and C1) green and surface expressed GluR2 (A2, B2, and C2) red from control (A), mCherry-KIF5C (B), and mCherry-KIF5CΔMD (C) transfected neurons. Fluorescence co-localization shown in a yellow color from merged images (A3, B3, and C3) was used for analysis. Graphs show surface GluR2 puncta (D) and surface GluR2 intensity (E). Surface GluR2 number: (mCherry) 6.30 ± 0.29 (n= 30

neurites from 30 neurons); (mCherry-KIF5C) 11.41 ± 0.54 (n= 27 neurites from 27 neurons); (mCherry-KIF5C Δ MD) 3.83 ± 0.22 (n= 26 neurites from 26 neurons). Surface GluR2 intensity: (mCherry) 100.01 ± 5.58 (n= 30 neurites from 30 neurons); (mCherry-KIF5C) 201.02 ± 8.71 (n= 27 neurites from 27 neurons); (mCherry-KIF5C Δ MD) 74.03 ± 4.97 (n= 26 neurites from 26 neurons). *** $p < 0.001$. Data: means \pm SEM. Scale bar: 50 μ m.

Significant increase and decrease between the number of surface expressed GluR2 proteins and their signal intensities were observed from neurons transfected either mCherry-KIF5C or mCherry-KIF5C Δ MD, respectively (Figure 5-14. D and E). A significant increase in the number of surface expressed GluR2 clusters and their signal intensities was seen in neurons expressed with mCherry-KIF5C. Conversely, a significant decrease was seen in both parameters in neurons expressing mCherry-KIF5C Δ MD (Figure 5-14. D and E).

These results show that GFP-KIF5C constructs can reproduce endogenous KIF5 motor function in terms of the localization of its cargos, N-Cadherin and GluR2. Altogether, the data provided above suggests that KIF5 might be a motor protein for N-Cadherin in a complex linked with GRIP1.

5-2-3. Interference of GluR2 and N-Cadherin surface expression

A biochemical approach was used to confirm whether N-Cadherin surface expression is regulated by KIF5. To examine the relationship of N-Cadherin and KIF5, a biotinylated surface expression experiment was carried out via expression of either GFP-KIF5C or GFP-KIF5C Δ MD with mRFP-N-Cadherin into HEK293TN cells. One day after transfection, biotinylation reagents were introduced to the cells in order to interact with surface expressed membrane proteins. Cells were solubilized to allow binding of biotinylated membrane proteins onto streptavidin. In parallel, control experiments were performed to see the effect of disruption of the track used by motor proteins, microtubules, by the application of 1 μ M Nocodazole. Transient receptor potential cation 1 (TRPC1) was used as a loading control since TRPC1 is ubiquitously expressed on the membrane without any relation to KIF5.

Surface expressed N-Cadherin was significantly reduced when cells expressing GFP-KIF5C Δ MD were compared to cells expressing GFP-KIF5C (Figure 5-15. B).

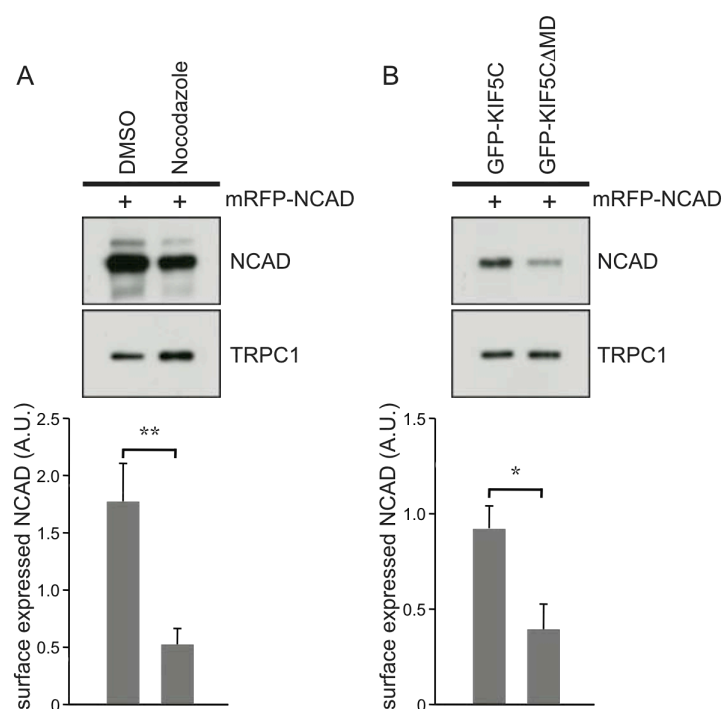


Figure 5-15. Decrease of N-Cadherin surface expression by overexpression of motor domain deleted form of KIF5C, KIF5CΔMD. mRFP-N-Cadherin was expressed with either GFP-fused full-length KIF5C (GFP-KIF5C) or GFP-fused KIF5C lacking its motor domain (GFP-KIF5CΔMD) into HEK293TN cells. One day after transfection, transfected cells were labeled with biotinylation solution. The biotinylated cell membrane proteins were bound onto streptavidin after solubilization of the cells. In parallel, DMSO or 1 μ M Nocodazole were applied to mRFP-N-Cadherin only transfected cells as positive or negative controls, respectively. After biotinylated binding and interaction, surface expressed proteins were detected with N-Cadherin. Transient receptor potential cation 1 (TRPC1) was used as a loading control. Surface expressed N-Cadherin was normalized with TRPC1. Graph shows the levels of surface expressed N-Cadherin. N-Cadherin detection: (DMSO) 1.43 \pm 0.21 (n= 7 experiments); (Nocodazole) 0.59 \pm 0.18 (n= 7 experiments); (GFP-KIF5C) 0.89 \pm 0.11 (n= 6 experiments); (GFP-KIF5CΔMD) 0.37 \pm 0.14. * p < 0.05 and ** p < 0.01. Data: means \pm SEM.

Moreover, control experiments showed significant reduction of N-Cadherin surface expression when the microtubules were disrupted by nocodazole (Figure 5-15 A). This result confirms the relationship between N-Cadherin and KIF5 in terms of surface expression of N-Cadherin. To further identify a new transport complex, GRIP1 was examined to observe its relationship with N-Cadherin for surface expression.

Previous studies (Schurek, 2006; Setou *et al.*, 2002) as well as my earlier presented results suggest that GRIP1 interacts with N-Cadherin and binds with KIF5. These results might suggest that a new transport complex consisting of N-Cadherin, GRIP1, and KIF5 may exist.

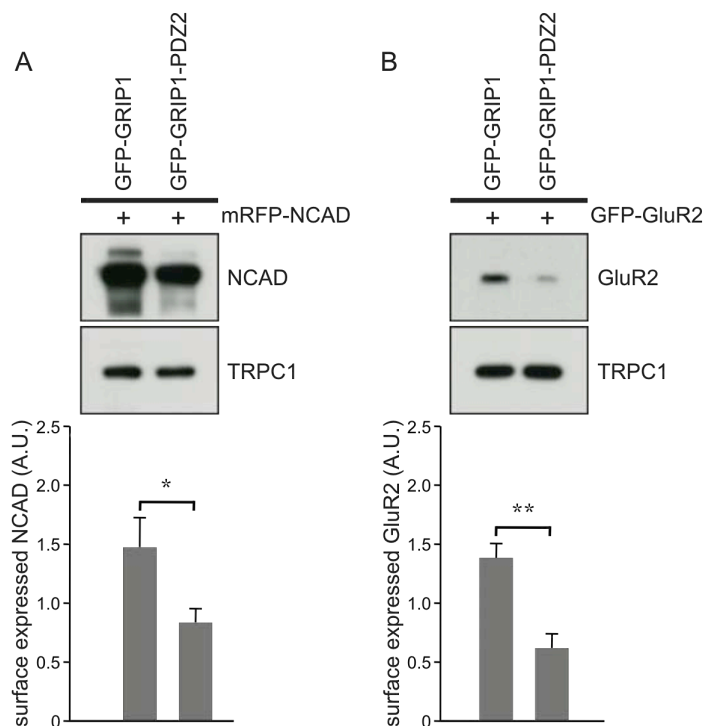


Figure 5-16. Decrease of N-Cadherin and GluR2 surface expression through the overexpression of the competitive form of GRIP1, GRIP1-PDZ2. mRFP-N-Cadherin was co-expressed into HEK293TN cells with either GFP-fused full-length GRIP1 (GFP-GRIP1) or GFP-fused GRIP1 with only its PDZ2 domain (GFP-GRIP1-PDZ2). One day after transfection, transfected cells were labeled with biotinylation solution. The biotinylated cell membrane proteins were bound to streptavidin after solubilization of the cells. After biotinylated binding, surface expressed proteins were detected with N-Cadherin (A) and GluR2 (B) specific antibodies. Transient receptor potential cation 1 (TRPC1) was used as a loading control. Surface expressed N-Cadherin and GluR2 levels were normalized with TRPC1. Graph shows levels of surface expressed N-Cadherin and GluR2. N-Cadherin detection: (GFP-GRIP1) 1.60 ± 0.22 ($n=7$ experiments); (GFP-GRIP1-PDZ2) 1.02 ± 0.15 ($n=7$ experiments). GluR2 detection: (GFP-GRIP1) 1.38 ± 0.13 ($n=5$ experiments); (GFP-GRIP1-PDZ2) 0.62 ± 0.13 ($n=5$ experiments). * $p < 0.05$ and ** $p < 0.01$. Data: means \pm SEM.

To show whether the new transport complex uses GRIP1 as its adaptor protein, I employed a GFP-fused competitive form of GRIP1 (GFP-GRIP1-PDZ2), which contains only a PDZ domain, PDZ2, from its seven PDZ domains since the PDZ2 domain of GRIP1 interacts with N-Cadherin (Schurek, 2006). Using this GFP-GRIP1-PDZ2 construct, surface expressed N-Cadherin and GluR2 were separately examined in HEK293TN cells. Because GRIP1 directly interacts with N-Cadherin via its PDZ2 domain of GRIP1, either GFP-GRIP1 or GFP-GRIP1-PDZ2 were co-expressed along with mRFP-N-Cadherin into HEK293TN cells to detect the level of N-Cadherin surface expression. As expected from my previous results, surface expressed N-Cadherin was reduced in the cells expressing GFP-GRIP1-PDZ2 (Figure 5-16. A).

I also examined GluR2 surface levels under expression of GFP-GRIP1-PDZ2. PDZ2 is not the binding region for GluR2 (Dong *et al.*, 1997). GluR2 interacts with GRIP1 through PDZ4, PDZ5, and additional 30 amino acids on the N-terminal side of its PDZ4 of GRIP1 (Dong *et al.*, 1997). However, the level of GluR2 surface expression was strikingly reduced in the cells expressing GFP-GRIP1-PDZ2 as compared to control cells expressing GFP-GRIP1 (Figure 5-16. B). This result suggests that GluR2 may participate as a component of the transport complex, N-Cadherin, GRIP1, and KIF5.

Several previous studies have reported that N-Cadherin interacts with GluR2 at the plasma membrane through their extracellular domains and that this interaction regulates several cellular functions such as spine regulation and metabotropic glutamate receptor dependent long-term depression (LTD) (Zhou *et al.*, 2011; Saglietti *et al.*, 2007). However, it has not been shown where the interaction between N-Cadherin and GluR2 occurs. If N-Cadherin and GluR2 are already dimerized during their transport within the cell, the newly proposed transport complex may exist to transport N-Cadherin and GluR2 to the cell membrane together. To characterize the possible transport complex, I generated a GFP-fused competitive form of GluR2 (GFP-GluR2N), which contains the extracellular domain of GluR2. To identify whether the GFP-GluR2N construct is usable and whether GluR2 interacts with N-Cadherin intracellularly, a co-immunoprecipitation experiment was carried out with HEK293TN cells using an extracellular domain specific GluR2 antibody. Either GFP-GluR2 or GFP-GluR2N were co-expressed with mRFP-N-Cadherin into HEK293TN cells. Cells were incubated for one day and proteins in the transfected cells were precipitated with the extracellular

domain specific GluR2 antibody to detect protein interactions. Interestingly, GFP-GluR2N interacted with N-Cadherin in a similar fashion to GFP-GluR2 (Figure 5-17). This result may be speculated to show that GluR2 interacts with N-Cadherin intracellularly because GFP-GluR2N is unlikely to be transported alone to the cell surface membrane as it does not contain the GRIP1 binding domain. Therefore, N-Cadherin and GluR2 might be transported together by KIF5.

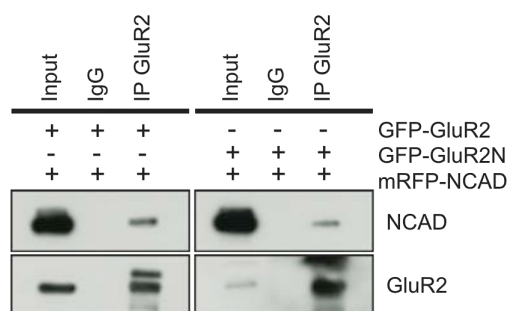


Figure 5-17. Cytosolic-interaction of extracellular N-terminal region of GluR2 with N-Cadherin. Co-immunoprecipitation was performed with HEK293TN cell after expression of mRFP-N-Cadherin with either GFP-fused full-length GluR2 (GFP-GluR2) or GFP-fused competitive form of GluR2 (GFP-GluR2N). Using a GluR2 specific antibody against the extracellular domain, GFP-GluR2 and GFP-GluR2N were precipitated and detected with GluR2 and N-Cadherin specific antibodies. Mouse IgG was used as a negative control.

To further characterize the relationship between GluR2 and the complex, N-Cadherin-GRIP1-KIF5, biotinylation surface expression experiments were performed to detect the levels of N-Cadherin surface expression using either GFP-GluR2 or GFP-GluR2N co-expressed with mRFP-N-Cadherin. N-Cadherin surface levels were significantly reduced when GFP-GluR2N was co-expressed as compared to co-expression of GFP-GluR2 (Figure 5-18). This result suggests that either direct (N-Cadherin and GluR2) or indirect (N-Cadherin and GluR2 separately bind via GRIP1) interactions between N-Cadherin and GluR2 may be sufficient for the transport of N-Cadherin and GluR2, although direct interactions between N-Cadherin and GluR2 at the plasma membrane was shown before (Zhou *et al.*, 2011; Saglietti *et al.*, 2007).

Together, these data suggest that a KIF5-driven transport complex consisting of N-Cadherin, GluR2, GRIP1, and KIF5, might be existed in the cell.

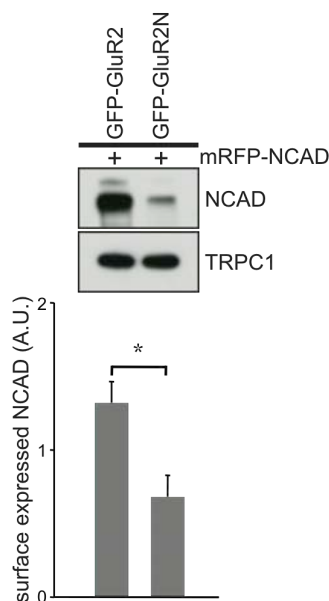


Figure 5-18. Decrease of N-Cadherin surface expression through co-transfection with extracellular N-terminal GluR2. N-Cadherin was co-expressed with either GFP-fused full-length GluR2 (GFP-GluR2) or GFP-fused competitive form of GluR2 (GFP-GluR2N). One day after transfection, transfected cells were labeled with biotinylation solution and the biotinylated cell membrane proteins were bound to streptavidin after solubilization of the cells. After biotinylated binding, surface expressed proteins were detected with N-Cadherin specific antibody. Transient receptor potential cation 1 (TRPC1) was used as a loading control. Surface expressed N-Cadherin was normalized against TRPC1. Graph shows the levels of surface expressed N-Cadherin. N-Cadherin detection: (GFP-GluR2) 1.32 ± 0.15 (n= 3 experiments); (GFP-GluR2N) 0.68 ± 0.15 (n= 3 experiments). * $p < 0.05$. Data: means \pm SEM.

5-2-4. A transport complex carrying different transmembrane proteins

According to my previous results, different approaches have shown that N-Cadherin and GluR2 are transported together by KIF5 linked with GRIP1. However, further specific identifications, such as co-localization and co-migration of N-Cadherin and GluR2 in the same vesicle, are needed in order to conclusively show the existence of a new transport complex, N-Cadherin-GluR2-GRIP1-KIF5. The interactions of the individual components were examined by co-immunoprecipitation. Using the vesicle-enriched intracellular P3 fraction of rat whole brain lysate, N-Cadherin was precipitated with its specific antibody. Each component, N-Cadherin, GluR2, GRIP1, and KIF5C, was detected (Figure 5-19),

as previously described (Figure 5-5 and Figure 5-8). No proteins were precipitated by control IgG.

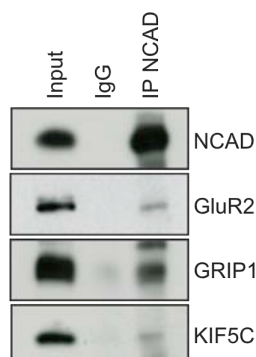


Figure 5-19. KIF5-drives a new quadruple interaction complex: N-Cadherin, GluR2, GRIP1, and KIF5. Co-immunoprecipitation was performed on vesicle-enriched intracellular P3 fraction of rat whole brain extract. N-Cadherin specific antibody was used to precipitate and proteins were detected with N-Cadherin, GluR2, GRIP1, and KIF5C specific antibodies. Mouse IgG was used as a negative control.

5-2-4-1. Co-localization of N-Cadherin and GluR2 in the same vesicles

To prove that N-Cadherin and GluR2 are co-transported as a single transport complex, electron microscopy was performed using two different sizes of immunogold particles, 10 nm for GluR2 and 15 nm for N-Cadherin, that were attached to secondary antibodies of N-Cadherin and GluR2. If N-Cadherin and GluR2 are transported as a single transport complex, both molecules must be co-localized in the same vesicle. The two molecules, N-Cadherin and GluR2, were labeled with immunogold. This experiment was carried out with the help of Dr. Michaela Schweizer, the service group leader of morphology in the Center for Molecular Neurobiology Hamburg (ZMNH).

Many co-localizations of N-Cadherin and GluR2 were observed in the endoplasmic reticulum (ER) network (Figure 5-20. A). The dark organelles in the ER network are mitochondria. The inset was magnified from the white box and showed multiple complexes of N-Cadherin and GluR2 in a vesicle. Arrows and arrowheads indicate GluR2 and N-Cadherin, respectively (Figure 5-20. A). Clearly, co-localized N-Cadherin and GluR2 were also found in the ER network around the nucleus (shown in the upper left-hand side on the figure) (Figure 5-20. B). Notably, a single vesicle containing two small immunogold particles (GluR2; indicated by

arrows) and a large immunogold particle (N-Cadherin; indicated by arrowhead) was observed in the ER network and was magnified (Figure 5-20 B).

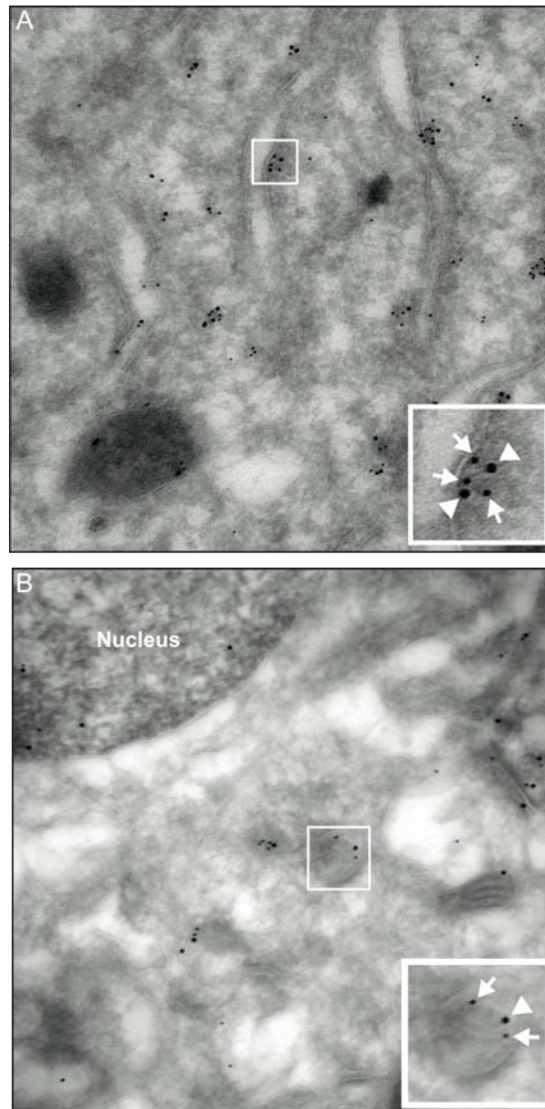


Figure 5-20. Immunogold electron microscopy co-localization of N-Cadherin and GluR2 in the same vesicle. Based on the original methods from Slot and Geuze and Tokuyasu (Slot & Geuze, 2007; Tokuyasu, 1973), a slightly modified immunolabeling method was performed on hippocampal CA1 cryosections. GluR2 and N-Cadherin were labeled with 10 nm and 15 nm sizes of immunogold, respectively. (A) Two different sizes of immunogold particles were found near the endoplasmic reticulum (ER) network in the soma and were multimerized in the same vesicles. Inset shows a magnified image of the white box. (B) Immunolabeled particles were found close to the nucleus and in a membrane-bound vesicle, which was shown inset. White arrows and arrowheads indicate 10 nm particles for GluR2 and 15 nm particles for N-Cadherin on the figures, respectively.

This result showing the co-localized N-Cadherin and GluR2 by electron microscopy clearly confirmed previous results, which stated that N-Cadherin and GluR2 first interact intracellularly. However, some of particles appear to be separately transported, as mentioned in previous reports suggesting that N-Cadherin and GluR2 may be transported by KIF3 and KIF5, respectively (Teng *et al.*, 2005; Setou *et al.*, 2002).

5-2-4-2. Co-migration of N-Cadherin and GluR2

Previous results have suggested that N-Cadherin and GluR2 interact intracellularly and that the interacting proteins are transported by the KIF5 motor protein in complex with GRIP1. However, movement of the transport complex was not clear in terms of co-migration of N-Cadherin and GluR2. Therefore, I employed live cell imaging to test their anterograde co-migration in the cell. Before analysing co-migration of N-Cadherin and GluR2, anterograde N-Cadherin single migration was tested.

To perform live cell imaging of anterograde N-Cadherin movement, DIV10 cultured hippocampal neurons were transfected with mRFP-N-Cadherin. One day after transfection, mRFP-N-Cadherin mobility was observed under established conditions for live cell time-lapse microscopy. Data were obtained every 5 sec for 5 min. mRFP-N-Cadherin single particles are shown, spanning both mobile and immobile particles (Figure 5-21. A). Red arrow number 1 showed mainly anterograde movement, whereas red arrows 2 and 3 showed movement that changed from the anterograde to retrograde direction (Figure 5-21. A). In contrast with the mobile particles, the black arrowhead showed a particle in stationary state throughout the entire observation (Figure 5-21. A). The kymograph represents the movement of each particle throughout the entire time period (Figure 5-21. B). The *x-axis* indicates the distance of the movement and the *y-axis* indicates the time period in the kymograph. Therefore, the thick, white line (declination in the lower right-hand direction) represents a particle indicated by the red arrow number 1, whereas the weak, white line (no inclination over the time period) represents a particle indicated by the black arrowhead (Figure 5-21. B). However, movements of two particles indicated by the red arrows 2 and 3 are hardly found on the kymograph due to their low signal intensities.

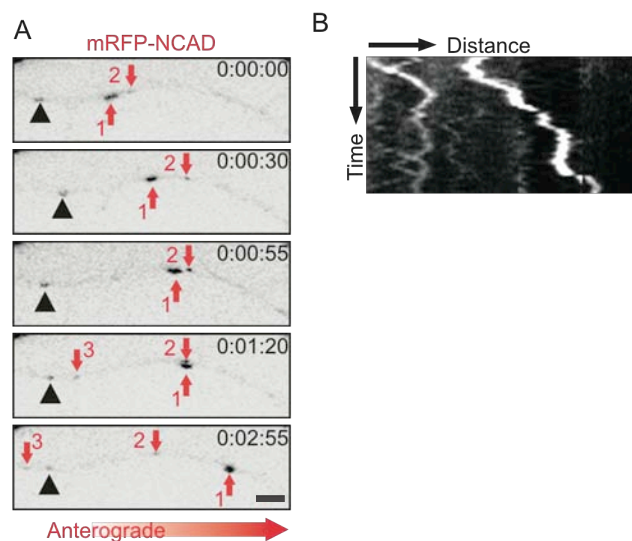


Figure 5-21. Single migration of N-Cadherin in the anterograde direction in dendrites. Time-lapse imaging was performed one day after single transfection of a neuron expressing mRFP-N-Cadherin by Calcium Phosphate Transfection Method (see 4-4-4) in a pre-warmed plastic hood (see 4-5). (A) Over the time period of 5 min, 4 mRFP autofluorescences, which indicate transfected mRFP-N-Cadherin, were observed within depicted dendritic region. The moving particles were represented with red arrows and the immobile particle was represented with the black arrowhead. Over the time period, one particle (red arrow 1) moved in the anterograde direction and two particles (red arrow 2 and 3) changed their movement directions from anterograde to retrograde. One particle, which is indicated with the black arrowhead, was immobile. The movements were represented with kymograph in (B) over the entire time period. Scale bar: 2 μ m.

Co-migration of N-Cadherin and GluR2 was observed using the same experimental technique as for the experiment shown in Figure 5-21. mRFP-N-Cadherin and GFP-GluR2 were introduced into DIV10 cultured hippocampal neurons. One day after transfection, co-migration of mRFP-N-Cadherin and GFP-GluR2 was observed using live cell time-lapse microscopy. Only anterograde co-migration of mRFP-N-Cadherin and GFP-GluR2 was chosen, although several types of mRFP-N-Cadherin movement were observed as seen in the previous N-Cadherin single migration (Figure 5-21 A). The co-migration was highlighted with red and green broken circles around mRFP-N-Cadherin and GFP-GluR2, respectively. The trace in the panel of GFP-GluR2 shows the dendrite outline (Figure 5-22. A). Over the observation time of 5 min, an anterograde movement of mRFP-N-Cadherin and GFP-GluR2 was observed (Figure 5-22. A).

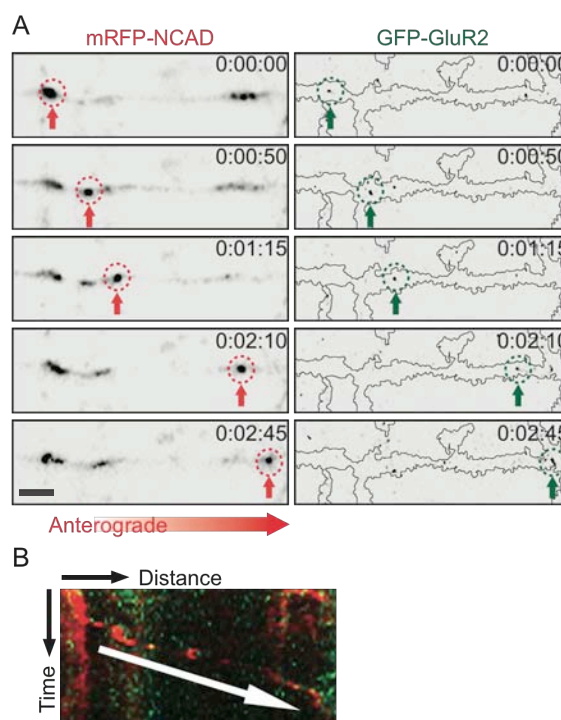


Figure 5-22. Co-migration of N-Cadherin and GluR2 in the anterograde direction in dendrites. Time-lapse imaging was performed one day after co-transfection of neurons expressing mRFP-N-Cadherin and GFP-GluR2 by Calcium Phosphate Transfection Method (see 4-4-4) in a pre-warmed plastic hood (see 4-5). (A) Movement of mRFP-N-Cadherin and GFP-GluR2 were separately represented on two panels and co-migrations of mRFP-N-Cadherin and GFP-GluR2 over the time period were indicated by red and green arrows, respectively. The dendritic outline was visualized by a trace in the GFP-GluR2 panel. (B) The movements of mRFP-N-Cadherin and GFP-GluR2 were analyzed by kymographs separately and the kymographs were merged together with red and green colors for mRFP-N-Cadherin and GFP-GluR2, respectively. Yellow dots show co-migration of mRFP-N-Cadherin and GFP-GluR2 over the entire time period. Scale bar: 3 μ m.

Two kymographs were separately obtained from the time-lapse videos of mRFP-N-Cadherin and GFP-GluR2 and these two kymographs were merged with their representing colors (red and green colors indicate mRFP-N-Cadherin and GFP-GluR2, respectively) (Figure 5-22. B). The white arrow in Figure 5-22 B indicates the direction of co-migratory yellow particles.

Therefore, these results together with previous findings might be speculated that KIF5 is a transport motor protein for N-Cadherin. In addition, the interaction between N-Cadherin and KIF5 represents a new transport complex linked with GRIP1. Moreover, the new transport complex includes GluR2, an AMPA receptor

subunit. This describes KIF5-driven a novel transport complex to transport N-Cadherin and GluR2 in a single vesicle.

5-2-5. Association of the complex with Sec8

To facilitate exocytosis of vesicles, the exocyst complex, which is octameric protein complex involved in vesicle trafficking and targeting, is necessary. The exocyst complex regulates the exocytosis of vesicles by directing vesicle fusion. One exocyst component, which is attached to a vesicle, can interact with another exocyst component, which is attached to the plasma membrane, to facilitate the exocytosis of the vesicle (Hsu *et al.*, 1999). The exocyst complex consists of eight proteins, Sec3, Sec5, Sec6, Sec8, Sec10, Sec15, Sec70, and Sec84 (Ting *et al.*, 1995). The AMPA receptor exocytosis is controlled by fusion of the Sec8 exocyst complex via a PDZ-dependent protein interaction (Gerges *et al.*, 2006).

Thus, I tested interaction between GRIP1 and Sec8 by immunoprecipitation because recent study identified that GRIP1 as an adaptor protein interacts with Sec8 exocyst component for exocytosis of the complex. Using vesicle-enriched intracellular P3 fraction of rat whole brain lysate, proteins were precipitated by a GRIP1 specific antibody. The obtained samples were detected by Sec8 and GRIP1 specific antibodies to observe whether they interact. As shown in Figure 5-23 C, it was revealed that GRIP1 and Sec8 are possibly co-precipitated. To characterize whether the new transport complex consisting of N-Cadherin, GluR2, GRIP1, and KIF5 interacts with Sec8, the same precipitation experiment was carried out with a Sec8 specific antibody. The immunoprecipitation experiment from vesicle-enriched intracellular P3 fraction of rat whole brain lysate showed that Sec8 interacts with two cargo proteins, N-Cadherin and GluR2, and the adaptor protein, GRIP1 (Figure 5-23. A). Furthermore, an immunoprecipitation experiment with an N-Cadherin specific antibody was performed to examine whether immunoprecipitation is reproducible in the opposite direction. The immunoprecipitation experiment showed that Sec8 also co-precipitate with N-Cadherin, suggesting an interaction of these protein in the vesicle-enriched fraction derived from rat brain lysate (Figure 5-23. B).

These results suggest that the new transport complex, N-Cadherin-GluR2-GRIP1-KIF5, moves in the anterograde direction. In addition, the interaction of N-Cadherin, GluR2, and GRIP1 with Sec8, a known component of the exocyst

complex, suggesting a continuous exocytosis of these proteins after the anterograde transport mediated by KIF5.

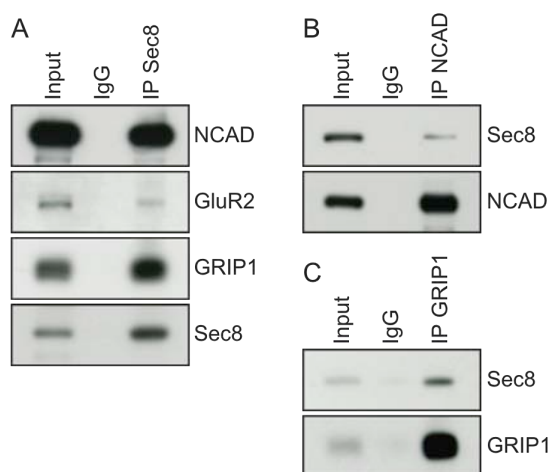


Figure 5-23. Association of a new transport complex with an exocyst protein, Sec8.

Co-immunoprecipitation was performed from vesicle-enriched intracellular P3 fraction of rat whole brain extraction using (A) exocyst protein, Sec8, (B) N-Cadherin, and (C) GRIP1. Precipitated P3 fractions were detected with N-Cadherin, GluR2, GRIP1, and Sec8 specific antibodies in (A). (B and C) were performed to observe the direct interactions between Sec8 and N-Cadherin and GRIP1, respectively. Mouse IgG was used as a negative control.

5-2-6. Interference of spine density by inhibiting complex formation

Chemical synapses are specialized junctions formed by different neurons allowing these cells to form circuits in the CNS. Each neuron can have thousands of synapses with neighboring cells. To date, N-Cadherin as a cell adhesion molecule and AMPA receptor as a neurotransmitter receptor have both been reported that N-Cadherin is essential for pre- and postsynaptic adhesion and, through this adhesion, plays a key role for neurite outgrowth, synaptogenesis, and dendritic arborization, whereas AMPA receptor is the primary synaptic receptor for fast excitatory transmission (Platt *et al.*, 2007; Yu and Malenka, 2003; Benson and Tanaka, 1998). Recently, two approaches suggested that extracellular interactions between N-Cadherin and GluR2 are involved in cellular and biological regulations, such as spines formation and synaptic plasticity (Zhou *et al.*, 2011; Saglietti *et al.*, 2007).

Thus, I investigated spine density after interfering with components of the new transport complex via either disrupted KIF5C or competitive formed GRIP1, which inhibits the interaction of N-Cadherin to GRIP1. To examine spine density, either GFP-KIF5C Δ MD or GFP-GRIP1-PDZ2 with mRFP construct with no insert were expressed into DIV10 cultured hippocampal neurons, and cells were incubated for 36 h. Red autofluorescent from mRFP was analyzed after confirming GFP signal in the neurons. Dendritic protrusions were counted on dendrites.

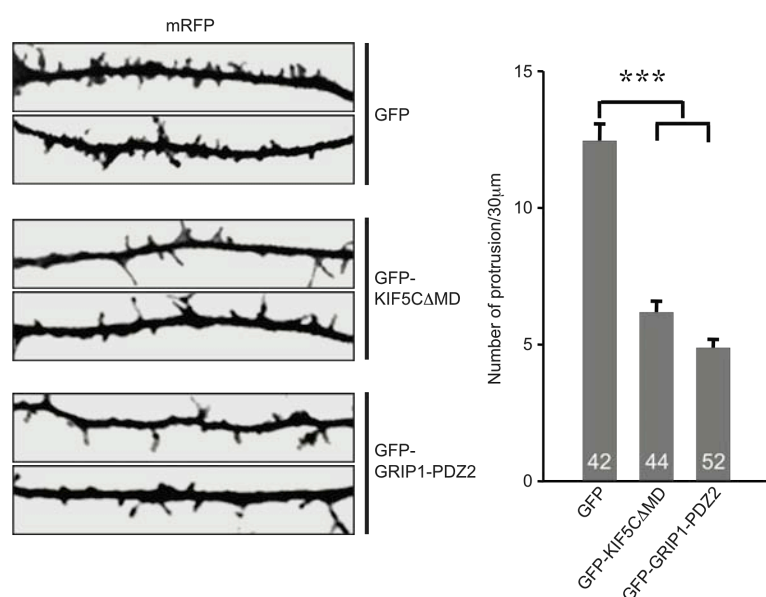


Figure 5-24. Reduction of spine numbers by interference of N-Cadherin transport.

KIF5C lacking its motor domain (GFP-KIF5C Δ MD) and GRIP1 only containing PDZ2 domain (GFP-GRIP1-PDZ2) were separately co-expressed into DIV10 hippocampal neurons together with an mRFP construct with no insert. GFP alone was also expressed as a control. The entire neuron was visualized by mRFP red fluorescence and the number of protrusions from the visualized neuron was counted in each group. Graphs show the numbers of difference from each group. Protrusion number: (GFP) 12.45 ± 0.62 (n= 42 neurites from 22 neurons); (GFP-KIF5C Δ MD) 6.18 ± 0.40 (n= 44 neurites from 28 neurons); (GFP-GRIP1-PDZ2) 4.89 ± 0.31 (n= 52 neurites from 33 neurons). *** $p < 0.001$. Data: means \pm SEM.

The numbers of protrusions from neurons either expressing GFP-KIF5C Δ MD or expressing GFP-GRIP1-PDZ2 were significantly reduced in comparison with control neurons expressing GFP construct with no insert (Figure 5-24). This result suggests that interference of the new transport complex through either disruption

of its motor protein KIF5C or inhibition of N-Cadherin binding to GRIP1 decreased the numbers of protrusion on dendrites. This suggests a role of the new transport complex, N-Cadherin-GluR2-GRIP1-KIF5 might be related with spine density.

6. Discussion

6-1. Project 1: Polyglutamylation specifically inhibits gephyrin-mediated KIF5 movement

This project is part of a publication under the title: “Synaptic activation modifies microtubules underlying transport of postsynaptic cargo” (Maas *et al.*, 2009). This project researched the movement of a transport complex, glycine receptor (GlyR)-gephyrin-KIF5, under the regulation of neuronal activation triggered by strychnine. Upon neuronal activation, several posttranslational modifications occur on the microtubules, one of which, polyglutamylation, specifically inhibits the movement of the gephyrin-mediated KIF5 transport complex. However, polyglutamylation of tubulin did not interfere with KIF5 movement, which is associated with another adaptor protein, GRIP1 (Maas *et al.*, 2009). In this project, I investigated the relationship between polyglutamylation and the gephyrin-mediated KIF5 transport complex.

6-1-1. Application of a glycine receptor antagonist induces polyglutamylation

Previous studies have reported that several forms of posttranslational modifications such as acetylation, tyrosination, detyrosination, $\Delta 2$ tubulin modification, phosphorylation, palmitoylation, glycylation, and glutamylation appear on microtubules (Janke and Kneussel, 2010; Hammond *et al.*, 2008; Verhey and Gaertig, 2007; Westermann and Weber, 2003). These modifications give rise to functionally diverse microtubules. In terms of polyglutamylation, varying numbers of glutamate residues are added to the C-terminal tail of both α - and β -tubulin. Polyglutamylation is a prevalent modification process of stable microtubule populations in flagellar axoneme, basal bodies, centrioles, the mitotic spindle, and neuronal cells (Verhey and Gaertig, 2007; Westermann and Weber, 2003; Lehtreck and Geimer, 2000; Bobinnec *et al.*, 1998; Bre *et al.*, 1994). Here, my results demonstrated that increased neuronal activity caused by inhibition of the glycine receptor induces polyglutamylation of tubulin. However, this

phenomenon warrants further investigation in order to decipher the differences between the levels of polyglutamylation in control and strychnine application. In addition, it is worth investigation whether the differences arise directly from changes in polyglutamylation of tubulin caused by increased neuronal activity, given that increased neuronal activity affects many intracellular functions.

Accumulating evidence indicates that polyglutamylation affects the interaction between microtubules and their associated proteins. Several approaches show a strong increase in the affinity of microtubule-associated proteins (MAPs) to the microtubules and this affinity correlates with the length of glutamate residues involved in polyglutamylation (Bonnet *et al.*, 2001; Larcher *et al.*, 1996). Three glutamate side chains on a tubulin cause a strong affinity between microtubules and MAPs, whereas glutamate side chains with more than three residues decreases this affinity (Bonnet *et al.*, 2001; Larcher *et al.*, 1996). Moreover, a different study shows that the interactions between microtubules and MAPs are increased under strychnine-mediated blockade of glycinergic transmission (Maas *et al.*, 2009). However, this finding has not been characterized in terms of length of polyglutamylation.

6-1-2. Functional inactivation of polyglutamylase increases mRFP-gephyrin transport into neurites

Recent studies have shown that glutamylase enzymes are involved in polyglutamylation and that these enzymes are members of the tubulin tyrosine ligase-like (TTL) domain protein family (Rogowski *et al.*, 2009; Wloga *et al.*, 2009; van Dijk *et al.*, 2007; Ikegami *et al.*, 2006; Janke *et al.*, 2005). In mammals, eight TTL domain-containing proteins, TTL1, TTL4, TTL5, TTL6, TTL7, TTL9, TTL11, and TTL13, are tubulin polyglutamylases. These enzymes differ in their preference for chain initiation and elongation as well as their specificity for α - or β -tubulin (van Dijk *et al.*, 2007; Ikegami *et al.*, 2006; Janke *et al.*, 2005). For example, Ikegami *et al.* demonstrated that TTL7 is a specific β -tubulin polyglutamylase and is highly expressed in neurons. Knockdown of TTL7 led to a decrease in neuronal outgrowth in neuronal PC12 cells (Ikegami *et al.*, 2006). In addition, neuronal polyglutamylase activity is mainly regulated by one enzyme, TTL1, which is composed of five subunits, PGs 1-5 (van Dijk *et al.*, 2007; Janke *et al.*, 2005). Based on these findings, I showed that by knocking down one

subunit of TTLL1 (PGs1) using Lentivirus carrying shRNA-PGs1, the polyglutamylase enzyme in the neurons was reduced and that this reduction caused a decrease of polyglutamylation on tubulin. This result confirms that polyglutamylation on tubulin is regulated by polyglutamylase enzymes. Although previous approaches have shown that polyglutamylase activity is essential for polyglutamylation, deglutamylase activity has also been discovered in neurons (Audebert *et al.*, 1993). However, it is yet to be determined whether or not deglutamylases are involved in the specific regulation of glutamate side chains.

Polyglutamylation may influence the transport system because it occurs on tubulin. Each tubulin is a component of microtubules, which are major tracks for motor proteins like the kinesins and dyneins. A recent study demonstrated that genetic knockout of TTLL1 in mice leads to the absence of PGs1 (a non-catalytic subunit of the TTLL1 α -tubulin glutamylase) and consequent decrease of KIF1A levels in neurites. Moreover, these mice showed a significant decrease in the density of synaptic vesicles, which are cargos for KIF1A in the axon terminals. At the same time, the distribution pattern of the KIF3A and KIF5 motor proteins was unaltered (Ikegami *et al.*, 2007). These results, together with a previous study (Ikegami *et al.*, 2006) suggest that polyglutamylation is capable of either increasing or decreasing the function of various motor proteins under different conditions.

Another recent study showed that strychnine-induced neuronal activation may specifically regulate the distribution of gephyrin because the distribution of mRFP fusion gephyrin was highly inhibited in neurons treated with strychnine (Maas *et al.*, 2009). Notably, an increase in the activity of inhibitory glycine receptors did not alter the distribution of mRFP-gephyrin (Maas *et al.*, 2009). In line with these findings, my results provided further evidence showing that the distribution of gephyrin as an adaptor protein for KIF5 and the glycine receptor (GlyR), was compromised under neuronal activity which up-regulates tubulin polyglutamylation. On the other hand, the distribution of mRFP-gephyrin was rescued by knockdown of polyglutamylase. Consistent with previous data showing that decreased levels of TTLL1 and TTLL7 interferes with the function of KIF1A and neuronal outgrowth, respectively, decreased levels of TTLL1 by knockdown of PGs1 enhances the movement of the KIF5-gephyrin complex. My data therefore suggest that polyglutamylation can negatively affect the GlyR-gephyrin-KIF5 transport complex. Polyglutamylation seems to act specifically on the gephyrin adaptor protein, due to

previous indications that polyglutamylation does not affect the movement of a different KIF5-driven transport complex, GluR2-GRIP1-KIF5 (Maas *et al.*, 2009). It is interesting that one KIF5-driven transport complex (GlyR-gephyrin-KIF5) delivers glycine receptors to inhibitory postsynaptic sites, whereas another KIF5-driven transport complex (GluR2-GRIP1-KIF5) delivers GluR2-containing AMPA receptors to excitatory postsynaptic sites. It is well known that induction of neuronal activity can be triggered by either an increase of AMPA receptors or a decrease of glycine receptors at the postsynaptic membrane. This suggests that the levels of polyglutamylation of tubulin might be increased by neuronal activity. Thus, it appears that the transport complexes containing either an inhibitory or excitatory neurotransmitter receptor may be differentially regulated depending on neuronal activity. Hence, an adaptor protein may function to detect changes in polyglutamylation of tubulin. This regulation may be critical for the functional properties of motor proteins under specific neuronal conditions.

6-2. Project 2: KIF5-driven novel transport complex, N-Cadherin-GluR2-GRIP1-KIF5C

Trafficking of N-Cadherin is essential for spine formation as well as for the transfer of information into or out of cells. Although several proposals exist, the specific transport mechanism for N-Cadherin remains elusive. Here, I demonstrate a KIF5-driven transport of N-Cadherin via the GRIP1 adaptor protein. Moreover, the transport of N-Cadherin is coupled with the GluR2-containing AMPA receptor. The co-transport of N-Cadherin and GluR2 is interesting due to accumulating studies showing that the relationship between N-Cadherin and GluR2 subunit at synapses plays a role in several synaptic functions (Zhou *et al.*, 2011; Arikath *et al.*, 2009; Ochiishi *et al.*, 2008; Saglietti *et al.*, 2007; Silverman *et al.*, 2007). In particular, Zhou *et al.* and Saglietti *et al.* demonstrated that the interaction between the extracellular domains of N-Cadherin and GluR2 is essential for spine formation and synaptic strength (Zhou *et al.*, 2011; Saglietti *et al.*, 2007). If the interaction of these two proteins is necessary for the regulation of several synaptic functions, their different transport mechanisms might effectively be involved in synaptic targeting.

According to my study, a novel transport complex, N-Cadherin-GluR2-GRIP1-KIF5, exists in cells. My data also shows that N-Cadherin and GluR2 undergo co-transport in the same vesicle and this co-transport might be involved in spine density.

6-2-1. GRIP1 interacts with N-Cadherin through its PDZ2 domain

Previous investigations have shown that N-Cadherin is essential for excitatory synapse formation by linking the presynaptic and postsynaptic membranes. Furthermore, these studies show that N-Cadherin interacts through δ -catenin with either GRIPs or ABP, which bind to AMPA receptors (Arikath *et al.*, 2009; Ochiishi *et al.*, 2008; Silverman *et al.*, 2007). The interaction of GRIPs or ABP to δ -catenin is mediated by the PDZ2 domain of GRIPs or ABP (see Figure 6-1) (Silverman *et al.*, 2007). These interactions are not only essential for synapse formation and maintenance, but also allow various intra- and extracellular signals to be processed via these receptors and cell adhesion molecules (Silverman *et al.*,

2007). These cellular functions play critical roles in regulating neuronal synaptic plasticity, such as long-term potentiation (LTP) and long-term depression (LTD). As mentioned earlier, although the functional regulation of N-Cadherin at synapses is well established, its transport machinery remains largely elusive. Recently, it was shown that GRIP1 directly interacts with N-Cadherin via its PDZ2 domain (Figure 2-4; Schurek, 2006). GRIP1 is a well characterized protein, which functions either as a scaffolding protein or as an adaptor protein. In its role as an adaptor protein, GRIP1 functions as a mediator by linking the GluR2-containing AMPA receptor (Dong *et al.*, 1997) and the KIF5 motor protein (Setou *et al.*, 2002). Based on the discovery that N-Cadherin interacts directly with GRIP1 (Schurek, 2006), GRIP1 may be a good candidate for uncovering a new transport complex for N-Cadherin trafficking.

6-2-2. N-Cadherin interacts and co-localizes with the GluR2-GRIP1-KIF5C complex

In the GluR2-GRIP1-KIF5 transport complex, GluR2 and KIF5 are independently linked to GRIP1 through its different PDZ domains. More specifically, GluR2 interacts with PDZ4, PDZ5, and the additional 30 amino acids on the N-terminal side of the PDZ4 of GRIP1 (Dong *et al.*, 1997), whereas KIF5 interacts between PDZ6 and PDZ7 domains (Setou *et al.*, 2002) (see Figure 6-1). Although KIF5 preferentially moves into axons, it migrates in association with GRIP1 into dendrites (Nakata and Hirokawa, 2003). Therefore, GRIP1 functions as an adaptor protein in the transportation of AMPA receptors into dendrites.

In addition to a previous report (Schurek, 2006), the two experiments carried out here showed that GRIP1 interacts with N-Cadherin. It is conceivable, therefore, that the interaction between N-Cadherin and GRIP1 may involve additional synaptic components. This is because GRIP1 also functions as a scaffolding protein for the GluR2 and GluR3-AMPA receptor subunits at excitatory synapses and N-Cadherin acts as a cell adhesion molecule at the same synapses. In general, AMPA receptors show high turnover rates at the synaptic specialization. This turnover occurs either through lateral diffusion between synaptic and extra-synaptic plasma membrane domains or through active translocation between synaptic and intracellular compartments (Choquet, 2010; Groc and Choquet, 2008; Triller and Choquet, 2008; Groc *et al.*, 2007). Through the interaction

between N-Cadherin and AMPA receptors, AMPA receptor clusters are anchored and immobilized in the postsynaptic membrane. This anchorage of AMPA receptors plays a critical role for AMPA receptor properties such as synaptic strength.

Two motor proteins, the heterotrimeric KIF3 complex (Teng *et al.*, 2005) or KIF5 (Yanagisawa *et al.*, 2004; Chen *et al.*, 2003; Mary *et al.*, 2002) are involved in N-Cadherin trafficking to the surface membrane. By using conditional knockout mice for the *Kap3* gene, Teng *et al.* showed that the heterotrimeric KIF3 complex, KIF3A-KIF3B-KAP3 (kinesin-associated protein 3), transports N-Cadherin in association with β -catenin to the neuronal cell surface membrane and that this trafficking regulates the developing neuroepithelium (Teng *et al.*, 2005). For this transport complex, an interaction between KAP3 (a non-motor subunit in the complex) and β -catenin is necessary because KAP3 regulates the association of the KIF3 motor domain with its cargos (in this case, the β -catenin and N-Cadherin complex). In contrast to the KIF3-mediated N-Cadherin transport, other groups have shown that KIF5 transports N-Cadherin in association with p120-catenin to the neuronal cell surface membrane (Yanagisawa *et al.*, 2004; Chen *et al.*, 2003; Mary *et al.*, 2002). In this case, p120-catenin acts as an interaction partner for KIF5. p120-catenin plays various characteristic functions compared with the α -, β -, and γ -catenins. p120-catenin binds to the juxtamembrane region of N-Cadherin, thereby modulating N-Cadherin dimerization and adhesive function. Using time-lapse video microscopy in fibroblasts, Mary *et al.* observed that the localization of N-Cadherin between the intracellular pool and the plasma membrane is dynamically regulated during embryonic development and that this regulation is related with KIF5 (Mary *et al.*, 2002). One year later, Chen *et al.* identified that the N-terminus of p120-catenin is involved in the trafficking of N-Cadherin to the cell surface membrane because the N-terminal of p120-catenin interacts with KIF5 (Chen *et al.*, 2003). Disruption of an interaction either between N-Cadherin and p120-catenin or between p120-catenin and KIF5 delayed accumulation of N-Cadherin at the cell surface (Chen *et al.*, 2003). These results show that two motor proteins, KIF3 and KIF5, transport N-Cadherin in the anterograde direction along the microtubules and that KIF3 and KIF5 need β -catenin and p120-catenin as adaptor proteins, respectively (Teng *et al.*, 2005; Yanagisawa *et al.*, 2004; Chen *et al.*, 2003; Mary *et al.*, 2002). The mechanisms for regulating the interaction between motor and adaptor proteins are largely different. With respect to the

interaction between N-Cadherin and β -catenin, β -catenin needs to be dephosphorylated prior to interacting with N-Cadherin, whereas p120-catenin needs to be phosphorylated in order to interact with N-Cadherin. By phosphorylation and dephosphorylation the interaction of N-Cadherin with these adaptor molecules, β -catenin and p120-catenin, seems to be regulated. Moreover, it is already known that β -catenin is associated with N-Cadherin at the cell surface but is also associated with transcription factors and DNA in the nucleus, where it functions as a transcriptional regulator. In contrast with β -catenin and p120-catenin, GRIP1 may function more effectively as an adaptor if it is involved in the trafficking of both N-Cadherin and GluR2-containing AMPA receptors to the cell surface membrane.

My data show that N-Cadherin co-localizes and interacts with each component of the GluR2-GRIP1-KIF5C complex. These results support the hypothesis that GRIP1 is an adaptor protein for trafficking of N-Cadherin. This is because a previous study suggested that as an adaptor, GRIP1 interacts directly with the KIF5 motor protein and steers the motor to dendrites (Setou *et al.*, 2002). Moreover, the results imply that KIF5 might be a motor protein for N-Cadherin linked with GRIP1. Although it has been reported that KIF5 is involved in N-Cadherin transport (Yanagisawa *et al.*, 2004; Chen *et al.*, 2003; Mary *et al.*, 2002), my results extend the current view, showing that GRIP1 is an important component of this motor-cargo complex.

6-2-3. KIF5C is a motor protein for N-Cadherin

Previous studies have identified the relationships between GRIP1 and other proteins. The GRIP1-PDZ4-5 domain binds to the C-terminus of the GluR2/3 subunit of AMPA receptors (Wyszynski *et al.*, 1999; Srivastava *et al.*, 1998; Dong *et al.*, 1997), whereas the GRIP1-PDZ6 interacts with either the C-terminus of ephrin-B1 ligand and EphB2/EphA7 receptor tyrosine kinases (Bruckner *et al.*, 1999; Lin *et al.*, 1999; Torres *et al.*, 1998) or with the C-terminus of the liprin- α family of multidomain proteins (Wyszynski *et al.*, 2002). Distribution of GRIP1 to the postsynaptic membrane regulates the localization of several proteins together with their motor proteins. A transport complex, GluR2-GRIP1-KIF5, is largely known from two independent findings that characterized an interaction between either GluR2 and GRIP1 (Dong *et al.*, 1997) or GRIP1 and KIF5 (Setou *et al.*,

2002). Setou *et al.* showed that most of GRIP1 disappears from the periphery of the cells when KIF5B knockout mice were observed and abundantly appears in intracellular clusters in the soma of a cell (Setou *et al.*, 2002). Thus, the result indicated that an association of GRIP1 with KIF5 steers to the dendrites. Consistent with this data, another study showed that KIF5 interacting with GRIP1 moves toward the dendrites to transport EphB receptors and that this transport regulates dendrite morphogenesis (Hoogenraad *et al.*, 2005). In neurons expressing GRIP1-siRNA, Hoogenraad *et al.* observed an increased accumulation of KIF5 in the cell body, whereas the level of p150^{Glued}, an accessory protein of dynein, did not alter its localization in the cell body (Hoogenraad *et al.*, 2005). In contrast with GRIP1, when the kinesin-binding scaffolding protein JSAP1, JNK/SAPK-associated protein 1, interacts with KIF5 via kinesin-light chain (KLC) KIF5 predominantly moves toward the somatoaxon area, (Verhey *et al.*, 2001; Bowman *et al.*, 2000; Ito *et al.*, 1999). These data indicate that GRIP1 is a major adaptor protein for KIF5 and is a regulator for the movement of KIF5 to the dendrites. Here, my results confirmed a similar function for GRIP1, namely that distribution of GRIP1 is regulated by the KIF5C motor protein. When neurons expressed a dominant-negative KIF5C construct characterized by the deletion of its motor domain, the distribution of GRIP1 was largely changed to either aggregation in the cell body or removal from the dendrites when compared to control cells expressing GFP construct with no insert. In contrast, GRIP1 was highly distributed either over the cell body or over the dendrites when wildtype KIF5C was overexpressed.

Accordingly, I analyzed distribution of N-Cadherin in neurons expressing either GFP alone, GFP-fused full-length KIF5C, or GFP-fused dominant-negative KIF5C. As a result, I observed distribution of N-Cadherin similar to the distribution of mRFP-GRIP1. Moreover, it revealed that GFP-KIF5C regulates surface expression of N-Cadherin because N-Cadherin cell surface levels decreased when co-expressed with dominant-negative GFP-KIF5C. These results suggest that transport of N-Cadherin is mediated by KIF5 for its surface expression and localization. Although a transport complex, N-Cadherin-p120-catenin-KIF5, showing that KIF5 transports N-Cadherin via the N-terminal domain of p120-catenin has been already reported (Yanagisawa *et al.*, 2004; Chen *et al.*, 2003; Mary *et al.*, 2002), my results introduce another KIF5-driven transport complex, N-Cadherin-GRIP1-KIF5. Combining the previous finding that GRIP1 directly interacts with N-

Cadherin (Schurek, 2006) with my results indicate that the three potential components, N-Cadherin, GRIP1, and KIF5, for a new transport complex interact with each other. Moreover, another motor protein, KIF3, also transports N-Cadherin together with β -catenin (Teng *et al.*, 2005). The transport of N-Cadherin could be mediated by various transport systems because N-Cadherin is essential for many cellular functions. The level of difference in distribution between GRIP1 and N-Cadherin is only slightly observed. Although one transport complex for N-Cadherin is interfered with by disrupting its motor protein, another transport complex exists, which uses KIF3, for N-Cadherin transport (Teng *et al.*, 2005). However, GRIP1 has been identified as an adaptor protein for KIF5 (Hoogenraad *et al.*, 2005; Setou *et al.*, 2002). This could be a possible explanation why the distribution of GRIP1 is more affected than the distribution of N-Cadherin through the disruption of the KIF5 motor protein.

Although it is well established that KIF5 is the major motor protein involved with the transport of GluR2 through the GRIP1 adaptor (Setou *et al.*, 2002), some other transport systems to transport AMPA receptors, including GluR2, exist (Ko *et al.*, 2003; Shin *et al.*, 2003). The interaction between the liprin- α -AMPA receptors-GRIP1 complex and GIT1, a multidomain protein with GTPase-activating protein activity for the ADP-ribosylation factor family of small GTPases known to regulate protein trafficking and the actin cytoskeleton, could transport AMPA receptors to the postsynaptic membrane (Ko *et al.*, 2003). Moreover, Shin *et al.* showed that the liprin- α -AMPA receptors-GRIP1 complex interacts with the neuron-specific kinesin motor protein KIF1 and that this transport complex regulates trafficking of AMPA receptors (Shin *et al.*, 2003). However, previous data along with my results demonstrated that KIF5 can effectively transport AMPA receptors, particularly the GluR2-containing AMPA receptor (Setou *et al.*, 2002).

6-2-4. Functional ablation of KIF5 and GRIP1 decrease GluR2 and N-Cadherin surface expression

It has been well characterized that the kinesin superfamily consists of transport motor proteins that move along microtubule tracks to transport a variety of cargos to the cell surface over long distances (Seiler *et al.*, 1997; Hirokawa, 1996). In addition, disruption of the microtubules by nocodazole treatment completely inhibits the anterograde and retrograde transport machinery (Mary *et al.*, 2002).

Because the level of N-Cadherin surface expression is decreased both through disruption of microtubules by nocodazole treatment and through interference of the motor protein function by dominant-negative GFP-KIF5C, my results suggested that N-Cadherin surface levels are related with KIF5 motor protein along the microtubules. Although it has been reported that the interaction complex between the N-terminal of p120-catenin and N-Cadherin is transported by KIF5 (Yanagisawa *et al.*, 2004; Chen *et al.*, 2003; Mary *et al.*, 2002), my results described different transport complex in terms of adaptor protein. The functional interference of GRIP1 revealed a relationship between N-Cadherin and GRIP1 for level of N-Cadherin surface expression. When expressing a competitive blockade peptide GRIP1 (GFP-GRIP1-PDZ2), which contains only PDZ2 out of 7 PDZ domains, N-Cadherin surface expression is significantly decreased as compared to cells expressing wildtype GFP-GRIP1. Together with a previous report showing that N-Cadherin directly interacts with GRIP1 (Schurek, 2006), these results suggest that N-Cadherin-GRIP1-KIF5 travels together in one complex and that this complex may be related with surface expression of N-Cadherin.

I controlled that GRIP1 controls surface expression of GluR2 (Steiner *et al.*, 2005). When expressing GFP-GRIP1-PDZ2, the levels of surface expressed GluR2 decreased as compared with cells expressing GFP-GRIP1. This is an unexpected result because the interaction region between GluR2 and GRIP1 is different than that between N-Cadherin and GRIP1. Thus, these two molecules, N-Cadherin and GluR2, do not share an interaction region on GRIP1. Moreover, although the surface expression of N-Cadherin should be inhibited by GFP-GRIP1-PDZ2 expression, the level of GluR2 surface expression shouldn't be changed. However, the level of GluR2 surface expression was changed by GFP-GRIP1-PDZ2. These results suggest that there is some relationship between N-Cadherin and GluR2 during their transport. Interestingly, recent studies showed evidence that an interaction between N-Cadherin and the GluR2-containing AMPA receptor is essential and that the interaction highly regulates presynaptic development and function as well as long-lasting changes in synaptic strength, including LTP and LTD (Zhou *et al.*, 2011; Saglietti *et al.*, 2007). In particular, Saglietti *et al.* demonstrated in neurons that N-Cadherin is a major extracellular binding partner of GluR2. Using exogenous GluR2, they demonstrated that GluR2 induces bigger and more abundant spines through the interaction between N-Cadherin and GluR2 regulates spines formation (Saglietti *et al.*, 2007). However, Saglietti *et al.*

indicated that the interaction between N-Cadherin and GluR2 occurs extracellularly (Saglietti *et al.* 2007).

The AMPA receptors are essential for determining synaptic strength and synaptic trafficking of AMPA receptors is highly regulated (Malinow and Malenka, 2002). Although many approaches have suggested that AMPA receptor trafficking and surface expression are important, only one major mechanism that AMPA receptor trafficking is governed the regulated interaction of intracellular C-termini of AMPA receptors subunits with PDZ domain-containing proteins has been considered (Chung *et al.*, 2003; Xia *et al.*, 1999; Srivastava *et al.*, 1998; Dong *et al.*, 1997). Recently, some studies have suggested that AMPA receptors are regulated together with N-Cadherin (Zhou *et al.*, 2011; Saglietti *et al.*, 2007; Nuriya and Hugarir, 2006; Dunah *et al.*, 2005). Dunah *et al.* demonstrated that the leukocyte common antigen-related (LAR) receptor promotes the synaptic recruitment of AMPA receptors, N-Cadherin, and β -catenin and that these molecules are associated with each other. Finally, these associations promote the growth of dendritic spines (Dunah *et al.*, 2005). In support of this, Nuriya and Hugarir showed that a biochemical interaction between N-Cadherin and AMPA receptors occurs in the brain as well as in heterologous cell lines and that this interaction is related with β -catenin. Through this triple interaction, N-Cadherin and AMPA receptors are linked together, and this link plays several key roles in the structural and functional plasticity of synapses (Nuriya and Hugarir, 2006).

In general, N-Cadherin is present in both pre- and postsynaptic membranes, whereas the GluR2-containing AMPA receptor is dominantly localized on the postsynaptic membrane. However, previous results were not clarified about whether the biochemical interaction between N-Cadherin and AMPA receptors is *cis*-dimerization. Through a discovery that the N-terminal domain of the GluR2 subunit promotes spine growth in cultured neurons (Passafaro *et al.*, 2003), it was possible to show using cell aggregation and bead aggregation experiments that N-Cadherin and AMPA receptors bind on both side of the synapses via in *cis*- and in *trans*-dimerizations (Saglietti *et al.*, 2007). Using a competitive GluR2 peptide (GluR2N), which contains only the 92 amino acids at the N-terminus of GluR2 (extracellular domain of GluR2), an interaction between N-Cadherin and GluR2 was examined in HEK293 cells. Because HEK293TN cells express no AMPA receptors, N-Cadherin is not possible to show interaction between N-Cadherin and GluR2 at extracellular membrane without expressing full-length GluR2 construct.

However, HEK293TN cell expressing GFP-GluR2N (no binding site for motor protein) showed interaction between N-Cadherin and GluR2N. The result suggested that the interaction between N-Cadherin and GluR2 occurs intracellularly before transport to the membrane. Moreover, the surface expression of N-Cadherin was significantly decreased when cells expressed GFP-GluR2N. These results suggested that trafficking of N-Cadherin is controlled by the GluR2-containing AMPA receptor subunit.

6-2-5. GluR2 and N-Cadherin are formed in the same vesicle and undergo co-transport

Previous studies have identified that N-Cadherin and GluR2-containing AMPA receptor, including GluR2, interact either directly or indirectly and that several molecules are independently involved in the trafficking of N-Cadherin and GluR2 (Zhou *et al.*, 2011; Saglietti *et al.*, 2007; Nuriya and Haganir, 2006; Dunah *et al.*, 2005; Setou *et al.*, 2002; Dong *et al.*, 1997). These approaches together with my previous results implied that a relationship between N-Cadherin and GluR2 exist and that this relationship may occur during their transport. In addition, Zhou *et al.* and Saglietti *et al.* demonstrated that N-Cadherin directly interacts with GluR2-containing AMPA receptors (Zhou *et al.*, 2011; Saglietti *et al.*, 2007). Although they suggested that the interaction between N-Cadherin and GluR2 occurs extracellularly, they did not directly examine where the association between N-Cadherin and GluR2 occurs. Here, I showed that N-Cadherin interacts with GluR2 as well as with other components of a transport complex, GluR2-GRIP1-KIF5. This result indicated the interaction occurs intracellularly although it is yet unclear whether the interaction between N-Cadherin and GluR2 is a direct or an indirect interaction.

Using live cell observation of fluorescently labeled receptors, the AMPA receptor turnover, namely their exocytosis, internalization, and lateral diffusion, has been intensively studied (Choquet, 2010; Hirling, 2009; Jaskolski and Henley, 2009; Groc *et al.*, 2007). However, the intracellular transport machinery for the AMPA receptor still remains elusive. In brief, AMPA receptors are associated in the endoplasmic reticulum (ER) network after translation and the associated AMPA receptors exit the ER network and enter the Golgi compartment where they become fully glycosylated. Newly synthesized AMPA receptors have to travel a

long distance along their cytoskeletal tracks, such as microtubules and actin filaments, to their final synaptic target regions. Additionally, interaction between synthesized AMPA receptors and some cytosolic proteins enhance the exit of the AMPA receptors from the ER network (Perez *et al.*, 2001; Dev *et al.*, 1999). For example, the GluR2 C-terminus has a PDZ consensus motif (-SVKI), which binds with PDZ-containing proteins, such as protein interacting with C-kinase 1 (PICK1) and GRIP1 (Chung *et al.*, 2003; Perez *et al.*, 2001; Dev *et al.*, 1999; Dong *et al.*, 1999; Xia *et al.*, 1999; Osten *et al.*, 1998). In particular, this interaction is required for the exit of GluR2-containing AMPA receptors from the ER network (Greger *et al.*, 2002).

Thus, it is conceivable that N-Cadherin and GluR2 are co-localized and co-transported together, when two molecules, N-Cadherin and GluR2, are placed in the same vesicle. An immunogold-labeled electron microscope result identified that N-Cadherin and GluR2 co-localize on the ER lumen. Other observations clearly show that N-Cadherin and GluR2 are formed in the same vesicle. This result can be interpreted to show that N-Cadherin and GluR2 co-localized in the same vesicle are independently connected with GRIP1 since it has been demonstrated that GRIP1 can directly interact with both N-Cadherin (Schurek, 2006) and GluR2 (Dong *et al.*, 1997) (see Figure 6-1). Previous studies have explained that the exit of GluR2 from the ER network is dependent on the interaction of GluR2 with PDZ-containing proteins (Greger *et al.*, 2002; Dong *et al.*, 1999). The PDZ-containing protein, GRIP1, directly interacts with KIF5 (Setou *et al.*, 2002) as well as with the C-terminal PDZ motif of GluR2 (Dong *et al.*, 1997). Through these interactions, the transport complex moves in the anterograde direction along the microtubules. My previous results suggested that a novel transport complex exists, which transports N-Cadherin and GluR2 together in the same vesicle. Although previous studies have reported that N-Cadherin is transported by two different motor proteins, KIF3 (Teng *et al.*, 2005) and KIF5 (Yanagisawa *et al.*, 2004; Chen *et al.*, 2003; Mary *et al.*, 2002), its movement has not been examined so far in the neurons. Thus, using live cell time-lapse microscopy, I showed that N-Cadherin moves both in the anterograde and retrograde directions, and that some N-Cadherin particles remain stationary in the neurons. I additionally showed that N-Cadherin and GluR2 co-migrated over the time.

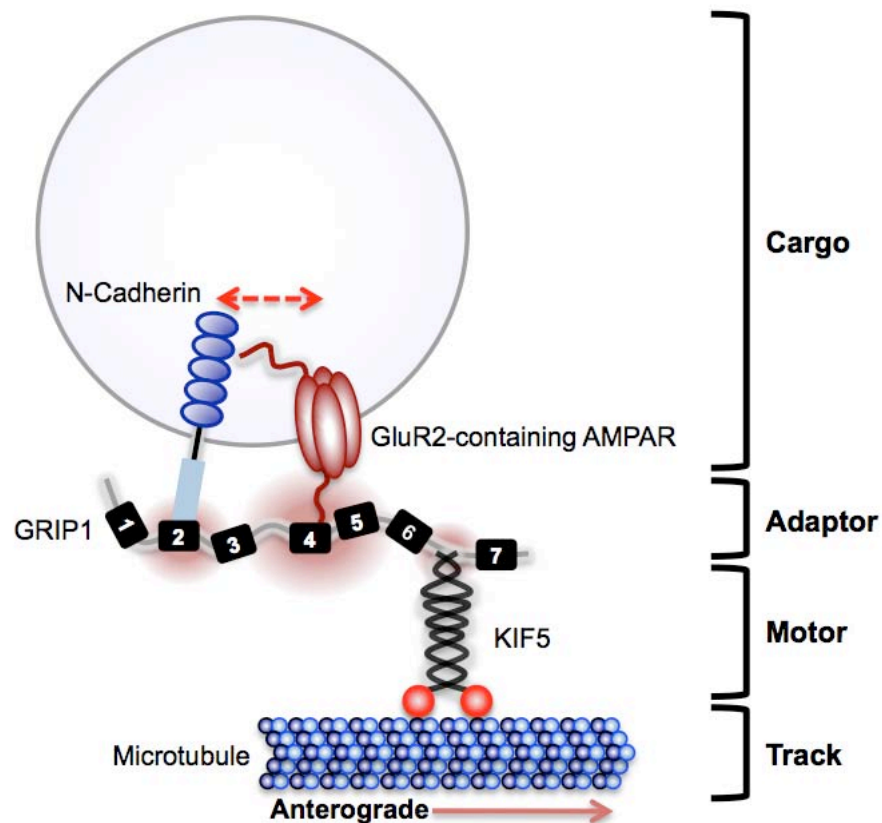


Figure 6-1. Hypothetical model of a KIF5-driven new transport complex. N-Cadherin is transported together with the GluR2-containing AMPA receptor in the same vesicle. KIF5 walks on microtubules in the anterograde direction and interacts with GRIP1 as previously mentioned (Setou *et al.*, 2002). GRIP1 interacts with the GluR2-containing AMPA receptor (Dong *et al.*, 1997) as well as with N-Cadherin through PDZ2 domain of GRIP1 (Schurek, Diplomarbeit, 2006). Each point of interaction is marked by a red background gradient circle. The new transport complex consists of N-Cadherin, GluR2, GRIP1, and KIF5.

Therefore, these results strongly suggest that N-Cadherin and GluR2 interact with each other and that these molecules migrate in the same vesicle via the GRIP1 adaptor. The novel transport complex is comprised of N-Cadherin, GluR2, GRIP1, and KIF5.

The hypothetical model for this novel transport complex is shown in Figure 6-1. GRIP1, a multi-PDZ-containing protein, acting as an adaptor protein is essential for this transport complex and there are three binding sites for the other components of the transport complex. GRIP1 can interact with both N-Cadherin

and with the GluR2-containing AMPA receptor; N-Cadherin interacts with the PDZ2 domain of GRIP1 (Schurek, 2006) and GluR2 interacts with the PDZ4, PDZ5, and the additional 30 amino acids on the N-terminal side of the PDZ4 of GRIP1 (Dong *et al.*, 1997). Finally, these three interacting components are associated with a motor protein, KIF5 (Setou *et al.*, 2002). Therefore, this novel transport complex moves in the anterograde direction along the microtubules. Moreover, a direct interaction between N-Cadherin and GluR2 occurs in the vesicle. Although previous studies suggested that the interaction between N-Cadherin and GluR2 appears between their extracellular domains in the extracellular space (Zhou *et al.*, 2011; Saglietti *et al.*, 2007), my results show that the interaction occurs intracellularly during their transport.

6-2-6. KIF5C and N-Cadherin/GRIP1 binding is involved in the regulation of spine numbers

The exocytosis event is crucial for cellular processes, such as morphogenesis, cell growth, and cell migration. It is well established that most intracellular membrane sorting in eukaryotic cells is governed by the small GTPases of the Rab family (Zerial and McBride, 2001). For example, recycling endosomes, which are driven by the small GTPase Rab11, mediate the activity-dependent delivery of GluR1-containing AMPA receptors into the synapses while another small GTPase, Rab8, regulates synaptic insertion of GluR1 (Hattula *et al.*, 2006; Gerges *et al.*, 2004; Park *et al.*, 2004). Therefore, the exocytosis of GluR1-containing AMPA receptors is controlled at least two distinct membrane compartments by the small GTPases, Rab8 and Rab11. Rab11-containing endosomes are localized at the base of dendritic spines, whereas Rab8 is located more proximally, toward the postsynaptic membrane (Park *et al.*, 2006; Gerges *et al.*, 2004). In addition, it has reported that the exocyst complex, which consists of Sec3, Sec5, Sec6, Sec8, Sec10, Sec15, Exo70, and Exo84, is also involved in the exocytosis event through their interactions with the vesicles and the membrane. Interference with the Exo70 subunit of the exocyst inhibits exocytosis of AMPA receptors because the Exo70 regulates AMPA receptors-containing vesicular fusion with synaptic membranes (Gerges *et al.*, 2006). Moreover, Sec8 was suggested to control the movement of AMPA receptors to the postsynaptic membrane via PDZ-containing protein-dependent interactions (Mao *et al.*, 2010; Gerges *et al.*, 2006). In particular, Mao

et al. demonstrated that GluR2 interacts with both GRIP1 and Sec8 (Mao *et al.*, 2010). My study importantly demonstrated the interaction between N-Cadherin, GluR2, GRIP1, and Sec8. This result suggested that Sec8 as an exocyst component might be involved in the movement of the novel transport complex in terms of interaction between Sec8 and either N-Cadherin or GluR2.

At the synapses, glutamate receptors and cell adhesion molecules are essential for biological processes such as synaptic formation and synaptic strength. AMPA receptors mainly conduct fast excitatory synaptic transmission in the CNS and these AMPA receptors together with N-Cadherin are involved in many of cellular and biological regulations, such as spines formation and synaptic plasticity (Zhou *et al.*, 2011; Saglietti *et al.*, 2007). One preliminary electrophysiology approach remarkably showed that interfering with N-Cadherin surface expression largely decreases AMPA receptor current as compared to control (personal communication with Prof. Dr. J. R. Schwarz). In detail, AMPA receptor currents were decreased when surface expression of N-Cadherin was reduced due to the expression of GFP-GRIP1-PDZ2. GFP-GRIP1-PDZ2 interacts with N-Cadherin in a competitive manner and thereby inhibits the transport of N-Cadherin. The decreased levels of AMPA receptor currents correlated with the expression of GFP-GRIP1-PDZ2 in the neurons. During the neurogenesis it is likely that both molecules, N-Cadherin and GluR2, might be necessary to precisely respond to change in neuronal activity.

Furthermore, I showed that the spine density is decreased by either interfering KIF5 motor function or with N-Cadherin transport. A previous study suggested that inhibition of the extracellular interaction between N-Cadherin and GluR2 reduces spine density and alters miniature excitatory postsynaptic currents (Saglietti *et al.*, 2007). In addition to this study, my results indicated that N-cadherin surface expression can be disrupted by interference with either the motor protein KIF5C or the interaction between N-Cadherin and GRIP1 intracellularly, leading to a decrease in spine density.

Together, these results suggest a new transport complex consisting of N-Cadherin, GluR2, and GRIP1 driven by KIF5 along the microtubule cytoskeleton in an anterograde direction. Although both N-Cadherin and GluR2 are also independently transported, these findings offer a new possibility how N-Cadherin and GluR2-containing AMPA receptor are co-transported. This might be necessary during synaptic plasticity to change synaptic strength.

6-3. Outlook

In this study, I demonstrated that N-Cadherin and GluR2-containing AMPA receptors independently interact with the adaptor protein, GRIP1, through two distinct PDZ domain regions of GRIP1 and that this trimerized complex is finally linked to the motor protein, KIF5. Moreover, dendritic spine numbers were decreased in neurons either by interfering with N-Cadherin binding to the complex or by disrupting motor function of the complex. Therefore, co-migration of N-Cadherin and GluR2 seems to be important to regulate the spine density on dendrites.

Previous studies have suggested that N-Cadherin and GluR2 each have separate transport complexes targeting the molecules to the synapses. It is believed that, during the initiation phase in synapse formation, cell adhesion molecules, such as N-Cadherin, are transported to the synapse. Afterward, during the elongation phase, the expression of receptors, such as AMPA and NMDA receptors, are increased at the postsynaptic membrane to facilitate and communicate between the pre- and postsynapse. Thus, it is conceivable that independent trafficking of N-Cadherin and GluR2-containing AMPA receptors occurs through different transport complexes. However, during the elongation phase of synapse formation, a larger number of these molecules are still needed for synaptic functions and synaptic formation. Here, the co-transport of N-Cadherin and GluR2 might effectively play several roles in the development of functional synapses.

To prove this regulation by the novel transport complex consisting of N-Cadherin, GluR2, GRIP1, and KIF5, further investigation must follow. The functional interference of N-Cadherin transport has been examined in this study but further investigations with a similar concept are needed. For example, interference with either GluR2 transport or KIF5 binding by blocking the specific interaction regions on GRIP1 should be investigated. Through the interference of the complex, pre- and postsynaptic functions should be investigated using electrophysiological studies. In addition, a neuronal activity inducing experiment may be interesting to observe in neurons either interfering with the function of the complex or induced neuronal activity compared to their control. Moreover, although specific exocytosis of the novel transport complex can be explained, the single inhibition of the exocyst complex helps to understand further transport mechanisms. Finally, an *in*

vivo approach will be required to characterize the function of the novel transport complex.

References

Abe, K., Chisaka, O., Van Roy, F., Takeichi, M. (2004). Stability of dendritic spines and synaptic contacts is controlled by alpha N-catenin. *Nat Neurosci.* 7:357-363.

Aiga, M., Levinson, J.N., Bamji, S.X. (2010). N-cadherin and neuroligins cooperate to regulate synapse formation in Hippocampal cultures. *J Biol Chem.* 286(1):851-8.

Aizawa, H., Sekine, Y., Takemura, R., Zhang, Z., Nangaku, M., Hirokawa, N. (1992). Kinesin family in murine central nervous system. *J Cell Biol.* 119:1287-1296.

Alexander, J.E., Hunt, D.F., Lee, M.K., Shabanowitz, J., Michel, H., Berlin, S.C., MacDonald, T.L., Sundberg, R.J., Rebhun, L.I., Frankfurter, A. (1991). Characterization of posttranslational modifications in neuron-specific class III beta-tubulin by mass spectrometry. *Proc Natl Acad Sci U S A.* 88,4685-4689.

Andersson, O., Stenqvist, A., Attersand, A., von Euler, G. (2001). Nucleotide sequence, genomic organization, and chromosomal localization of genes encoding the human NMDA receptor subunits NR3A and NR3B. *Genomics* 78(3):178-84.

Aoki, E., Semba, R., Keino, H., Kato, K., Kashiwamata, S. (1988). Glycine-like immunoreactivity in the rat auditory pathway. *Brain Res.* 442,63-71.

Arikkath, J., Peng, I.F., Ng, Y.G., Israely, I., Liu, X., Ullian, E.M., Reichardt, L.F. (2009). Delta-catenin regulates spine and synapse morphogenesis and function in hippocampal neurons during development. *J Neurosci.* 29(17):5435-42.

Arimura, N., Kimura, T., Nakamuta, S., Taya, S., Funahashi, Y., Hattori, A., Shimada, A., Me´nager, C., Kawabata, S., Fujii, K., Iwamatsu, A., Segal, R.A., Fukuda, M., Kaibuchi, K. (2009). Anterograde transport of TrkB in axons is

- mediated by direct interaction with Slp1 and Rab27. *Dev Cell* 16,675–686.
- Armstrong, N., Sun, Y., Chen, G.Q., Gouaux, E. (1998). Structure of a glutamate-receptor ligand-binding core in complex with kainate. *Nature* 395(6705):913–7.
- Asztély, F. and Gustafsson, B. (1996). Ionotropic glutamate receptors. Their possible role in the expression of hippocampal synaptic plasticity. *Mol Neurobiol.* 12(1):1–11.
- Audebert, S., Desbruyères, E., Gruszczynski, C., Koulakoff, A., Gros, F., Denoulet, P., Eddé, B. (1993). Reversible polyglutamylation of alpha- and beta-tubulin and microtubule dynamics in mouse brain neurons. *Mol Biol Cell* 4,615–626.
- Baas, P.W., Deitch, J.S., Black, M.M., Banker, G.A. (1988). Polarity orientation of microtubules in hippocampal neurons: Uniformity in the axon and nonuniformity in the dendrite. *Proc. Natl. Acad. Sci. USA* 85,8335–8339.
- Baas, P.W., Black, M.M., Banker, G.A. (1989). Changes in microtubule polarity orientation during the development of hippocampal neurons in culture. *J. Cell Biol.* 109,3085–3094.
- Baude, A., Nusser, Z., Roberts, J.D., Mulvihill, E., McIlhinney, R.A., Somogyi, P. (1993). The metabotropic glutamate receptor (mGluR1 alpha) is concentrated at perisynaptic membrane of neuronal subpopulations as detected by immunogold reaction. *Neuron* 11(4):771-87.
- Bazzoni, G. and Dejana, E. (2004). Endothelial cell-to-cell junctions: molecular organization and role in vascular homeostasis. *Physiol Rev.* 84,869–901.
- Bear, M.F. and Abraham, W.C. (1996). Long-term depression in hippocampus. *Annu Rev Neurosci.* 19:437-62.
- Benson, D.L. and Tanaka, H. (1998). N-cadherin redistribution during synaptogenesis in hippocampal neurons. *J. Neurosci.* 18,6892–6904.

- Bettler, B. and Tiao, J.Y. (2006). Molecular diversity, trafficking and subcellular localization of GABAB receptors. *Pharmacol Ther.* 110, 533–543.
- Bobinnec, Y., Moudjou, M., Fouquet, J.P., Desbruyères, E., Eddé, B., Bornens, M. (1998). Glutamylation of centriole and cytoplasmic tubulin in proliferating non-neuronal cells. *Cell Motil Cytoskeleton* 39,223–232.
- Bonanomi, D., Benfenati, F., Valtorta, F. (2006). Protein sorting in the synaptic vesicle life cycle. *Prog Neurobiol.* 80:177-217.
- Bonnet, C., Boucher, D., Lazereg, S., Pedrotti, B., Islam, K., Denoulet, P., Larcher, J.C. (2001). Differential binding regulation of microtubule-associated proteins MAP1A, MAP1B, and MAP2 by tubulin polyglutamylation. *J Biol Chem.* 276,12839–12848.
- Bormann, J. and Feigenspan, A. (1995). GABAC receptors. *Trends Neurosci.* 18, 515–519.
- Bourne, J. and Harris, K.M. (2007). Do thin spines learn to be mushroom spines that remember? *Curr Opin Neurobiol.* 17(3):381–86.
- Bowman, A.B., Kamal, A., Ritchings, B.W., Philp, A.V., McGrail, M., Gindhart, J.G., Goldstein, L.S. (2000). Kinesin-dependent axonal transport is mediated by the sunday driver (SYD) protein. *Cell* 103(4):583-94.
- Boyer, C., Schikorski, T., and Stevens, C.F. (1998). Comparison of hippocampal dendritic spines in culture and in brain. *J Neurosci.* 18(14):5294-300.
- Brackenbury, R., Rutishauser, U., Edelman, G.M. (1981). Distinct calcium-independent and calcium-dependent adhesion systems of chicken embryo cells. *Proc Natl Acad Sci U S A.* 78(1):387–91.
- Brady, S.T. (1985). A novel brain ATPase with properties expected for the fast axonal transport motor. *Nature* 317,73–75.

- Bre, M.H., de Nechaud, B., Wolff, A., Fleury, A. (1994). Glutamylated tubulin probed in ciliates with the monoclonal antibody GT335. *Cell Motil Cytoskeleton* 27,337–349.
- Brown, A. (2003). Axonal transport of membranous and nonmembranous cargoes: a unified perspective. *J Cell Biol.* 160(6):817-21.
- Brückner, K., Pablo, Labrador, J., Scheiffele, P., Herb, A., Seeburg, P.H., Klein, R. (1999). EphrinB ligands recruit GRIP family PDZ adaptor proteins into raft membrane microdomains. *Neuron* 22(3):511-24.
- Cai, Q., Gerwin, C., Sheng, Z.H. (2005). Syntabulin-mediated anterograde transport of mitochondria along neuronal processes. *J Cell Biol.* 170,959–969.
- Cavallaro, U. and DeJana, E. (2011). Adhesion molecule signalling: not always a sticky business. *Nat Rev Mol Cell Biol.* 12(3):189-97.
- Chang, F.L. and Greenough, W.T. (1984). Transient and enduring morphological correlates of synaptic activity and efficacy change in the rat hippocampal slice. *Brain Res.* 309, 35–46.
- Chavas, J. and Marty, A. (2003). Coexistence of excitatory and inhibitory GABA synapses in the cerebellar interneuron network. *J Neurosci.* 23:2019–2031.
- Chen, X., Kojima, S., Borisy, G.G., Green, K.J. (2003). p120 catenin associates with kinesin and facilitates the transport of cadherin-catenin complexes to intercellular junctions. *J Cell Biol.* 163(3):547-57.
- Cheney, R.E. and Baker, J.P. (1999). Myosins, divergent. In Guidebook to the Cytoskeletal and Motor Proteins, *T.E. Kreis and R. Vale, eds.* (Oxford: Oxford University Press), pp. 453–456.
- Choquet, D. (2010). Fast AMPAR trafficking for a high-frequency synaptic transmission. *Eur J Neurosci.* 32(2):250-60.

- Chung, H.J., Xia, J., Scannevin, R.H., Zhang, X., Huganir, R.L. (2000). Phosphorylation of the AMPA receptor subunit GluR2 differentially regulates its interaction with PDZ domain-containing proteins. *J Neurosci.* 20:7258–7267.
- Chung, H.J., Steinberg, J.P., Huganir, R.L., Linden, D.J. (2003). Requirement of AMPA receptor GluR2 phosphorylation for cerebellar long-term depression. *Science* 300:1751– 1755.
- Colin, E., Zala, D., Liot, G., Rangone, H., Borrell-Page`s, M., Li, X.J., Saudou, F., Humbert, S. (2008). Huntingtin phosphorylation acts as a molecular switch for anterograde/retrograde transport in neurons. *EMBO J.* 27,2124–2134.
- Collingridge, G.L. and Bliss, T.V. (1995). Memories of NMDA receptors and LTP. *Trends Neurosci.* 18(2):54-6.
- Conde, C. and Caceres, A. (2009). Microtubule assembly, organization and dynamics in axons and dendrites. *Nat. Rev. Neurosci.* 10,319–332.
- Couve, A., Moss, S.J., Pangalos, M.N. (2000). GABAB receptors: a new paradigm in G protein signaling. *Mol Cell Neurosci.* 16, 296–312.
- Cull-Candy, S., Brickley, S., Farrant, M. (2001). NMDA receptor subunits: diversity, development and disease. *Curr Opin Neurobiol.* 11(3):327–35.
- Curtis, D.R., Phillis, J.W., Watkins, J.C. (1960). The chemical excitation of spinal neurones by certain acidic amino acids. *J Physiol.* 150:656–82.
- Daggett, L.P., Johnson, E.C., Varney, M.A., Lin, F.F., Hess, S.D., Deal, C.R., Jachec, C., Lu, C.C., Kerner, J.A., Landwehrmeyer, G.B., Standaert, D.G., Young, A.B., Harpold, M.M., Veliçelebi, G. (1998). The human N-methyl-D-aspartate receptor 2C subunit: genomic analysis, distribution in human brain, and functional expression. *J Neurochem.* 71(5):1953-68.
- Danglot, L., Rostaing, P., Triller, A., Bessis, A. (2004). Morphologically identified glycinergic synapses in the hippocampus. *Mol Cell Neurosci.* 27(4):394-403.

- Danysz, W. and Parsons, C.G. (1998). Glycine and N-methyl-D-aspartate receptors: Physiological significance and possible therapeutic applications. *Pharmacol Rev.* 50,597-664.
- Debanne, D., Daoudal, G., Sourdet, V., Russier, M. (2003). Brain plasticity and ion channels. *J Physiol Paris.* 97(4-6): 403–14.
- Dejana, E., Tournier-Lasserre, E., Weinstein, B.M. (2009). The control of vascular integrity by endothelial cell junctions: molecular basis and pathological implications. *Dev Cell* 16,209–221.
- di Penta, A., Mercaldo, V., Florenzano, F., Munck, S., Ciotti, M.T., Zalfa, F., Mercanti, D., Molinari, M., Bagni, C., Achsel, T. (2009). Dendritic LSM1/ CBP80-mRNPs mark the early steps of transport commitment and translational control. *J Cell Biol.* 184,423–435.
- Dev, K.K., Nishimune, A., Henley, J.M., Nakanishi, S. (1999). The protein kinase C alpha binding protein PICK1 interacts with short but not long form alternative splice variants of AMPA receptor subunits. *Neuropharmacology* 38: 635–644.
- Dingledine, R., Borges, K., Bowie, D., Traynelis, S.F. (1999). The glutamate receptor ion channels. *Pharmacol Rev.* 51:7–61.
- Doherty, G.J. and McMahon, H.T. (2008). Mediation, Modulation and Consequences of Membrane-Cytoskeleton Interactions. *Annual Review of Biophysics* 37:65–95.
- Dombeck, D.A., Kasischke, K.A., Vishwasrao, H.D., Ingelsson, M., Hyman, B.T., Webb, W.W. (2003). Uniform polarity microtubule assemblies imaged in native brain tissue by second-harmonic generation microscopy. *Proc. Natl. Acad. Sci. USA* 100,7081–7086.
- Dong, H., O'Brien, R.J., Fung, E.T., Lanahan, A.A., Worley, P.F., Huganir, R.L. (1997). GRIP: A synaptic PDZ domain-containing protein that interacts with AMPA receptors. *Nature* 386:279–284.

- Dong, H., Zhang, P., Song, I., Petralia, R.S., Liao, D., Huganir, R.L. (1999). Characterization of the glutamate receptor-interacting proteins GRIP1 and GRIP2. *J Neurosci.* 19:6930–6941.
- Dumoulin, A., Rostaing, P., Bedet, C., Lévi, S., Isambert, M.F., Henry, J.P., Triller, A., Gasnier, B. (1999). Presence of the vesicular inhibitory amino acid transporter in GABAergic and glycinergic synaptic terminal boutons. *J Cell Sci.* 112 (Pt 6):811-23.
- Dunah, A.W., Hueske, E., Wyszynski, M., Hoogenraad, C.C., Jaworski, J., Pak, D.T., Simonetta, A., Liu, G., Sheng, M. (2005). LAR receptor protein tyrosine phosphatases in the development and maintenance of excitatory synapses. *Nat Neurosci.* 8, 458–467.
- Eddé, B., Rossier, J., Le Caer, J.P., Desbruyères, E., Gros, F., Denoulet, P. (1990). Posttranslational glutamylation of alpha-tubulin. *Science* 247,83–85.
- Ehlers, M.D., Mammen, A.L., Lau, L.F., Huganir, R.L. (1996). Synaptic targeting of glutamate receptors. *Curr Opin Cell Biol.* 8:484–489.
- Elia, L.P., Yamamoto, M., Zang, K., Reichardt, L.F. (2006). p120 catenin regulates dendritic spine and synapse development through Rho-family GTPases and cadherins. *Neuron* 51:43-56.
- Endoh, T. (2004). Characterization of modulatory effects of postsynaptic metabotropic glutamate receptors on calcium currents in rat nucleus tractus solitarius. *Brain Res.* 1024(1-2):212–24.
- Elste, A.M. and Benson, D.L. (2006). Structural basis for developmentally regulated changes in cadherin function in synapses. *J Comp Neurol.* 495:324-335.
- Fejtova, A., Davydova, D., Bischof, F., Lazarevic, V., Altroch, W.D., Romorini, S., Schone, C., Zuschratter, W., Kreutz, M.R., Garner, C.C., Ziv NE, Gundelfinger, E.D. (2009). Dynein light chain regulates axonal trafficking and synaptic levels of Bassoon. *J Cell Biol.* 185,341–355.

- Feng, G., TINTRUP, H., KIRSCH, J., NICHOL, M.C., KUHSE, J., BETZ, H., SANES, J.R. (1998). Dual requirement for gephyrin in glycine receptor clustering and molybdoenzyme activity. *Science* 282,1321–1324
- Fouquet, J.P., Edde, B., Kann, M.L., Wolff, A., Desbruyeres, E., Denoulet, P. (1994). Differential distribution of glutamylated tubulin during spermatogenesis in mammalian testis. *Cell Motil Cytoskeleton* 27,49–58.
- Fuchs, E. and Cleveland, D.W. (1998). A structural scaffolding of intermediate filaments in health and disease. *Science* 279(5350):514–9.
- Fuhrmann, J.C., Kins, S., Rostaing, P., El Far, O., Kirsch, J., Sheng, M., Triller, A., Betz, H., Kneussel, M. (2002). Gephyrin interacts with Dynein light chains 1 and 2, components of motor protein complexes. *J Neurosci.* 22,5393–5402.
- Gauthier, L.R., Charrin, B.C., Borrell-Page`s, M., Dompierre, J.P., Rangone, H., Cordelie`res, F.P., De Mey, J., MacDonald, M.E., Lessmann, V., Humbert, S., Saudou, F. (2004). Huntingtin controls neurotrophic support and survival of neurons by enhancing BDNF vesicular transport along microtubules. *Cell* 118,127–138.
- Gerges, N.Z., Backos, D.S., Esteban, J.A. (2004). Local control of AMPA receptor trafficking at the postsynaptic terminal by a small GTPase of the Rab family. *J Biol Chem.* 279:43870–43878.
- Gerges, N.Z., Backos, D.S., Rupasinghe, C.N., Spaller, M.R., Esteban, J.A. (2006). Dual role of the exocyst in AMPA receptor targeting and insertion into the postsynaptic membrane. *EMBO J.* 25:1623–1634.
- Goldstein, L.S. (1993). With apologies to scheherazade: tails of 1001 kinesin motors. *Annu Rev Genet.* 27:319–351.
- Greger, I.H., Khatri, L., Kong, X., Ziff, E.B. (2003). AMPA receptor tetramerization in mediated by Q/R editing. *Neuron* 40(4):763-74.

- Greger, I.H., Ziff, E.B., Penn, A.C. (2007). Molecular determinants of AMPA receptor subunit assembly. *Trends Neurosci.* 30(8):407–16.
- Groc, L., Lafourcade, M., Heine, M., Renner, M., Racine, V., Sibarita, J.B., Lounis, B., Choquet, D., Cognet, L. (2007). Surface trafficking of neurotransmitter receptor: comparison between single-molecule/quantum dot strategies. *J Neurosci.* 27(46):12433-7.
- Groc, L. and Choquet, D. (2008). Measurement and characteristics of neurotransmitter receptor surface trafficking. *Mol Membr Biol.* 25(4):344-52.
- Guillaud, L., Wong, R., Hirokawa, N. (2008). Disruption of KIF17-Mint1 interaction by CaMKII-dependent phosphorylation: A molecular model of kinesin-cargo release. *Nat Cell Biol.* 10,19–29.
- Gumbiner, B.M. (2005). Regulation of cadherin-mediated adhesion in morphogenesis. *Nat Rev Mol Cell Biol.* 6:622–34.
- Guo, X., Macleod, G.T., Wellington, A., Hu, F., Panchumarthi, S., Schoenfield, M., Marin, L., Charlton, M.P., Atwood, H.L., Zinsmaier, K.E. (2005). The GTPase dMiro is required for axonal transport of mitochondria to Drosophila synapses. *Neuron* 47,379–393.
- Ha, J., Lo, K.W., Myers, K.R., Carr, T.M., Humsi, M.K., Rasoul, B.A., Segal, R.A., Pfister, K.K. (2008). A neuron-specific cytoplasmic dynein isoform preferentially transports TrkB signaling endosomes. *J Cell Biol.* 181,1027– 1039.
- Hammond, J.W., Cai, D., Verhey, K.J. (2008). Tubulin modifications and their cellular functions. *Curr Opin Cell Biol.* 20(1):71-6.
- Harris, K.M., Jensen, F.E., and Tsao, B. (1992). Three-dimensional structure of dendritic spines and synapses in rat hippocampus (CA1) at postnatal day 15 and adult ages: implications for the maturation of synaptic physiology and long-term potentiation. *J Neurosci.* 12,2685–2705.

- Hattula, K., Furuholm, J., Tikkanen, J., Tanhuanpaa, K., Laakkonen, P., Peranen, J. (2006). Characterization of the Rab8-specific membrane traffic route linked to protrusion formation. *J Cell Sci.* 119:4866–4877.
- Hsu, S.C., Hazuka, C.D., Foletti, D.L., Scheller, R.H. (1999). Targeting vesicles to specific sites on the plasma membrane: The role of the sec6/8 complex. *Trends Cell Biol.* 9:150–153.
- Hebb, D. (1949). The organization of behavior. *The organization of behavior.* New York, John Wiley.
- Hirai, H., Kirsch, J., Laube, B., Betz, H., Kuhse, J. (1996). The glycine binding site of the N-methyl-D-aspartate receptor subunit NR1: identification of novel determinants of co-agonist potentiation in the extracellular m3-m4 loop region. *Proc Natl Acad Sci U S A.* 93, 6031-6036.
- Hirling, H. (2009). Endosomal trafficking of AMPA-type glutamate receptors. *Neuroscience* 158:36–44.
- Hirokawa, N. (1993). Axonal transport and the cytoskeleton. *Curr Opin Neurobiol.* 3:724–731.
- Hirokawa, N. (1996). The molecular mechanism of organelle transport along microtubules: the identification and characterization of KIFs (kinesin superfamily proteins). *Cell Struct Funct.* 21(5):357-67.
- Hirokawa, N. (1998). Kinesin and dynein superfamily proteins and the mechanism of organelle transport. *Science* 279, 519–526.
- Hirokawa, N., and Noda, Y. (2008). Intracellular transport and kinesin superfamily proteins, KIFs: Structure, function, and dynamics. *Physiol Rev.* 88,1089–1118.
- Hirokawa, N., Niwa, S., Tanaka, Y. (2010). Molecular motors in neurons: transport mechanisms and roles in brain function, development, and disease. *Neuron* 68(4):610-38.

- Hollenbeck, P.J. Saxton, W.M. (2005). The axonal transport of mitochondria. *J Cell Sci.* 118,5411–5419.
- Hollmann, M., O'Shea-Greenfield, A., Rogers, S.W., and Heinemann, S. (1989). Cloning by functional expression of a member of the glutamate receptor family. *Nature* 342:643–648.
- Hollmann, M. and Heinemann, S. (1994). Cloned glutamate receptors. *Annu Rev Neurosci.* 17:31–108.
- Hollmann, M. (1999). Structure of ionotropic glutamate receptors, Ionotropic Glutamate Receptors in the CNS. *P. Jonas and H. Monyer, Eds., Berlin, Springer:3-119.*
- Hoogenraad, C.C., Milstein, A.D., Ethell, I.M., Henkemeyer, M., Sheng, M. (2005). GRIP1 controls dendrite morphogenesis by regulating EphB receptor trafficking. *Nat Neurosci.* 8(7):906-15.
- Horiguchi, K., Hanada, T., Fukui, Y., Chishti, A.H. (2006). Transport of PIP3 by GAKIN, a kinesin-3 family protein, regulates neuronal cell polarity. *J Cell Biol.* 174, 425–436.
- Horning, M.S. and Mayer, M.L. (2004). Regulation of AMPA receptor gating by ligand binding core dimmer. *Neuron* 41(3):379-388.
- Huang, J.D., Brady, S.T., Richards, B.W., Stenolen, D., Resau, J.H., Copeland, N.G., Jenkins, N.A. (1999). Direct interaction of microtubule- and actin- based transport motors. *Nature* 397,267–270.
- Ikegami, K., Mukai, M., Tsuchida, J., Heier, R.L., Macgregor, G.R., Setou, M. (2006). TTL7 is a mammalian beta-tubulin polyglutamylase required for growth of MAP2-positive neurites. *J Biol Chem.* 281:30707-30716.
- Ikegami, K., Heier, R.L., Taruishi, M., Takagi, H., Mukai, M., Shimma, S., Taira, S., Hatanaka, K., Morone, N., Yao, I., Campbell, P.K., Yuasa, S., Janke, C.,

- Macgregor, G.R., Setou, M. (2007). Loss of alpha-tubulin polyglutamylation in ROSA22 mice is associated with abnormal targeting of KIF1A and modulated synaptic function. *Proc Natl Acad Sci U S A*. 104:3213-3218.
- Ishii, T., Moriyoshi, K., Sugihara, H., Sakurada, K., Kadotani, H., Yokoi, M., Akazawa, C., Shigemoto, R., Mizuno, N., Masu, M., Nakanish, S. (1993). Molecular characterization of the family of the N-methyl-D-aspartate receptor subunits. *J Biol Chem*. 5;268(4):2836-43.
- Ito, M., Yoshioka, K., Akechi, M., Yamashita, S., Takamatsu, N., Sugiyama, K., Hibi, M., Nakabeppu, Y., Shiba, T., Yamamoto, K.I. (1999). JSAP1, a novel jun N-terminal protein kinase (JNK)-binding protein that functions as a Scaffold factor in the JNK signaling pathway. *Mol Cell Biol*. 19(11):7539-48.
- Janke, C., Rogowski, K., Wloga, D., Regnard, C., Kajava, A.V., Strub, J.M., Temurak, N., van Dijk, J., Boucher, D., van Dorselaer, A., Suryavanshi, S., Gaertig, J., Eddé, B. (2005). Tubulin polyglutamylase enzymes are members of the TTL domain protein family. *Science* 308:1758-1762.
- Janke, C. and Kneussel, M. (2010). Tubulin post-translational modifications: encoding functions on the neuronal microtubule cytoskeleton. *Trends Neurosci*. 33(8):362-72.
- Jaskolski, F. and Henley, J.M. (2009). Synaptic receptor trafficking: the lateral point of view. *Neuroscience* 158:19–24.
- Jeyifous, O., Waites, C.L., Specht, C.G., Fujisawa, S., Schubert, M., Lin, E.I., Marshall, J., Aoki, C., de Silva, T., Montgomery, J.M., Garner, C.C., Green, W.N. (2009). SAP97 and CASK mediate sorting of NMDA receptors through a previously unknown secretory pathway. *Nat Neurosci*. 12,1011–1019.
- Jin, Y. and Garner, C.C. (2008). Molecular mechanisms of presynaptic differentiation. *Annu Rev Cell Dev Biol*. 24, 237-262.
- Johansson, M., Rocha, N., Zwart, W., Jordens, I., Janssen, L., Kuijl, C., Olkkonen,

- V.M., Neefjes, J. (2007). Activation of endosomal dynein motors by stepwise assembly of Rab7-RILP-p150Glued, ORP1L, and the receptor betalll spectrin. *J Cell Biol.* 176,459–471.
- Kamal, A., Almenar-Queralt, A., LeBlanc, J.F., Roberts, E.A., Goldstein, L.S. (2001). Kinesin-mediated axonal transport of a membrane compartment containing β -secretase and presenilin-1 requires APP. *Nature* 414,643–648.
- Kanai, Y., Dohmae, N., Hirokawa, N. (2004). Kinesin transports RNA: Isolation and characterization of an RNA-transporting granule. *Neuron* 43,513–525.
- Kandal, E., Schwartz, J., Jessel, T.M. (2000). Principles of neural science. 4th edition. *Mcgraw-Hill Publ. Comp.*, New York, USA
- Karki, S. and Holzbaaur, E.L. (1999). Cytoplasmic dynein and dynactin in cell division and intracellular transport. *Curr Opin Cell Biol.* 11, 45–53.
- Karp, Gerald (2005). *Cell and Molecular Biology: Concepts and Experiments*. USA: John Wiley & Sons. p. 355.
- Kasai, H., Matsuzaki, M., Noguchi, J., Yasumatsu, N., Nakahara, H. (2003). Structure-stability-function relationships of dendritic spines. *Trends Neurosci.* 26(7):360-8.
- Kim, A. J. and Endow, S. A. (2000). *J Cell Sci.* 113,3681–3682.
- Kim, D.Y., Kim, S.H., Choi, H.B., Min, C., Gwag, B.J. (2001). High abundance of GluR1 mRNA and reduced Q/R editing of GluR2 mRNA in individual NADPH-diaphorase neurons. *Mol Cell Neurosci.* 17(6):1025–33.
- Kim, E.Y., Schrader, N., Smolinsky, B., Bedet, C., Vannier, C., Schwarz, G., Schindelin, H. (2006). Deciphering the structural framework of glycine receptor anchoring by gephyrin. *EMBO J.* 25,1385–1395.
- Kim, H., Han, J.R., Park, J., Oh, M., James, S.E., Chang, S., Lu, Q., Lee, K.Y., Ki,

- H., Song, W.J., Kim, K. (2008). Delta-catenin-induced dendritic morphogenesis. An essential role of p190RhoGEF interaction through Akt1-mediated phosphorylation. *J Biol Chem.* 283:977-987.
- Kins, S., Betz, H., Kirsch, J. (2000). Collybistin, a newly identified brain-specific GEF, induces submembrane clustering of gephyrin. *Nat Neurosci.* 3(1):22–9.
- Ko, J., Kim, S., Valtschanoff, J.G., Shin, H., Lee, J.R., Sheng, M., Premont, R.T., Weinberg, R.J., Kim, E. (2003). Interaction between liprin-alpha and GIT1 is required for AMPA receptor targeting. *J Neurosci.* 23:1667–1677.
- Korkotian, E., Holcman, D., Segal, M. (2004). Dynamic regulation of spine-dendrite coupling in cultured hippocampal neurons. *Eur J Neurosci.* 20(10):2649-63.
- Kornau, H-C., Seeburg, P.H., Kennedy, M.B. (1997). Interaction of ion channels and receptors with PDZ domain proteins. *Curr Opin Neurobiol.* 7:368 –373.
- Krnjevic, K. and Phillis, J.W. (1963). Ionophoretic studies of neurones in the mammalian cerebral cortex. *J Physiol.* 165:274–304.
- Larcher, J.C., Boucher, D., Lazereg, S., Gros, F., Denoulet, P. (1996). Interaction of kinesin motor domains with α - and β -tubulin subunits at a tau-independent binding site. Regulation by polyglutamylation. *J Biol Chem.* 271,22117–22124.
- Laube, B., Hirai, H., Sturgess, M., Betz, H., Kuhse, J. (1997). Molecular determinants of agonist discrimination by NMDA receptor subunits: Analysis of the glutamate binding site on the NR2B subunit. *Neuron* 18, 493-503.
- Lawrence, C.J., Dawe, R.K., Christie, K.R., Cleveland, D.W., Dawson, S.C., Endow, S.A., Goldstein, L.S., Goodson, H.V., Hirokawa, N., Howard, J., Malmberg, R.L., McIntosh, J.R., Miki, H., Mitchison, T.J., Okada, Y., Reddy, A.S., Saxton, W.M., Schliwa, M., Scholey, J.M., Vale, R.D., Walczak, C.E., Wordeman, L. (2004). A standardized kinesin nomenclature. *J Cell Biol.* 167,19–22.

- Lechtreck, K.F. and Geimer, S. (2000). Distribution of polyglutamylated tubulin in the flagellar apparatus of green flagellates. *Cell Motil Cytoskeleton* 47,219–235.
- Lee, S.H., Peng, I.F., Ng, Y.G., Yanagisawa, M., Bamji, S.X., Elia, L.P., Balsamo, J., Lilien, J., Anastasiadis, P.Z., Ullian, E.M., Reichardt, L.F. (2008) Synapses are regulated by the cytoplasmic tyrosine kinase Fer in a pathway mediated by p120catenin, Fer, SHP-2, and beta-catenin. *J Cell Biol.* 183:893-908.
- Leonard, A.S., Davare, M.A., Horne, M.C., Garner, C.C., Hell, J.W. (1998). SAP97 is associated with the alpha-amino-3-hydroxy-5-methylisoxazole-4-propionic acid receptor GluR1 subunit. *J Biol Chem.* 273 (31):19518–24.
- Lin, D., Gish, G.D., Songyang, Z., Pawson, T. (1999). The carboxyl terminus of B class ephrins constitutes a PDZ domain binding motif. *J Biol Chem.* 274,3726–3733.
- Liu, Y. and Zhang, J. (2000). Recent development in NMDA receptors. *Chin Med J.* 113(10):948–56.
- Luduena, R.F. (1998). Multiple forms of tubulin: different gene products and covalent modifications. *Int Rev Cytol.* 178, 207–275.
- Lüscher, C., Nicoll, R.A., Malenka, R.C., Muller, D. (2000). Synaptic plasticity and dynamic modulation of the postsynaptic membrane. *Nat Neurosci.* 3(6):545-50.
- Lynch, J.W. (2004). Molecular structure and function of the glycine receptor chloride channel. *Physiological reviews* 84 (4):1051–95.
- Maas, C., Tagnaouti, N., Loebrich, S., Behrend, B., Lappe-Siefke, C., Kneussel, M. (2006). Neuronal cotransport of glycine receptor and the scaffold protein gephyrin. *J Cell Biol.* 172,441–451.
- Maas, C., Belgardt, D., Lee, H.K., Heisler, F.F., Lappe-Siefke, C., Magiera, M.M., van Dijk, J., Hausrat, T.J., Janke, C., Kneussel, M. (2009). Synaptic activation

modifies microtubules underlying transport of postsynaptic cargo. *Proc Natl Acad Sci U S A.* 26;106(21):8731-6.

MacRae, T.H. (1997). Tubulin post-translational modifications — enzymes and their mechanisms of action. *Eur J Biochem.* 244, 265–278.

Malinow, R. and Malenka, R.C. (2002). AMPA receptor trafficking and synaptic plasticity. *Annu Rev Neurosci.* 25,103–126.

Malosio, M.L., Marquèze-Pouey, B., Kuhse, J., Betz, H. (1991). Widespread expression of glycine receptor subunit mRNAs in the adult and developing rat brain. *EMBO J.* 10(9):2401-9.

Makrigiannakis, A., Coukos, G., Christofidou-Solomidou, M., Gour, B.J., Radice, G.L., Blaschuk, O., Coutifaris, C. (1999). N-cadherin-mediated human granulosa cell adhesion prevents apoptosis: a role in follicular atresia and luteolysis? *Am J Pathol.* 154:1391–406.

Mao, L., Takamiya, K., Thomas, G., Lin, D.T., Huganir, R.L. (2010). GRIP1 and 2 regulate activity-dependent AMPA receptor recycling via exocyst complex interactions. *Proc Natl Acad Sci U S A.* 107(44):19038-43.

Mary, J., Redeker, V., Le Caer, J. P., Prome, J. C., Rossier, J. (1994). Class I and IVa β -tubulin isotypes expressed in adult mouse brain are glutamylated. *FEBS Lett.* 353,89–94.

Mary, S., Charrasse, S., Meriane, M., Comunale, F., Travo, P., Blangy, A., Gauthier-Rouvière, C. (2002). Biogenesis of N-cadherin-dependent cell-cell contacts in living fibroblasts is a microtubule-dependent kinesin-driven mechanism. *Mol Biol Cell* 13(1):285-301.

Matsuda, S., Mikawa, S., Hirai, H. (1999). Phosphorylation of serine-880 in GluR2 by protein kinase C prevents its C terminus from binding with glutamate receptor-interacting protein. *J Neurochem.* 73:1765–1768.

- May, S.R., Ashique, A.M., Karlen, M., Wang, B., Shen, Y., Zarbalis, K., Reiter, J., Ericson, J., Peterson, A.S. (2005). Loss of the retrograde motor for IFT disrupts localization of Smo to cilia and prevents the expression of both activator and repressor functions of Gli. *Dev Biol.* 287,378–389.
- Mayer, M.L. and Armstrong, N. (2004). Structure and function of glutamate receptor ion channels. *Annu Rev Physiol.* 66:161-81.
- Mayer, M.L. (2005). Glutamate receptor ion channels. *Curr Opin Neurobiol.* 15(3):282–288.
- Mcbain, C.J. and Mayer, M.L. (1994). N-methyl-D-aspartic acid receptor structure and function. *Physiol Rev.* 74, 723-760.
- Megías M, Emri Z, Freund TF, Gulyás AI. (2001). Total number and distribution of inhibitory and excitatory synapses on hippocampal CA1 pyramidal cells. *Neuroscience* 102(3):527-40.
- Meyer, G., Kirsch, J., Betz, H., Langosch, D. (1995). Identification of a gephyrin binding motif on the glycine receptor beta subunit. *Neuron* 15(3):563-72.
- Miki, H., Setou, M., Kaneshiro, K., Hirokawa, N. (2001). All kinesin super- family protein, KIF, genes in mouse and human. *Proc Natl Acad Sci U S A.* 98,7004–7011.
- Minton, A.P. (1992). Confinement as a determinant of macromolecular structure and reactivity. *Biophys. J.* 63 (4):1090–100.
- Mitchison, T. and Kirschner, M. (1984). Dynamic instability of microtubule growth. *Nature* 312 (5991): 237–42.
- Miyazawa, A., Fujiyoshi, Y., Unwin, N. (2003). Structure and gating mechanism of the acetylcholine receptor pore. *Nature* 423(6943):949–955.

- Monyer, H., Burnashev, N., Laurie, D.J., Sakmann, B., Seeburg, P.H. (1994). Developmental and regional expression in the rat brain and functional properties of four NMDA receptors. *Neuron* 12(3):529-40.
- Muresan, Z., and Muresan, V. (2005). Coordinated transport of phosphorylated amyloid- β precursor protein and c-Jun NH2-terminal kinase-interacting protein-1. *J Cell Biol.* 171, 615–625.
- Nakanishi, S. and Masu, M. (1994). Molecular diversity and functions of glutamate receptors. *Annu Rev Biophys Biomol Struct.* 23:319-48.
- Nakata, T. and Hirokawa, N. (2003). Microtubules provide directional cues for polarized axonal transport through interaction with kinesin motor head. *J Cell Biol.* 162,1045–1055.
- Niwa, S., Tanaka, Y., Hirokawa, N. (2008). KIF1B β - and KIF1A-mediated axonal transport of presynaptic regulator Rab3 occurs in a GTP-dependent manner through DENN/MADD. *Nat Cell Biol.* 10,1269–1279.
- Noda, Y., Sato-Yoshitake, R., Kondo, S., Nangaku, M., Hirokawa, N. (1995). KIF2 is a new microtubule-based anterograde motor that transports membranous organelles distinct from those carried by kinesin heavy chain or KIF3A/B. *J Cell Biol.* 129,157–167.
- Nogales, E., Whittaker, M., Milligan, R. A., Downing, K. H. (1999). High-resolution model of the microtubule. *Cell* 96,79–88.
- Nuriya, M. and Huganir, R.L. (2006). Regulation of AMPA receptor trafficking by N-cadherin. *J Neurochem.* 97, 652–661.
- O'Brien, R.J., Lau, L.F., Huganir, R.L. (1998). Molecular mechanisms of glutamate receptor clustering at excitatory synapses. *Curr Opin Neurobiol.* 8:364–369.
- Ochiishi, T., Futai, K., Okamoto, K., Kameyama, K., Kosik, K.S. (2008). Regulation of AMPA receptor trafficking by delta-catenin. *Mol Cell Neurosci.* 39(4):499-507.

- Okada, Y., Yamazaki, H., Sekine-Aizawa, Y., Hirokawa, N. (1995). The neuron-specific kinesin superfamily protein KIF1A is a unique monomeric motor for anterograde axonal transport of synaptic vesicle precursors. *Cell* 81,769–780.
- Ong, L.L., Kim, N., Mima, T., Cohen-Gould, L., Mikawa, T. (1998). Trabecular myocytes of the embryonic heart require N-cadherin for migratory unit identity. *Dev Biol.* 193:1–9.
- Osten, P., Srivastava, S., Inman, G.J., Vilim, F.S., Khatri, L., Lee, L.M., States, B.A., Einheber, S., Milner, T.A., Hanson, P.I., Ziff, E.B. (1998). The AMPA receptor GluR2 C terminus can mediate a reversible, ATP-dependent interaction with NSF and alpha- and beta-SNAPs. *Neuron* 21:99–110.
- Ottersen OP, Davanger S, Storm-Mathisen J. (1987). Glycine-like immunoreactivity in the cerebellum of rat and Senegalese baboon, *Papio papio*: a comparison with the distribution of GABA-like immunoreactivity and with [3H]glycine and [3H]GABA uptake. *Exp Brain Res.* 66(1):211-21.
- Ozawa, S., Kamiya, H., Tsuzuki, K. (1998). Glutamate receptors in the mammalian central nervous system. *Prog Neurobiol.* 54(5):581-618.
- Palmada, M. and Centelles, J. (1998). Excitatory amino acid neurotransmission. Pathways for metabolism, storage and reuptake of glutamate in brain. *Front Biosci.* 3:d701–18.
- Paoletti, P. and Neyton, J. (2007). NMDA receptor subunits: function and pharmacology. *Curr Opin Pharmacol.* 7(1):39–47.
- Park, M., Penick, E.C., Edwards, J.G., Kauer, J.A., Ehlers, M.D. (2004). Recycling endosomes supply AMPA receptors for LTP. *Science* 305:1972–1975.
- Park, M., Salgado, J.M., Ostroff, L., Helton, T.D., Robinson, C.G., Harris, K.M., Ehlers, M.D. (2006). Plasticity-induced growth of dendritic spines by exocytic trafficking from recycling endosomes. *Neuron* 52:817–830.

- Passafaro, M., Nakagawa, T., Sala, C., Sheng, M. (2003). Induction of dendritic spines by an extracellular domain of AMPA receptor subunit GluR2. *Nature* 424,677–681.
- Pérez-Otaño, I. and Ehlers, M.D. (2005). Homeostatic plasticity and NMDA receptor trafficking. *Trends Neurosci.* 28(5):229–38.
- Perez, J.L., Khatri, L., Chang, C., Srivastava, S., Osten, P., Ziff, E.B. (2001). PICK1 targets activated protein kinase Calpha to AMPA receptor clusters in spines of hippocampal neurons and reduces surface levels of the AMPA-type glutamate receptor subunit 2. *J Neurosci.* 21:5417–5428.
- Perry, R.B. and Fainzilber, M. (2009). Nuclear transport factors in neuronal function. *Semin Cell Dev Biol.* 20,600-606.
- Peters, A. and Kaiserman-Abramof, I.R. (1970). The small pyramidal neuron of the rat cerebral cortex. The perikaryon, dendrites and spines. *Am J Anat.* 127, 321–355.
- Pfeiffer, F., Graham, D., Betz, H. (1982). Purification by affinity chromatography of the glycine receptor of rat spinal cord. *J Biol Chem.* 257(16):9389-93.
- Pfister, K.K., Fisher, E.M., Gibbons, I.R., Hays, T.S., Holzbaur, E.L., McIntosh, J.R., Porter, M.E., Schroer, T.A., Vaughan, K.T., Witman, G.B., King, S.M., Vallee, R.B. (2005). Cytoplasmic dynein nomenclature. *J Cell Biol.* 171,411–413.
- Pfister, K.K., Shah, P.R., Hummerich, H., Russ, A., Cotton, J., Annuar, A.A., King, S.M., Fisher, E.M. (2006). Genetic analysis of the cytoplasmic dynein subunit families. *PLoS Genet.* 2(1):e1.
- Platt, S.R. (2007). The role of glutamate in central nervous system health and disease--a review. *Vet J.* 173(2):278–86.
- Poulopoulos, A., Aramuni, G., Meyer, G., Soykan, T., Hoon, M., Papadopoulos, T., Zhang, M., Paarmann, I., Fuchs, C., Harvey, K., Jedlicka, P., Schwarzacher, S.W.,

- Betz, H., Harvey, R.J., Brose, N., Zhang, W., Varoqueaux, F. (2009). Neuroligin 2 drives postsynaptic assembly at perisomatic inhibitory synapses through gephyrin and collybistin. *Neuron* 63(5):628–42.
- Purves, D., George J. Augustine, David Fitzpatrick, William C. Hall, Anthony-Samuel LaMantia, James O. McNamara, Leonard E. White. (2008). *Neuroscience, 4th Ed.*, Sinauer Associates. pp. 129–131.
- Rácz, B., Blanpied, T.A., Ehlers, M.D., Weinberg, R.J. (2004). Lateral organization of endocytic machinery in dendritic spines. *Nat Neurosci.* 7(9):917-8.
- Rajendra, S., Lynch, J.W., Schofield, P.R. (1997). The glycine receptor. *Pharmacology and Therapeutics* 73 (2):121–146.
- Redeker, V., Levilliers, N., Schmitter, J.M., Le Caer, J.P., Rossier, J., Adoutte, A., Bré, M.H. (1994). Polyglycylation of tubulin: a posttranslational modification in axonemal microtubules. *Science* 266,1688–1691.
- Regnard, C., Desbruyères, E., Huet, J.C., Beauvallet, C., Pernollet, J.C., Eddé, B. (2000). Polyglutamylation of nucleosome assembly proteins. *J Biol Chem.* 275,15969–15976.
- Rogowski, K., Juge, F., van Dijk, J., Wloga, D., Strub, J.M., Levilliers, N., Thomas, D., Bré, M.H., Van Dorsselaer, A., Gaertig, J., Janke, C. (2009). Evolutionary divergence of enzymatic mechanisms for posttranslational polyglycylation. *Cell* 137,1076–1087
- Rosenmund, C., Stern-Bach, Y., Stevens, C.F. (1998). The tetrameric structure of a glutamate receptor channel. *Science* 280(5369):1596–9.
- Roy, S., Winton, M.J., Black, M.M., Trojanowski, J.Q., Lee, V.M. (2007). Rapid and intermittent cotransport of slow component-b proteins. *J Neurosci.* 27(12):3131-8.
- Roy, S., Winton, M.J., Black, M.M., Trojanowski, J.Q., Lee, V.M. (2008).

Cytoskeletal requirements in axonal transport of slow component-b. *J Neurosci.* 28,5248–5256.

Rüdiger, M., Plessman, U., Klöppel, K.D., Wehland, J., Weber, K. (1992). Class II tubulin, the major brain beta tubulin isotype is polyglutamylated on glutamic acid residue 435. *FEBS Lett.* 308,101–105.

Rudolph, U. and Mohler, H. (2004). Analysis of GABAA receptor function and dissection of the pharmacology of benzodiazepines and general anesthetics through mouse genetics. *Annu Rev Pharmacol Toxicol.* 44, 475–498.

Saglietti, L., Dequidt, C., Kamieniarz, K., Rousset, M.C., Valnegri, P., Thoumine, O., Beretta, F., Fagni, L., Choquet, D., Sala, C., Sheng, M., Passafaro, M. (2007). Extracellular interactions between GluR2 and N-cadherin in spine regulation. *Neuron* 54(3):461-77.

Satoh, D., Sato, D., Tsuyama, T., Saito, M., Ohkura, H., Rolls, M.M., Ishikawa, F., Uemura, T. (2008). Spatial control of branching within dendritic arbors by dynein-dependent transport of Rab5-endosomes. *Nat Cell Biol.* 10,1164– 1171.

Schapitz, I. (2009). Mikrotubuli-assoziiertes Transport von postsynaptischem NLG1 in *Rattus norvegicus* (Berkenhout, 1769) und *Mus musculus* (Linnaeus, 1758). *Dissertation*. University of Hamburg, Germany.

Scheiffele, P. (2003). Cell-cell signaling during synapse formation in the CNS. *Annu Rev Neurosci.* 26:485–508.

Schoch, S. and Gundelfinger, E.D. (2006). Molecular organization of the presynaptic active zone. *Cell Tissue Res.* 326, 379-391.

Schroer, T.A. (2004). Dynactin. *Annu Rev Cell Dev Biol.* 20,759–779.

Schurek, B. (2006). Untersuchung der Interaktion von GRIP1 mit dem synaptischen Protein N-Cadherin. *Diplomarbeit*. University of Hamburg, Germany.

- Seeburg, P.H. (1993). The TiPS/TINS lecture: the molecular biology of mammalian glutamate receptor channels. *Trends Pharmacol Sci.* 14(8):297-303.
- Seiler, S., Nargang, F.E., Steinberg, G., Schliwa, M. (1997). Kinesin is essential for cell morphogenesis and polarized secretion in *Neurospora crassa*. *EMBO J.* 16(11):3025-34.
- Setou, M., Nakagawa, T., Seog, D.H., Hirokawa, N. (2000). Kinesin super-family motor protein KIF17 and mLin-10 in NMDA receptor-containing vesicle transport. *Science* 288,1796–1802.
- Setou, M., Seog, D.H., Tanaka, Y., Kanai, Y., Takei, Y., Kawagishi, M., and Hirokawa, N. (2002). Glutamate-receptor-interacting protein GRIP1 directly steers kinesin to dendrites. *Nature* 417, 83–87.
- Shapiro, L., Fannon, A.M., Kwong, P.D., Thompson, A., Lehmann, M.S., Grubel, G., Legrand, J.F., Als-Nielsen, J., Colman, D.R., Hendrickson, W.A. (1995). Structural basis of cell–cell adhesion by cadherins. *Nature* 374:327-337.
- Sheng, M. (1996). PDZs and receptor/channel clustering: rounding up the latest suspects. *Neuron* 17:575–578.
- Sheng, M. and Kim, E. (1996). Ion channel associated proteins. *Curr Opin Neurobiol.* 6:602–608.
- Sheng, M. and Hoogenraad, C.C. (2007). The postsynaptic architecture of excitatory synapses: a more quantitative view. *Annu Rev Biochem.* 76:823-47.
- Sheng, M. and Wyszynski, M. (1997). Ion channel targeting in neurons. *Bioessays* 19:847–853.
- Shi, S.H., Hayashi, Y., Petralia, R.S., Zaman, S.H., Wenthold, R.J., Svoboda, K., Malinow, R. (1999). Rapid spine delivery and redistribution of AMPA receptors after synaptic NMDA receptor activation. *Science* 284(5421):1811–6.

- Shin, H., Wyszynski, M., Huh, K.H., Valtschanoff, J.G., Lee, J.R., Ko, J., Streuli, M., Weinberg, R.J., Sheng, M., Kim, E. (2003). Association of the kinesin motor KIF1A with the multi-modular protein Liprin-alpha. *J Biol Chem.* 278: 11393–11401.
- Sieghart, W. and Sperk, G. (2002). Subunit composition, distribution and function of GABAA receptor subtypes. *Curr Top Med Chem.* 2, 795–816.
- Silverman, J.B., Restituto, S., Lu, W., Lee-Edwards, L., Khatri, L., Ziff, E.B. (2007). Synaptic anchorage of AMPA receptors by cadherins through neural plakophilin-related arm protein AMPA receptor-binding protein complexes. *J Neurosci.* 27(32):8505-16.
- Sine, S. and Engel, A. (2006). Recent advances in Cys-loop receptor structure and function. *Nature* 440(7083):448–55.
- Singer, J.H., Talley, E.M., Bayliss, D.A., Berger, A.J. (1998). Development of glycinergic synaptic transmission to rat brain stem motoneurons. *J Neurophysiol.* 80(5):2608-20.
- Sola, M., Bavro, V.N., Timmins, J., Franz, T., Ricard-Blum, S., Schoehn, G., Ruigrok, R.W., Paarmann, I., Saiyed, T., O'Sullivan, G.A., Schmitt, B., Betz, H., Weissenhorn, W. (2004). Structural basis of dynamic glycine receptor clustering by gephyrin. *EMBO J.* 23,2510–2519.
- Song, I. and Huganir, R.L. (2002). Regulation of AMPA receptors during synaptic plasticity. *Trends Neurosci.* 25(11):578–88.
- Spacek, J. and Harris, K.M. (1997). Three-dimensional organization of smooth endoplasmic reticulum in hippocampal CA1 dendrites and dendritic spines of the immature and mature rat. *J Neurosci.* 17(1):190–203.
- Srivastava, S., Osten, P., Vilim, F.S., Khatri, L., Inman, G., States, B., Daly, C., DeSouza, S., Abagyan, R., Valtschanoff, J.G., Weinberg, R.J., Ziff, E.B. (1998). Novel anchorage of GluR2/3 to the postsynaptic density by the AMPA receptor-

binding protein ABP. *Neuron* 21:581–591.

Su, Q., Cai, Q., Gerwin, C., Smith, C.L., Sheng, Z.H. (2004). Syntabulin is a microtubule-associated protein implicated in syntaxin transport in neurons. *Nat Cell Biol.* 6,941–953.

Sucher, N.J., Awobuluyi, M., Choi, Y.B., Lipton, S.A. (1996). NMDA receptors: from genes to channels. *Trends Pharmacol Sci.* 17, 348-355.

Sudhof, T.C. (2004). The synaptic vesicle cycle. *Annu Rev Neurosci.* 27, 509-547.

Sugihara, H., Moriyoshi, K., Ishii, T., Masu, M., Nakanishi, S. (1992). Structures and properties of seven isoforms of the NMDA receptor generated by alternative splicing. *Biochem Biophys Res Commun.* 30;185(3):826-32.

Sun, Y., Aiga, M., Yoshida, E., Humbert, P.O., Bamji, S.X. (2009). Scribble interacts with beta-catenin to localize synaptic vesicles to synapses. *Mol Biol Cell* 20:3390-3400.

Stan, A., Pielarski, K.N., Brigadski, T., Wittenmayer, N., Fedorchenko, O., Gohla, A., Lessmann, V., Dresbach, T., Gottmann, K. (2010). Essential cooperation of N-cadherin and neuroligin-1 in the transsynaptic control of vesicle accumulation. *Proc Natl Acad Sci U S A.* 107:11116-11121.

Steiner P, Alberi S, Kulangara K, Yersin A, Sarria JC, Regulier E, Kasas S, Dietler G, Muller D, Catsicas S, Hirling H. (2005). Interactions between NEEP21, GRIP1 and GluR2 regulate sorting and recycling of the glutamate receptor subunit GluR2. *EMBO J.* 24(16):2873-84.

Stepanova, T., Slemmer, J., Hoogenraad, C.C., Lansbergen, G., Dortland, B., De Zeeuw, C.I., Grosveld, F., van Cappellen, G., Akhmanova, A., Galjart, N. (2003). Visualization of microtubule growth in cultured neurons via the use of EB3-GFP (end-binding protein 3-green fluorescent protein). *J. Neurosci.* 23,2655–2664.

Takai, Y., Ikeda, W., Ogita, H., Rikitake, Y. (2008a). The immunoglobulin-like cell

adhesion molecule nectin and its associated protein afadin. *Annu Rev Cell Dev Biol.* 24,309–342.

Takai, Y., Miyoshi, J., Ikeda, W., Ogita, H. (2008b) Nectins and nectin-like molecules: roles in contact inhibition of cell movement and proliferation. *Nat Rev Mol Cell Biol.* 9,603–615.

Takeda, S., Yamazaki, H., Seog, D.H., Kanai, Y., Terada, S., Hirokawa, N. (2000). Kinesin superfamily protein 3 (KIF3) motor transports fodrin-associated vesicles important for neurite building. *J Cell Biol.* 148,1255–1265.

Tanaka, Y., Zhang, Z., Hirokawa, N. (1995). Identification and molecular evolution of new dynein-like protein sequences in rat brain. *J Cell Sci.* 108,1883–1893.

Tanaka, Y., Kanai, Y., Okada, Y., Nonaka, S., Takeda, S., Harada, A., Hirokawa, N. (1998). Targeted disruption of mouse conventional kinesin heavy chain, kif5B, results in abnormal perinuclear clustering of mitochondria. *Cell* 93,1147–1158.

Teng, J., Rai, T., Tanaka, Y., Takei, Y., Nakata, T., Hirasawa, M., Kulkarni, A.B., Hirokawa, N. (2005). The KIF3 motor transports N-cadherin and organizes the developing neuroepithelium. *Nat Cell Biol.* 7,474–482.

Terada, S., Kinjo, M., Hirokawa, N. (2000). Oligomeric tubulin in large transporting complex is transported via kinesin in squid giant axons. *Cell* 103,141–155.

Terada, S., Kinjo, M., Aihara, M., Takei, Y., Hirokawa, N. (2010). Kinesin-1/Hsc70-dependent mechanism of slow axonal transport and its relation to fast axonal transport. *EMBO J.* 29,843–854.

Thompson, R.F. and Langford, G.M. (2002). Myosin superfamily evolutionary history. *The Anatomical Record* 268(3):276–289.

Ting, A.E., Hazuka, C.D., Hsu, S.C., Kirk, M.D., Bean, A.J., Scheller, R.H. (1995). rSec6 and rSec8, mammalian homologs of yeast proteins essential for secretion. *Proc Natl Acad Sci U S A.* 92:9613–9617.

- Tolle, T.R., Berthele, A., Zieglgansberger, W., Seeburg, P.H., Wisden, W. (1993). The differential expression of 16 NMDA and non-NMDA receptor subunits in the rat spinal cord and in periaqueductal gray. *J Neurosci.* 13, 5009-5028.
- Torres, R., Firestein, B.L., Dong, H., Staudinger, J., Olson, E.N., Huganir, R.L., Brecht, D.S., Gale, N.W., Yancopoulos, G.D. (1998). PDZ proteins bind, cluster, and synaptically colocalize with Eph receptors and their ephrin ligands. *Neuron* 21,1453–1463.
- Triller, A. and Choquet, D. (2008). New concepts in synaptic biology derived from single-molecule imaging. *Neuron* 59(3):359-74.
- Twelvetrees, A.E., Yuen, E.Y., Arancibia-Carcamo, I.L., MacAskill, A.F., Rostaing, P., Lumb, M.J., Humbert, S., Triller, A., Saudou, F., Yan, Z., Kittler, J.T. (2010). Delivery of GABAARs to synapses is mediated by HAP1-KIF5 and disrupted by mutant huntingtin. *Neuron* 65,53–65.
- van Dijk, J., Rogowski, K., Miro, J., Lacroix, B., Edde, B., Janke, C. (2007). A targeted multienzyme mechanism for selective microtubule polyglutamylation. *Mol Cell* 26(3):437-448.
- Vale, R.D., Reese, T.S., Sheetz, M.P. (1985). Identification of a novel force-generating protein, kinesin, involved in microtubule-based motility. *Cell* 42,39–50.
- Vale, R. D. and Fletterick, R. J. (1997). *Annu Rev Cell Dev Biol.* 13,745–777.
- Vale, R.D. (2003). The molecular motor toolbox for intracellular transport. *Cell* 112, 467–480.
- Verhey, K.J., Meyer, D., Deehan, R., Blenis, J., Schnapp, B.J., Rapoport, T.A., and Margolis, B. (2001). Cargo of kinesin identified as JIP scaffolding proteins and associated signaling molecules. *J Cell Biol.* 152, 959–970.
- Verhey, K.J. and Gaertig, J. (2007). The tubulin code. *Cell Cycle* 6(17):2152-60.

- Vestweber, D. (2008). VE-cadherin: the major endothelial adhesion molecule controlling cellular junctions and blood vessel formation. *Arterioscler Thromb Vasc Biol.* 28,223–232.
- Wagner, O.I., Esposito, A., Köhler, B., Chen, C.W., Shen, C.P., Wu, G.H., Butkevich, E., Mandalapu, S., Wenzel, D., Wouters, F.S., Klopfenstein, D.R. (2009). Synaptic scaffolding protein SYD-2 clusters and activates kinesin-3 UNC-104 in *C. elegans*. *Proc Natl Acad Sci U S A.* 106,19605–19610.
- Wallez, Y. and Huber, P. (2008). Endothelial adherens and tight junctions in vascular homeostasis, inflammation and angiogenesis. *Biochim Biophys Acta.* 1778,794–809.
- Westermann, S. and Weber, K. (2003). Post-translational modifications regulate microtubule function. *Nat Rev Mol Cell Biol.* 4:938-947.
- Wloga, D., Webster, D.M., Rogowski, K., Bré, M.H., Levilliers, N., Jerka-Dziadosz, M., Janke, C., Dougan, S.T., Gaertig, J. (2009). TTLL3 is a tubulin glycine ligase that regulates the assembly of cilia. *Dev Cell* 16,867–876.
- Wollmuth, L.P. and Sobolevsky, A.I. (2004). Structure and gating of the glutamate receptor ion channel. *Trends Neurosci.* 27(6):321-8.
- Wyszynski, M., Valtschanoff, J.G., Naisbitt, S., Dunah, A.W., Kim, E., Standaert, D.G., Weinberg, R., Sheng, M. (1999). Association of AMPA receptors with a subset of glutamate receptor-interacting protein in vivo. *J Neurosci.* 19(15):6528-37.
- Wyszynski, M., Kim, E., Dunah, A. W., Passafaro, M., Valtschanoff, J. G., Serrapages, C., Streuli, M., Weinberg, R. J., Sheng, M. (2002). Interaction between GRIP and liprin-alpha/SYD2 is required for AMPA receptor targeting. *Neuron* 34,39–52.
- Xia, J., Zhang, X., Staudinger, J., Huganir, R.L. (1999). Clustering of AMPA receptors by the synaptic PDZ domain-containing protein PICK1. *Neuron* 22:179–

187.

Xia, J., Chung, H.J., Wihler, C., Huganir, R.L., Linden, D.J. (2000). Cerebellar long-term depression requires PKC-regulated interactions between GluR2/3 and PDZ domain-containing proteins. *Neuron* 28:499–510.

Xia, C.H., Roberts, E.A., Her, L.S., Liu, X., Williams, D.S., Cleveland, D.W., Goldstein, L.S. (2003). Abnormal neurofilament transport caused by targeted disruption of neuronal kinesin heavy chain KIF5A. *J Cell Biol.* 161,55–66.

Xie, Z., Photowala, H., Cahill, M.E., Srivastava, D.P., Woolfrey, K.M., Shum, C.Y., Huganir, R.L., Penzes, P. (2008). Coordination of synaptic adhesion with dendritic spine remodeling by AF-6 and kalirin-7. *J Neurosci.* 28:6079-6091.

Yamada, S., Pokutta, S., Drees, F., Weis, W.I., Nelson, W.J. (2005). Deconstructing the cadherin–catenin-actin complex. *Cell* 123:889-901.

Yamagata, M., Sanes, J.R., Weiner, J.A. (2003). Synaptic adhesion molecules. *Curr Opin Cell Biol.* 15:621–32.

Yanagisawa, M., Kaverina, I.N., Wang, A., Fujita, Y., Reynolds, A.B., Anastasiadis, P.Z. (2004). A novel interaction between kinesin and p120 modulates p120 localization and function. *J Biol Chem.* 279(10):9512-21.

Yu, X. and Malenka, R.C. (2003). Beta-catenin is critical for dendritic morphogenesis. *Nat. Neurosci.* 6,1169–1177.

Zerial, M. and McBride, H. (2001). Rab proteins as membrane organizers. *Nat Rev Mol Cell Biol.* 2:107–117.

Zhao, C., Takita, J., Tanaka, Y., Setou, M., Nakagawa, T., Takeda, S., Yang, H.W., Terada, S., Nakata, T., Takei, Y., Saito, M., Tsuji, S., Hayashi, Y., Hirokawa, N. (2001). Charcot-Marie-Tooth disease type 2A caused by mutation in a microtubule motor KIF1Bbeta. *Cell* 105,587–597.

Zhou, Z., Hu, J., Passafaro, M., Xie, W., Jia, Z. (2011). GluA2 (GluR2) regulates metabotropic glutamate receptor-dependent long-term depression through N-cadherin-dependent and cofilin-mediated actin reorganization. *J Neurosci.* 31(3):819-33.

Zukin, R.S. and Bennett, M.V.L. (1995). Alternatively spliced isoforms of the NMDAR1 receptor subunit. *Trends Neurosci.* 18, 306-313.

8. Appendices

8-1. Abbreviations and units

ABP	AMPA receptor binding protein	DMEM	Dulbecco`s modified Eagle`s medium
AChR	nicotinicacetylcholine	DNA	Deoxyribonucleic acid
ADP	Adenosine diphosphate	Dync1h1	cytoplasmic dynein heavy chain 1
AMPA	α -amino-3-hydroxyl-5-methyl-4-isoxazole-propionate	Dync2h1	cytoplasmic dynein heavy chain 2
AMPAR	α -amino-3-hydroxyl-5-methyl-4-isoxazole-propionate receptor	ECL	enhanced chemiluminescence
APOER2	Apolipoprotein E receptor 2	ECM	extracellular matrix
APP	amyloid precursor protein	<i>E. coli</i>	Escherichia coli
AraC	Arabinofuranosyl Cytidine	ECs	Ectodomains
Arc	Activity-regulated Cytoskeleton	eGFP	enhanced green fluorescent protein
Arp1	actin-related protein 1	EDTA	Ethylenediaminetetraacetic acid
ATP	Adenosine-5'-triphosphate	EM	Electron microscopes
BDNF	brain-derived neurotrophic factor	EPSC	excitatory postsynaptic current
bp	base pare	ER	endoplasmic reticulum and others
BSA	Bovine serum albumin	<i>et al.</i>	and others
CaMKII	Calcium/calmodulin-dependent protein kinase II	EtBr	Ethidium bromide
CAMs	Cell adhesion molecules	FBS	Fetal bovine serum
cDNA	complementary DNA	GABA	γ -Aminobutyric acid
CNS	central nervous system	GABAR	γ -Aminobutyric acid receptor
Co-IP	Co-Immunoprecipitation	GAD	glutamic acid decarboxylase
Cys-loop	cysteine loops	GDP	Guanosine diposphate
DHC	dynein heavy chain	GFP	green fluorescent protein
DIC	dynein intermediate chain	GlyR	Glycine receptor
DIV	day in vitro	GPCR	G protein-coupled receptor
DLC	dynein light chain		

Appendice: Abbreviations and units

GRIP1	glutamate receptor interacting protein 1		proteins
GTP	Guanosine-5'-triphosphate	mGluRs	metabotropic glutamate receptors
HAP1	huntingtin-associated protein 1	Moco	molybdenum cofactor
HBS	Hepes Buffered Saline	mRFP	monomeric red fluorescent protein
HEK	human embryonic kidney	mRNA	Messenger RNA
HEPES	4-(2-hydroxyethyl)-1-piperazineethanesulfonic acid	mRNP	messenger ribonucleo-protein
HPSF	high purity salt free	MTOC	microtubule organizing center
HRP	horseradish peroxidase	NAP	nucleosomal assembly protein
IB	Immunoblotting	NB	Neurobasal
ICC	Immunocytochemistry	NCAD	N-Cadherin
Ig-CAMs	immunoglobulin-like CAMs	NL1	Neuroigin 1
IgG	immunoglobulin G	NMDA	<i>N</i> -Methyl-D-aspartate
iGluRs	ionotropic glutamate receptors	NMDAR	<i>N</i> -Methyl-D-aspartate receptor
JNK	c-Jun NH ₂ -terminal kinase	OD	optical density
JSAP1	JNK/SAPK-associated protein 1	PAGE	polyacrylamide gel electrophoresis
KAP	kinesin-associated protein	PBS	Phosphate-Buffered Saline
KHC	kinesin heavy chain	PCR	Polymerase chain reaction
KIF1	kinesin superfamily protein 1	PDZ	postsynaptic density protein / <i>Drosophila</i> disc large tumor suppressor/
KIF3	kinesin superfamily protein 3		zonula occludens-1 protein
KIF5	kinesin superfamily protein 5	PFA	Paraformaldehyde
KIF5C Δ MD	deleted motor domain of KIF5C	PGs1	Polyglutamylase 1
KLC	Kinesin light chain	PICK1	protein interacting with C kinase 1
LAR	Leukocyte common antigen-related	PIP ₃	phosphatidylinositol 3,4,5-triphosphate
LB	Luria-Bertani	PKC	Protein kinase C
LTD	long-term depression	PMSF	Phenylmethanesulfonyl fluoride
LTP	Long-term potentiation		
MAPs	microtubule-associated	PNS	peripheral nervous system

Appendice: Abbreviations and units

PSD	postsynaptic density	/	Liter
PSD95	postsynaptic density 95	min	Minute
PTMs	post-translational modifications	sec	Second
PTVs	Piccolo-Bassoon transport vesicles	f	Femto (10^{-15})
PVDF	polyvinylidene fluoride	p	Pico (10^{-12})
Q/R editing	glutamine/arginine editing	n	Nano (10^{-9})
RNA	Ribonucleic acid	μ	Micro (10^{-6})
rpm	revolutions per minute	m	Milli (10^{-3})
SAP97	synapse-associated protein 97	c h	Centi (10^{-2}) Hecto (10^2)
SAPK	stress-activated protein kinase	k M	Kilo (10^3) Mega (10^6)
SDS	sodium dodecyl sulfate	G	Giga (10^9)
SEM	standard error mean	T	Tera (10^{12})
shRNA	short hairpin RNA	P	Peta (10^{15})
siRNA	small interfering RNA		
SV2	synaptic vesicle 2		
TAE	Tris-Acetate-EDTA		
TBST	Tris-Buffered Saline Tween-20		
TRPC1	Transient receptor potential cation 1		
TTL	tubulin tyrosine ligase-like		
TrkB	Neurotrophic tyrosine kinase B		
UV	ultraviolet		
VIAAT	vesicular inhibitory amino acid transporter		
v/v	volume to volume		
%	per cent		
°C	degrees Celsius		
A.U.	arbitrary unit		
g	Gram		
h	Hour		

8-2. Figures and tables

8-2-1. List of figures

Fig. 2-1:	Structure of motor proteins	20
Fig. 2-2:	Intracellular transport in neurons	25
Fig. 2-3:	Schematic depiction of the N-Cadherin complex at excitatory synapses	32
Fig. 2-4:	Interaction of GRIP1 and N-Cadherin	34
Fig. 5-1:	Increase of polyglutamylation by strychnine-mediated blockade of GlyR	61
Fig. 5-2:	Knock-down of polyglutamylase by Lentivirus carrying shRNA-PGs1	62
Fig. 5-3:	Decrease of polyglutamylation by Lentivirus carrying shRNA-PGs1	63
Fig. 5-4:	Rescue of mRFP-gephyrin transport by Lentivirus carrying shRNA-PGs1	64
Fig. 5-5:	Interaction N-Cadherin with GluR2, and GRIP1	67
Fig. 5-6:	Triple co-localization of GRIP1, GluR2, and N-Cadherin	68
Fig. 5-7:	Localization of N-Cadherin with each component of GluR2-GRIP1-KIF5C	69
Fig. 5-8:	Association of N-Cadherin and GRIP1 with KIF5	69
Fig. 5-9:	Co-localization of GFP-fused GluR2, GRIP1, and N-Cadherin with synaptic vesicle 2	70
Fig. 5-10:	Co-immunoprecipitation of GluR2, GRIP1, and KIF5C with N-Cadherin in vitro	71
Fig. 5-11:	Subcellular distribution of mRFP-GRIP1 by motor protein, KIF5C	73
Fig. 5-12:	Subcellular distribution of mRFP-N-Cadherin by motor protein, KIF5C	74
Fig. 5-13:	Increase of N-Cadherin surface expression by motor protein, KIF5	76
Fig. 5-14:	Increase of GluR2 surface expression by the motor protein, KIF5	78
Fig. 5-15:	Decrease of N-Cadherin surface expression by overexpression of motor domain deleted form of KIF5C, KIF5C Δ MD	80
Fig. 5-16:	Decrease of N-Cadherin and GluR2 surface expression	

	through the overexpression of the competitive form of GRIP1, GRIP1-PDZ2	81
Fig. 5-17:	Cytosolic-interaction of extracellular N-terminal region of GluR2 with N-Cadherin	83
Fig. 5-18:	Decrease of N-Cadherin surface expression through co-transfection with extracellular N-terminal GluR2	84
Fig. 5-19:	KIF5-drives a new quadruple interaction complex: N-Cadherin, GluR2, GRIP1, and KIF5	85
Fig. 5-20:	Immunogold electron microscopy co-localization of N-Cadherin and GluR2 in the same vesicle	86
Fig. 5-21:	Single migration of N-Cadherin in the anterograde direction in dendrites	88
Fig. 5-22:	Co-migration of N-Cadherin and GluR2 in the anterograde direction in dendrites	89
Fig. 5-23:	Association of a new transport complex with an exocyst protein, Sec8	91
Fig. 5-24:	Reduction of spine numbers by interference of N-Cadherin transport	92
Fig. 6-1:	Hypothetical model of a KIF5-driven new transport complex	108

8-2-2. List of tables

Table 4-1:	Primary antibodies and their information	42
Table 4-2:	Secondary antibodies and their information	43
Table 4-3:	Oligonucleotides and their usage	43
Table 4-4:	Plasmids and their information	45
Table 4-5:	Viruses and their information	47

8-3. Curriculum Vitae

Education

- Present - **Ph.D. candidate**
 01. 2008 Department of Molecular Neurogenetics,
 Center for Molecular Neurobiology (ZMNH),
 University of Hamburg Medical School, Germany
 Head of department: Prof. Matthias Kneussel Ph.D.
- 2005 **Degree of Master of Science** in Biology
 Development & Neuroendocrine Research Laboratory,
 School of Biological Sciences,
 Seoul National University, South Korea
 Group leader: Prof. Kyungjin Kim Ph.D.
- Thesis:**
Adrenal peripheral clock:
Circadian rhythm of synthesis and secretion of glucocorticoid
- 2003 **Degree of Bachelor** in Biology
 Department of Life Science,
 School of Natural Science,
 Sung Kyun Kwan University, South Korea

Research / Teaching Experience

04. 2006 – 12. 2007 **Researcher**
 Department of Physiology and Biophysics,
 Department of Clinical Neuroscience,
 Faculty of Medicine, University of Calgary, Canada
01. 2005 – 04. 2006 **Research assistant**
 Department of Anatomy,
 School of Medicine, Korea University, South Korea
09. 2003 – 12. 2003 **Teaching assistant**
 School of Biological Sciences,
 Seoul National University, South Korea
 Subject: Advance biological experiment

8-4. List of publications

International publications

Maas, C., Belgardt, D., Lee, H.K., Heisler, F.F., Lappe-Siefke, C., Magiera, M.M., van Dijk, J., Hausrat, T.J., Janke, C., Kneussel, M. (2009). Synaptic activation modifies microtubules underlying transport of postsynaptic cargo. *Proc Natl Acad Sci U S A*. 26;106(21):8731-6.

Son, G.H., Chung, S., Choe, H.K., Kim, H.D., Baik, S.M., Lee, H.K., Lee, H.W., Choi, S., Sun, W., Kim, H., Cho, S., Lee, K.H., Kim, K. (2008). Adrenal peripheral clock controls the autonomous circadian rhythm of glucocorticoid by causing rhythmic steroid production. *Proc Natl Acad Sci U S A*. 105(52):20970-5.

Poster presentations

7th FENS Forum of European Neuroscience 2010. Amsterdam, The Netherlands: Hausrat, T.J., Myllynen, L., Heisler, F.F., Lee, H.K., Spilker, C., Gundelfinger, E.D., Kneussel, M. (2010). The RapGAP SPAR2 requires radixin binding for cytoskeletal anchoring at postsynaptic dendrites.

7th The Korean Society for Brain and Neural Science 2004. Seoul, South Korea: Lee, H.K., Kim, K. (2004). Adrenal peripheral clock: Circadian rhythm of synthesis and secretion of glucocorticoid.

9. Acknowledgements

It is a pleasure to thank the many people who made this dissertation possible.

I am extremely grateful to Prof. Dr. Matthias Kneussel for providing an opportunity to stay my life for Ph.D. at the ZMNH as well as for his advising and supporting of this project. Without his great supervising through my Ph.D. period, I would have been lost for my purpose. I also appreciate that my life could have some experience at here in Hamburg, which is a great city in Europe.

I would like to thank Prof. Dr. Christian Lohr for his kind agreement to be a referee for my dissertation and for his time. In addition, I wish to thank all the committee members, who are Prof. Dr. Alexander Haas, Prof. Dr. Lothar Renwartz, PD Dr. Sabine Hoffmeister-Ullerich, Dr. Kent Duncan, Dr. Petschenka Georg, Dr. Bettina Spitzweck, and Dr. Gabriele Loers, for their time. Especially, I thank Prof. Dr. Lothar Renwartz and PD Dr. Sabine Hoffmeister-Ullerich to be my referee for defense.

The words of appreciation go to all members of the department of Molecular Neurogenetics in the ZMNH. I am indebted to them for their support and help during the time. I am especially grateful to Frank, Torben, and Mary for their helping.

Lastly, and most importantly, I wish to thank my family, my parents, sisters, brother-in-law, and my wife Ji Na.